# DEVELOPING REPLACEABLE MEMBERS FOR STEEL LATERAL LOAD RESISTING SYSTEMS

A THESIS SUBMITTED TO
THE GRADUATE SCHOOL OF NATURAL AND APPLIED SCIENCES
OF
MIDDLE EAST TECHNICAL UNIVERSITY

BY

MEHMET BAKIR BOZKURT

IN PARTIAL FULFILLMENT OF THE REQUIREMENTS
FOR
THE DEGREE OF DOCTOR OF PHILOSOPHY
IN
CIVIL ENGINEERING

APRIL 2017

Approval of the thesis:

**DEVELOPING REPLACEABLE MEMBERS FOR STEEL LATERAL LOAD RESISTING SYSTEMS**

submitted by **MEHMET BAKIR BOZKURT** in partial fulfillment of the requirements for the degree of **Doctor of Philosophy in Civil Engineering Department, Middle East Technical University** by,

Prof. Dr. Gülbin Dural Ünver ______________________
Dean, Graduate School of **Natural and Applied Sciences**

Prof. Dr. İsmail Özgür Yaman ______________________
Head of Department, **Civil Engineering**

Prof. Dr. Cem Topkaya ______________________
Supervisor, **Civil Engineering Dept., METU**

**Examining Committee Members:**

Prof. Dr. Oğuzhan Hasançebi ______________________
Civil Engineering Dept., METU

Prof. Dr. Cem Topkaya ______________________
Civil Engineering Dept., METU

Prof. Dr. Özgür Anıl ______________________
Civil Engineering Dept., Gazi University

Assoc. Prof. Dr. Afşin Sarıtaş ______________________
Civil Engineering Dept., METU

Asst. Prof. Dr. Saeid Kazemzadeh Azad ______________________
Civil Engineering Dept., Atılım University

**Date:** 17.04.2017

**I hereby declare that all information in this document has been obtained and presented in accordance with academic rules and ethical conduct. I also declare that, as required by these rules and conduct, I have fully cited and referenced all material and results that are not original to this work.**

Name, Last name: MEHMET BAKIR BOZKURT

Signature:

# ABSTRACT

## DEVELOPING REPLACEABLE MEMBERS FOR STEEL LATERAL LOAD RESISTING SYSTEMS

BOZKURT, Mehmet Bakır
Ph.D., Department of Civil Engineering
Supervisor: Prof. Dr. Cem Topkaya

April 2017, 100 pages

Steel structures utilize lateral load resisting systems to provide sufficient strength, stiffness and ductility. Damaged structures need to be either demolished or retrofitted to recover their initial properties after a major earthquake. In steel structures, damage is concentrated to predefined fuse members and most other members are designed to behave elastic under seismic events. In buckling restrained braced frames (BRBFs) and eccentrically braced frames (EBFs), the fuse members are well defined and can be conveniently repaired. In the literature, experimented studies were conducted to develop fuse members for BRBFs and EBFs. This thesis reports findings of a three-phase experimental research program on steel encased buckling-restrained braces (BRBs) and a two-phase experimental research program on eccentrically braced frames with replaceable links.

The first experimental research program investigated the potential use of steel encased BRBs using subassemblage testing. Because steel encasements can provide lighter solutions, they are more advantageous compared to concrete or mortar filled encasements in terms of replacement of BRBs. Pursuant to this goal, a three-phase experimental research program consisting of thirteen tests was conducted where BRBs

were investigated under subassemblage testing. The first phase of the program aimed at studying the performance of steel encased BRBs which utilize constant width core plates. Test results indicated that these braces develop unacceptably high compression and tension resistances and the behaviors of these BRBs under uniaxial testing and subassemblage testing are markedly different. In second phase of the research program, a new type of BRB core, which utilizes a welded overlap, was developed to improve the cyclic performance observed in the first phase. Experimental results showed that the braces sustain axial strains that vary between 2.0 and 2.5% and resistances in tension and compression were found to improve significantly when compared with the findings of the first phase. Welded overlap core steel encased BRBs were found to sustain cumulative axial strains that are 419 times the yield strain when properly detailed. The third phase focused on connections of welded overlap steel encased BRBs. Two typical connection details, namely the pin connection and gusseted connection, were experimented by considering the collar detail as the prime variable. Test results indicate that the gusseted detail does not require collars to be used while the pinned detail mandates the use of collars for acceptable performance.

The second experimental research program concentrated on developing replaceable links for steel eccentrically braced frames. A replaceable link detail, which is based on splicing braces and the beam outside the link, was proposed. This detail eliminates the need to use hydraulic jacks and flame cutting operations for replacement purposes. The first phase of the research program concentrated on replaceable links with direct brace attachments while the second phase concentrated on links with gusset plate connected brace attachments. Performance of these proposed replaceable links was studied by conducting eight full-scale EBF tests with directly attached braces and eleven full-scale EBF tests with gusset plate connected braces under quasi-static cyclic loading. The link length ratio, stiffening of the link, loading protocol, connection type, bolt pretension, gap size of splice connections, and demand-to-capacity ratios of members were considered as the prime variables. The specimens primarily showed two types of failure modes: link web fracture and fracture of the flange at the link-to-brace connection. No failures were observed at the splice connections indicating that the proposed replaceable link details provide excellent response. The inelastic rotation capacity provided by the replaceable links satisfied the requirements of the AISC Seismic Provisions for Structural Steel Buildings (AISC341-10). The overstrength factor of the links exceeded 2.0 which is larger than the value assumed for EBF links by design provisions.  The high level of overstrength resulted in brace buckling in one of the specimens with direct connected brace and one of specimens with gusset plate connected brace which demonstrated the importance of overstrength factor used for EBF links.

Keywords: Buckling Restrained Brace, Eccentrically Braced Frame, Steel, Replaceable Link, Experimental Testing

# ÖZ


ÇELİK YATAY YÜK DİRENÇ SİSTEMLERİ İÇİN DEĞİŞTİRİLEBİLİR ELEMANLARIN GELİŞTİRİLMESİ

BOZKURT, Mehmet Bakır

Doktora, İnşaat Mühendisliği Bölümü

Tez Yöneticisi: Prof. Dr. Cem Topkaya

Nisan 2017, 100 sayfa

Çelik yapılar yeterli rijitlik ve süneklik sağlayabilmek için yatay yük direnç sistemlerinden faydalanırlar. Şiddetli bir deprem sonrasında hasar gören yapılar ya yıkılmalıdırlar ya da başlangıç özelliklerini geri kazanabilmek için güçlendirilmelidirler. Çelik yapılarda hasar, önceden tanımlanan enerji sönümleyici elemanlarda yoğunlaşır ve diğer tüm elemanlar sismik bir hareket durumunda elastik davranacak şekilde tasarlanır. Burkulması önlenmiş çelik çaprazlı perdelerde (BÖÇÇP'lerde) ve dışmerkez çelik çaprazlı perdelerde (DMÇÇP'lerde) bu enerji sönümleyici elemanlar çok iyi tanımlanmıştır ve rahatlıkla onarılabilir. Literatürde, BÖÇÇP'lerde ve DMÇÇP'lerde kullanılan enerji sönümleyici elemanların geliştirilmesi için deneysel çalışmalar gerçekleştirilmiştir. Bu tez çelik kılıflı BÖÇÇP'ler için üç aşamalı deneysel çalışmanın bulgularını ve değiştirilebilir bağ kirişli DMÇÇP'li sistemler için iki aşamalı deneysel çalışmanın bulgularını sunmaktadır.

Birinci deneysel araştırma programında, çelik kılıflı BÖÇÇP'lerin yarı çerçeve deneyleri yapılarak potansiyel kullanımları incelenmiştir. Çelik kılıflar daha hafif çözümler ortaya kolduğu için, BÖÇÇP'lerin değişimi açısından beton ve harç dolgulu kılıflara gore daha avantajlıdır. Bu amaca istinaden, on bir deneyden meydana gelen üç

aşamalı bir deneysel araştırma programı yarı çerçeve deneyleri altında uygulanmıştır. Bu programın birinci aşamasında, sabit genişlikli çekirdek plakanın kullanıldığı çelik kılıflı BÖÇÇP'lerinin performanslarının araştırılması amaçlanmıştır. Test sonuçları bu çaprazlarda kabul edilemeyen çekme ve basınç dayanımlarının oluştuğunu ve eksenel test ile yarı çerçeve teslerine maruz kalan BÖÇÇP elemanların davranışları arasında ciddi farkların olduğunu göstermiştir. Araştırma programının ikinci aşamasında, birinci aşamada gözlemlenen çevrimsel performansı iyileştirmek için kaynaklı olarak üst üste bindirilmiş çekirdek plakaların kullanıldığı yeni nesil bir BÖÇÇP geliştirilmiştir. Deneysel sonuçlar çapraz elemanların %2 ile %2.5 arasında değişen eksenel birim şekil değiştirmelerinde stabil dayanım gösterdiği ve çekme ile basınç dayanımlarında birinci aşamada elde edilen sonuçlarla kıyaslandığında ciddi iyieşmelerin olduğunu ortaya koymuştur. Kaynaklı üst üste bindirilmiş çekirdek plakalı BÖÇÇP'lerin düzgün detaylandırıldığı zaman akma birim şekil değiştirmenin 419 katına kadar kümülatif eksenel birim şekil değiştirmeye dayanabildiği gösterilmiştir. Araştırma programının üçüncü aşamasında, bu kaynaklı üst üste bindirilmiş çekirdek plakalı BÖÇÇP elemanların bağlantı detaylarına odaklanılmıştır. Mafsallı ve guse plakalı olmak üzere iki tipik bağlantı detayı ana değişken olarak çelik yaka sistemini göz önüne alarak test edilmiştir. Test sonuçları kabul edilen peformans için guse plakalı bağlantı detaylarında çelik yaka sistemine gerek olmadığını fakat mafsallı detaylarda bu elemanlara ihtiyaç olduğunu ortaya koymuştur.

İkinci deneysel araştırma programı dışmerkez çelik çapraz perdeli sistemler için değiştirilebilir bağ kirişlerinin geliştirilmesine yoğunlaşmıştır. Bağ kirişi dışındaki kat kirişi ve çapraz elemanların bölünmesi esasına dayanan bir değiştirilebilir bağ kiriş detayı önerilmiştir. Bu detay bağ kirişi elemanlarının değişimi esnasında ihtiyaç duyulan hidrolik piston ve alevli kesim gereksimini ortadan kaldırmıştır. Araştırma programının birinci aşamasında direkt çapraz bağlantılı değiştirilebilir bağ kirişine yoğunlaşılırken, ikinci aşamada guse plakalı çapraz bağlantılı değiştirilebilir bağ kirişlerine konsantre olunmuştur. Önerilen değiştirilebilir bağ kirişi elemanın performansı yarı-statik yükleme altında, sekiz adet direkt bağlanan çaprazlı tam ölçekli DMÇÇP'li sistemlerin deneyleri yapılarak ve on bir adet guse plaka ile bağlanan çaprazlı tam ölçekli DMÇÇP'li

sistemlerin deneyleri yapılarak ayrı ayrı incelenmiştir. Bağ kirişi uzunluk oranı, bağ kirişi berkitmeleri, yükleme protokolleri, bağlantı tipleri, cıvata önçekmesi, uç uca birleştirilen detaydaki boşluk ve elemanların talep kapasite oranları temel değişkenler olarak göz önüne alınmıştır. Temel olarak numuneler bağ kirişi gövde yırtılması ve bağ kirişi çapraz bağlantısındaki başlığın yırtılması şeklinde iki farklı göçme modu sergilemiştir. Çapraz ve kat kirişi eklerinde yer alan uç uca birleştirilmiş bağlantı detaylarında herhangi bir göçme gözlenmemesi önerilen değiştirilebilir bağ kirişi detayının mükemmel davranış sergilediğini ortaya koymuştur. Değiştirilebilir bağ kirişinin sağladığı plastik dönme kapasitesi Amerikan Yapısal Çelik Binalar için Sismik Şartnamesi (AISC341-10 (2010))'da tanımlanan koşulları yerine getirmiştir. Bağ kirişlerinin dayanım fazlalığı katsayısı DMÇÇP'li sistemler için tasarım şartnamelerinde kabul edilen 2.0 değerini aşmıştır. Dayanım fazlalığı katsayısının yüksek değeri direkt bağlantıya sahip çapraz elemanlı numunelerden bir tanesinde ve guse plakalı bağlantıya sahip çapraz elemanlı numunelerden bir tanesinde burkulmaya neden olmuştur ve bu durum DMÇÇP'li sistemlerde dayanım fazlalığı katsayısının önemini göstermiştir.

Anahtar Kelimeler: Burkulması Önlenmiş Çelik Çaprazlar, Dışmerkez Çelik Çaprazlı Perdeler, Çelik, Değiştirilebilir Bağ Kirişi, Deneysel Test

To My Family

# ACKNOWLEDGEMENTS

I wish to express my deepest gratitude to my supervisor Prof. Dr. Cem Topkaya for his invaluable support, guidance, comments, suggestions and insights throughout my research.

I wish to express my sincere thanks to Salim Azak, Özer Zeybek, Ali Özen, Nefise Shaban, Yasin Onuralp Özkılıç and Technical Staff Hasan Metin, Osman Keskin, Murat Demirel and Barış Esen who helped in the experiments.

I wish to express my hearty gratitude to my spouse Aslı, my daughters Naz and Zeynep for their patience, toleration and boundless supports.

This study presented herein was made possible through the funds (BAP-03-03-2014-002 and BAP-03-03-2016-003) from the College of Engineering of the Middle East Technical University.

This study was also supported by the Scientific and Technological Council of Turkey (TÜBİTAK) through grant number 114M251.

The help of Gözüm Çelik and Atak Mühendislik in fabricating the specimens is greatly appreciated.

The scholarship provided by TÜBİTAK during my study is acknowledged as well.

# TABLE OF CONTENTS

# LIST OF SYMBOLS AND ABBREVIATIONS

| | |
|---|---|
| A | Flange Buckling |
| b | Width |
| B | Bearing Type |
| B | Flange Fracture |
| BRB | Base Flat Bar |
| C | Fracture of Web at the Stiffener Weld |
| CGB | Compact Gusset Plate Connected Brace Attachment |
| CONT | Continuous |
| Cum | Cumulative |
| d | Depth of the Section |
| D | Double-Sided Stiffeners |
| D | Flange Buckling in Brace Connection Panel |
| DB | Direct Brace Attachment |
| Dim | Dimension |
| e | Link Length |
| E | Brace Buckling |
| $F_{actuator}$ | Force Applied by the Actuator |
| $F_y$ | Yield Strength |
| $F_u$ | Ultimate Strength |
| $F_{yL}$ | Lower Yield Stress |
| $F_{yu}$ | Upper Yield Stress |
| $F_{y,02}$ | Yield Stress at 0.2% Permanent Elongation |
| GB | Gusset Plate Connected Brace Attachment |
| GMAW | Gas Metal Arc Welding |
| h | Distance between the Pin Supports at Column Ends |
| H | Heat |
| INT1 | Intermittent (50-150) |
| INT2 | Intermittent (100-100) |

| | |
|---|---|
| $K$ | Cyclic Stress-Strain Curve Strength Coefficient |
| $K_{frame}$ | Elastic Stiffness of the Frame |
| $K_{link}$ | Elastic Stiffness of the Link |
| L | Frame Width Measured between the Pinned Column Bases |
| LP1 | AISC341-10 Loading Protocol |
| LP2 | AISC341-02 Loading Protocol |
| $M_e$ | Measured |
| $M_{rx}$ | Bending Moment Applied to the Member about x axis |
| $M_{cx}$ | Bending Moment Capacity of the Member about x axis |
| N | No |
| $N_m$ | Nominal |
| OFB | Overlapping Flat Bar |
| OS | Overstrength |
| $P_c$ | Axial Force Capacity of the Member |
| $P_{cr}$ | Critical Buckling Load |
| PGB | Gusset Plate Pin Connected Brace Attachment |
| PM | Demand to Capacity Ratio |
| $P_r$ | Axial Force Applied to the Member |
| Pre | Pretension |
| $P_{ysc}$ | Yield Load of Core Braces |
| S | Single-Sided Stiffeners |
| SC | Slip Critical |
| SCO | Slip Connection with Oversize Holes |
| Spec | Specimen |
| Sp | Specimen |
| Stf | Stiffeners |
| $t_f$ | Flange Thickness |
| $t_w$ | web thickness |
| $V_n$ | Nominal Shear Capacity |
| $V_{n,N}$ | Nominal Shear Strength |
| $V_{n,M}$ | Measured Shear Strength |

| | |
|---|---|
| Y | Yes |
| %E | Percent Elongation |
| $\beta$ | Compression Strength Adjustment Factor |
| $\gamma$ | Total Rotation Capacity |
| $\gamma_p$ | Inelastic Rotation Capacity |
| $\bar{\varepsilon}_p$ | Normalized Plastic Strain |
| $n$ | Cyclic Stress-Strain Curve Hardening Factor |
| $\theta$ | Total Story Drift Angle |
| $\theta_p$ | Inelastic Story Drift Angle |
| $\rho$ | Link Length Ratio |
| $\bar{\sigma}$ | Normalized Stress |
| $\omega$ | Strain Hardening Adjustment Factor |

# CHAPTER 1

# INTRODUCTION

## 1.1. General

Several lateral load resisting systems are available for steel structures against earthquake loads. These include but not limited to moment resisting frames (MRFs), concentrically braced frames (CBFs), eccentrically braced frames (EBFs), buckling restrained braced frames (BRBFs) and steel plate shear walls (SPSWs). Each system has its advantages and disadvantages. The following sections provide details for BRBF and EBF systems

## 1.2. Background of Buckling Restrained Braced Frames (BRBFs)

Buckling restrained braced frames are a special case of concentrically braced frames (CBFs). CBFs are composed of beams, columns and bracing members. Lateral stiffness of CBFs is proportional to axial stiffness of the bracing members. There are several configurations for CBF systems, some of which are illustrated in Figure 1.1. During a seismic event, braces are subjected to tension or compression. CBFs exhibit a pinched lateral load versus displacement response and are characterized as low ductility frames.

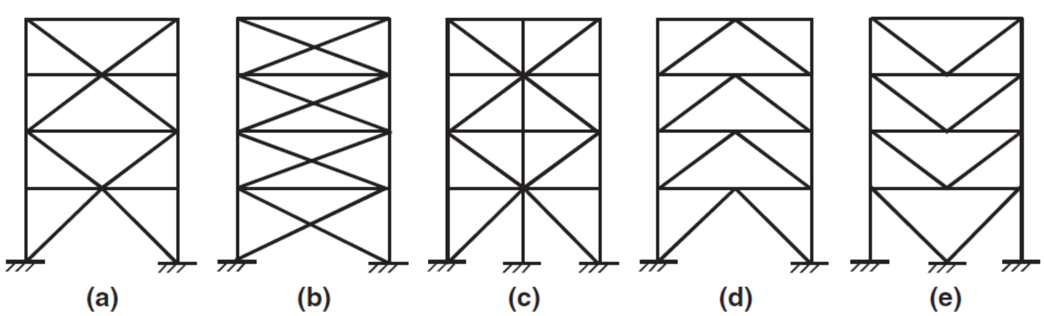


Figure 1.1 Typical CBF configurations (Bruneau et al. (2011))

Similar to CBFs, a typical steel BRBF is composed of beams, columns, and buckling restrained braces (BRBs). During a seismic event BRBs yield in tension and compression and contribute to energy dissipation. When compared with conventional steel braces, BRBs provide nearly equal tensile and compressive resistances. A typical BRB is composed of a core segment, debonding material and a buckling restraining mechanism.

A significant amount of research work has been performed in Japan and elsewhere in Asia over the last few decades for the development of BRBs (Xie (2005)). A detailed summary of findings are summarized in a report by Uang and Nakashima (2004). In general, BRBs can be classified into different categories depending on the type of core segment and the buckling restraining mechanism. Steel (Tremblay et al. and Devall (2006), Wu et al. (2014), Eryaşar (2009), Eryaşar and Topkaya (2010)) or aluminum (Usami et al. (2012), Wang et al. (2012), Wang et al. (2013)) can be selected for the material of the core segment. Buckling can be inhibited by a concrete or mortar filled steel encasing member which is usually a hollow structural steel section (Uang and Nakashima (2004)). The core segment can be restrained by steel sections only (Tremblay et al. (2006), Wu et al. (2014), Eryaşar (2009), Eryaşar and Topkaya (2010)) or with glass fiber-reinforced polymer pultruded tubes (Dusicka and Tinker (2013)).

Various geometries can be adopted for the core segment. As shown in Figure 1.2, typical cross sections used for the core segment can be rectangular sections (Tremblay et al. (2006), Wu et al. (2014), Eryaşar (2009), Eryaşar and Topkaya (2010)) or with glass fiber-reinforced polymer pultruded tubes (Dusicka and Tinker (2013)), built-up angle sections (Zhao et al. (210)), H-sections (Kim et al. (2015)) or steel rods (Park et al. (2012)). As shown in Figure 1.3, the cross-section of the core segment can be changed along the length to constrain yielding in a limited domain. In most of the BRBs the rectangular cross section is reduced at the center (Tremblay et al. (2006)). The advantage of this method is that the yielding segment length and capacity can be adjusted easily. The disadvantages are that the production of the core can be costly and the quality of workmanship plays an important role in BRB performance. This type of BRB core requires CNC cutting of plates to produce core segment with a certain radius. Stress concentrations can occur in the transition region if the workmanship is not of high quality and this in turn causes premature fractures in this region. A constant cross-section core segment can also be used (Eryaşar (2009), Eryaşar and Topkaya (2010)) which eliminates CNC cutting procedure; however, these core segments cannot be tailored easily to meet the stiffness requirements at the design stage. Other alternatives based on perforated core segments (Piedrafita et al. (2013), Piedrafita et al. (2015)) were also developed.

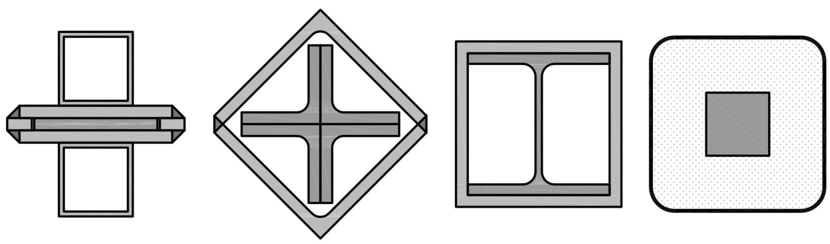

Figure 1.2 Typical cross sections for BRBs

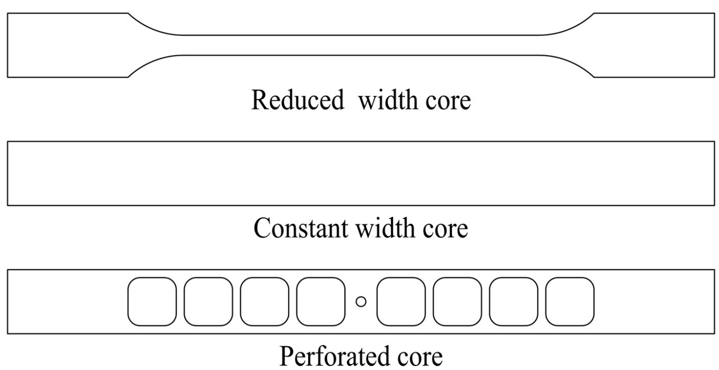


Figure 1.3 Core segment configurations for BRBs

In the United States design recommendations for BRBs have been incorporated into AISC 341-10 Seismic Provisions for Structural Steel Buildings (AISC341-10 (2010)). These provisions require qualifying cyclic tests to be performed on a subassemblage and a uniaxial test specimen. In a subassemblage test, BRBs are tested together with their connections under a loading condition that imposes rotation demands on a specimen.

The requirements for subassemblage test specimens are given in AISC341-10 (2010). Research conducted on BRBFs revealed that large flexural demands are produced at the BRB ends (Fahnestock et al. (2007), Zhao et al. (2012)) and this can cause an undesired behavior. Therefore, subassemblage testing needs to be performed to observe the behavior of a BRB under more realistic loading conditions. In addition, the connection performance (Lin et al. (2014), Chuang et al. (2015)) can be better studied using subassemblage testing or large scale testing (Lin et al. (2012)).

### 1.3. Background of Eccentrically Braced Frames (EBFs)

A typical steel EBF is composed of links, beams, columns, and braces. EBFs combine of the advantages of moment resisting frames (MRFs) and concentrically braced frames (CBFs). Therefore, EBFs are capable of high levels of ductility and they have high elastic stiffness. Development of EBFs started in Japan (Fujimoto et al. (1972), Tanabashi et al. (1974)) and USA (Roeder and Popov (1978), Hjelmstad and Popov (1983), Manheim and Popov (1983), Hjelmstad and Popov (1984), Malley and Popov (1984), Kasai and Popov (1985), Kasai and Popov (1986), Kasai and Popov (1986), Popov and Engelhardt (1988), Engelhardt and Popov (1989), Engelhardt and Popov (1989)) about 40 years ago. Research to date has resulted in the development of design specifications. A typical EBF can be designed according to the rules presented in Turkish Seismic Code (2007), AISC341-10 (2010) or EC8 (2004). A review of research on EBF systems is presented by Kazemzadeh Azad and Topkaya (2017).

An isolated segment of beam called the link controls energy dissipation of the EBFs. Type of yielding of the links is dependent on the length of the link. Short links generally yield under shear while long links yield under flexure. Intermediate length links yield under combined action of shear and flexure. Members other than the link are designed to remain elastic under seismic events. Experiments conducted on individual links showed stable hysteretic behavior which resulted in acceptance of these systems as high ductility systems. Different types of configurations for EBF systems are illustrated in Figure 1.4.

According to the current practice a structure may require extensive repair or replacement after a major earthquake. In general, repair of members is an expensive operation and may affect the use of a structure. EBFs are superior to many other lateral load resisting systems from a repair standpoint. Capacity design principles are utilized in design of EBFs which limit most of the inelastic action to the links. Beams outside the link, braces and columns are designed to remain essentially elastic during a seismic event. Fractures in links of EBFs were observed after the 2010 and 2011 New Zealand earthquakes (Clifton et al. (2011)). These links were subsequently replaced with new ones (Ramsay et al. (2013), Gardiner et al. (2013)).

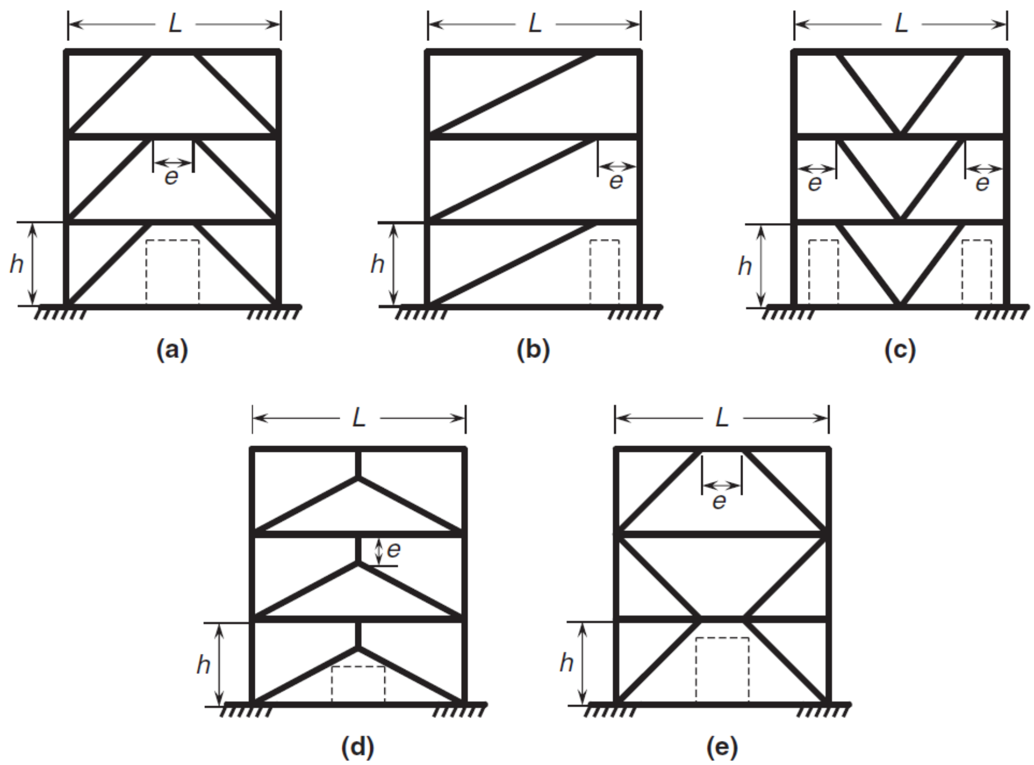


Figure 1.4 Typical EBF configurations (Bruneau et al. (2011))

In the current practice, the links and beams outside the link are designed as a single member which makes the replacement procedure rather difficult. In order to circumvent this problem, replaceable links were proposed over the years (Balut and Gioncu (2003), Mansour (2010)). Three replaceable link types were evaluated experimentally in the past which are shown in Figure 1.5. All three types have a common feature that bolted attachments are provided in the link ends to connect the link beam to the beams outside the link.

The first experimented type of replaceable link (Stratan and Dubina (2004), Stratan et al. (2003), Dubina et al. (2008), Sabau et al. (2014), Ioan et al. (2016)) utilizes flush end-plate bolted connections as shown in Figure 1.5a. This concept was studied at member level ((Stratan and Dubina (2004), Dubina et al. (2008)) as well as structure level (Sabau et al. (2014), Ioan et al. (2016)). The results of the experiments revealed that the behavior of these links is different from conventional shear links because of the pinched behavior (Stratan and Dubina (2004), Stratan et al. (2003), Dubina et al. (2008)). The deformations that take place at the bolts of the flush end-plate connection promote a pinched shear versus link rotation angle response. The amount of pinching can be significantly reduced by using short links that primarily yield in shear. The link length ratio $\rho = e/(M_p/V_p)$, where $e$ is the link length, $M_p$ is the plastic moment capacity, and $V_p$ is the plastic shear capacity of the link, is usually used to represent yielding behavior of a link. The flush end-plate bolted connection was recommended to be used for links with $\rho < 0.8$ (Stratan and Dubina (2004), Stratan et al. (2003), Dubina et al. (2008)). Quantifying the stiffness of these replaceable links is difficult because of the inherent flexibility of their connections; however, some recommendations were developed for practical applications (Dubina et al. (2008)). The applicability of these replaceable links was studied through full-scale pseudo-dynamic testing (Sabau et al. (2014), Ioan et al. (2016)). The dual system concept was utilized where EBFs are used together with moment resisting frames (MRFs). The idea here is to engage MRFs to reduce the residual drifts and provide a recentering capability to the system (Dubina et al. (2008), Dubina et al. (2011)). A three story-three bay structure was subjected to pseudo-dynamic loadings which produced different displacement demands at levels of Damage Limitation (DL), Significant Damage (SD), and Near Collapse (NC). The structure exhibited low residual top displacement of 5mm (0.05 percent roof drift) after the DL test. The links were replaced with new ones and the system re-centered itself by reducing the top displacement to 1 mm and 4 mm for two of the frames of the structure. One difficulty associated with the removal procedure was that a manually operated hydraulic jack was used to push the braces apart so that the links can be pulled apart. A low residual top story displacement of 13 mm (0.12 percent roof drift) was recorded after the SD test. Due to limitations in equipment capacity the final pseudo-dynamic test was replaced with a monotonic pushover test. The amount of residual displacement at the top story was recorded as 50mm (0.47%) after the pushover test. The second link replacement was subsequently performed and the top story displacements were observed to decrease to 10mm and 19mm for the two frames of the structure exhibiting excellent re-centering capability. For this replacement; however, flame cutting of the links was necessary. In addition, hydraulic jacks were used to place the new set of links in the structure.

The other two replaceable link types were experimented at the member level as well as a part of a one-story one-bay frame (Mansour (2010), Mansour et al. (2011)). The first of these types (Figure 1.5b) is an end-plated connection which is similar to the flush end-plate connection (Figure 1.5a) and the second one is web connected channel sections (Figure 1.5c). In the former connection, the end plate is extended to be able to provide bolts above and below the I-shaped link. The idea here is to eliminate pinching behavior by having an end connection which is much more rigid than the flush end-plate connection. Test results revealed (Mansour (2010), Mansour et al. (2011)) that a replaceable link with extended end plate connection exhibits similar behavior to a conventional I-shaped link. Link length ratios ($\rho$) of 1.16 and 1.6 were studied and the results showed that providing a stringent limit of $\rho<0.8$ is not necessary for these replaceable links. The application of an extended end plate requires that the depth of the beam outside of the link must be greater than the depth of the link section. While this requirement is useful for satisfying strength of the beams outside the link, which are subjected to a high level of axial load and bending moment, it can cause an over-design of these members. Replacement of these links under residual drift was not studied; however, sizing the link to be shorter by a few millimeters and filling the gap between the link end-plate and beam outside of the link with shims were proposed as a solution (Mansour et al. (2011)). Based on the experience gained from the links with flush end-plate connections (Sabau et al. (2014), Ioan et al. (2016)), it is expected that significant residual axial forces can be developed in these links which may require the use of hydraulic jacks and even flame cutting for removal and replacement.

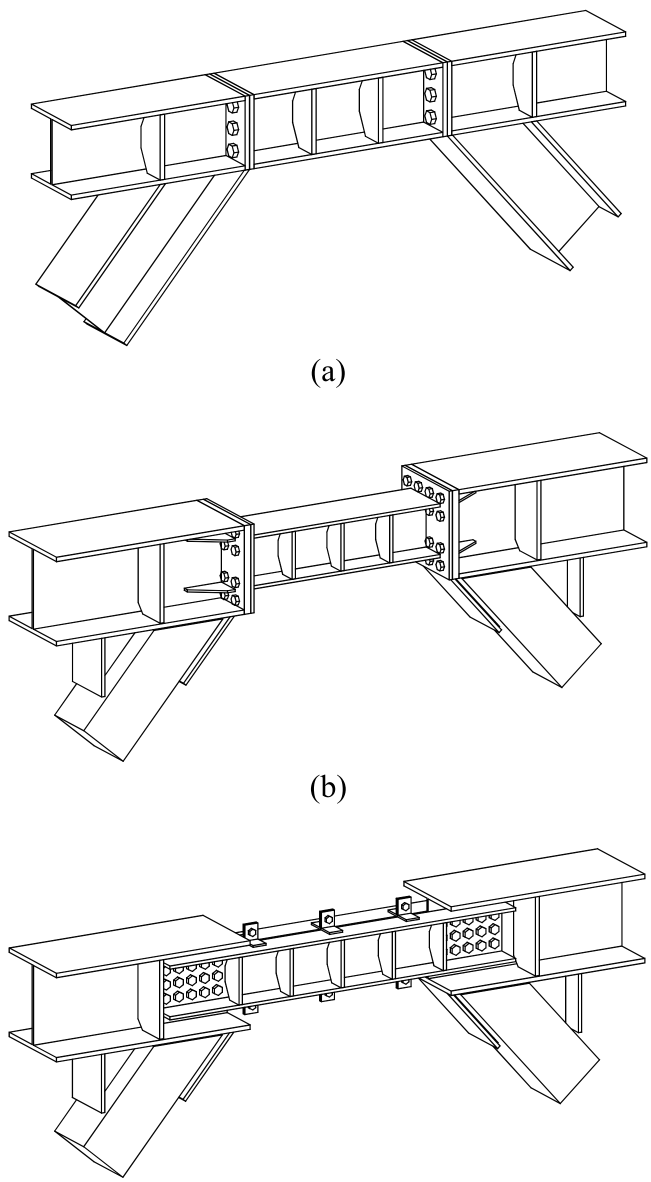

(a)

(b)

(c)

Figure 1.5 Replaceable link details

The web connected channel section replaceable link utilizes either channel sections or saw cut I-sections that are placed back-to-back and connected to beams outside the link through high-strength bolts. This link type may require cover plates to be welded to the flanges to increase the bending resistance and develop shear yielding links. In addition, the channel sections must be connected to each other to prevent lateral torsional buckling of these members. The bolts used to connect the channel links are subjected to eccentric shear and the design of these connections has a paramount importance in the performance of the link. Web connection reinforcement plates can be added in order to increase the bearing strength at bolt holes. The experimental results (Mansour (2010), Mansour et al. (2011)) indicated that this type of replaceable link provides a pinched behavior and the amount of pinching is influenced by the level of additional deformations that take place at the connections. These links on the other hand sustain larger inelastic rotations due the flexibility of their connections. Replacement of web bolted channel replaceable links was studied at a residual frame drift of 0.5 percent. All the bolt holes except the central one was post drilled to match the geometric configuration of the beam outside of the link holes that corresponded to the frame's residual drift. An acceptable performance was demonstrated for the replaced link. Design rules for replaceable links, which primarily developed based on these experimental findings (Mansour (2010), Mansour et al. (2011)), are presented in the Canadian Specification S16-14 (CAN/CSA S16-14).

### 1.4. Objectives and Scope

BRBFs and EBFs are more preferred systems among lateral load resisting systems in terms of repairment and retrofit of the steel structures damaged during an earthquake. In order to exhibit replaceability of the BRBs of BRBF systems and links of EBF systems, two experimental research programs were undertaken separately. First experimental research program was related to BRBs whereas second experimental research program was concerned with EBFs.

The aim of the first study was to examine potential use of steel encased BRBs which utilize constant width core plates and welded overlap core plates under subassemblage testing. In addition, two typical connection details, namely the pin connection and gusseted connection, were tested by taking into account the collar detail as the prime variable.

In the second experimental research program replaceable links for steel eccentrically braced frames were studied by making use of a nearly full-scale test setup. While the replaceable links with direct brace attachments were investigated in the first phase of this experimental program, replaceable links with gusset plated brace attachments were examined in the second phase. The aim of this research program was to come up with new replaceable links providing many advantages in terms of replaceability compared with the other replaceable links investigated to date for eccentrically braced frames.

### 1.5. Organization of Thesis

This thesis consists of three chapters which follow the chapter on Introduction. The brief contents on these chapters can be summarized as follows:

In Chapter 2, the details of a three-phase experimental research study on steel encased buckling restrained braces are given. The first phase of this research program focused on the use of constant width core plates while the second phase concentrated on the development of welded overlap core plates. Connection detailing for steel encased BRBs was studied in the third phase.

In Chapter 3, the details of a two-phase experimental research program on developing replaceable links for eccentrically braced frames are given. The first phase of this study concentrated on EBFs with direct brace attachments while the second phase focused on braces with gusset plates.

Finally, Chapter 4 summarizes the outcomes of all studies performed during the course of these two experimental research programs.

# CHAPTER 2

# STEEL ENCASED BUCKLING RESTRAINED BRACES

## 2.1. Background

Small scale steel encased BRBs that utilize a constant width steel core segment were studied by Eryaşar and Topkaya (2010) through a uniaxial test program. Different designs and attachment details for buckling restraining mechanisms were investigated. The test results revealed that properly detailed steel encased BRBs can sustain 2% axial strain and satisfy the cumulative deformation demands set forth by the Seismic Provisions for Structural Steel Buildings (AISC341-10 (2010)). An experimental study has been undertaken to extend the findings of Eryaşar and Topkaya (2010) to BRBs tested as a part of a subassemblage. Pursuant to this goal a three phase experimental program was developed. In the first phase, longer BRBs with constant cross section core plates were experimented to observe the differences between the BRB behaviors under uniaxial and subassemblage testing. In the second phase, a novel type of core segment named the welded overlap core (Figure 2.1) was proposed and studied through subassemblage testing. Connection detailing for welded overlap core steel encased BRBs was studied in the third phase. The idea behind the development of such a BRB core segment is to eliminate costly CNC cutting procedure and to be able to vary the cross sectional geometry of the core segment along its length. The details of the experimental study are presented herein.

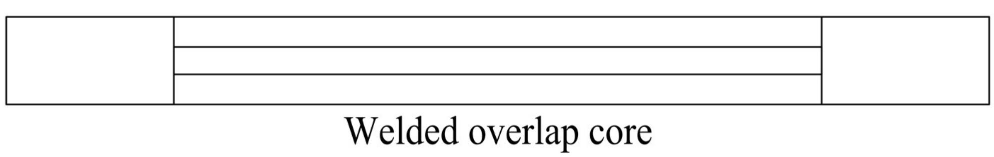


Figure 2.1 Proposed welded overlap core detail

## 2.2. Experimental Program

In the first and second phase of this research program, subassemblage testing was conducted using a setup that was mounted to a reaction wall and a reaction floor as shown in Figure 2.2. A floor beam which consists of two rectangular hollow sections was laid on the reaction floor and two pin supports that were 3000 mm apart from each other were connected to this floor beam. A column was attached to one of the pinned supports at its base. A BRB test specimen was connected to the top of the column and to the other of the pinned supports. The vertical distance between the center of the pin support and the workpoint of the brace to column connection was 2060 mm and resulted in a BRB length of 3639 mm measured from the workpoints. This geometry generated a brace angle of 34.5 degrees measured from the horizontal.

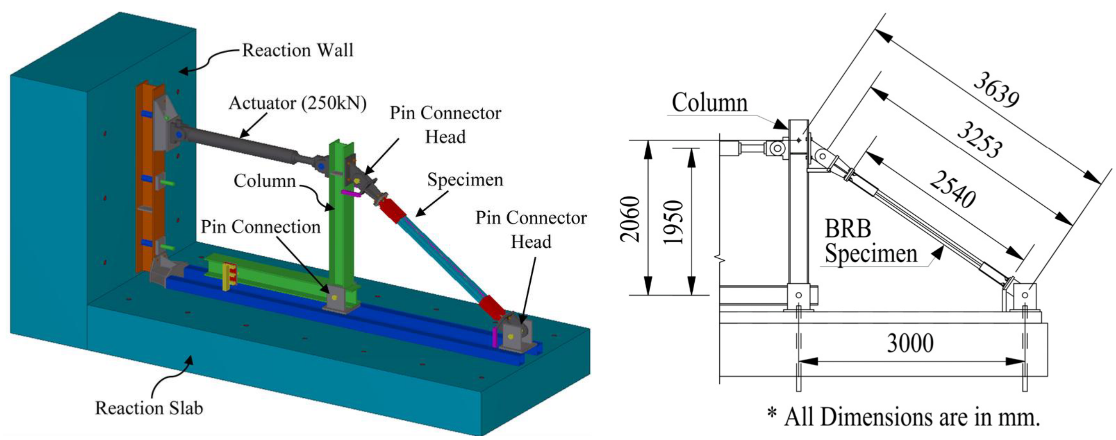


Figure 2.2 Rendering and dimensions of the test setup used for the first and second phase of the research program

Two pinned connector heads were used to fasten a BRB specimen to the column and pinned support as shown in Figures 2.2 and 2.3. Plates were welded to the ends of BRB specimens and 4 high strength bolts were used to fasten these plates to the connector heads. The pinned connections at both ends were used to properly position the specimen and helped to avoid any mismatch of connections due to construction tolerances. Once a BRB is installed in between the two pinned ends, the rotation of the pins were restrained by making use of struts that are made up of rectangular hollow sections. As shown in Figure 2.3 struts were welded on both sides of the connector heads after specimen installation. These struts effectively restrained any rotational motion that would take place in the pins. In essence both end connections simulate rigid connection behavior and the rotational demands that would form in the free end of the column were directly transferred to a BRB specimen.

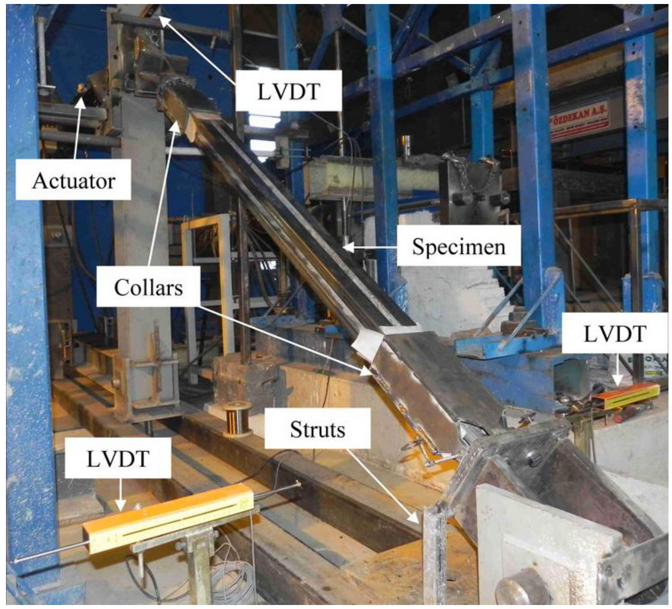


Figure 2.3 Photo of the test setup

Loading was applied by making use of a 250 kN capacity servo-controlled hydraulic actuator as shown in Figure 2.2. Strings placed on two sides of the specimen were used to monitor the axial deformations. One end of the string was fixed to the specimen while the other end was connected to a linear variable differential transformer (LVDT) as shown in Figure 2.3. A special fixture that enables rotation of the string with the global rotation of the specimen was used. The average of the two displacement readings was used to monitor the axial displacement.

In the third phase of this research program, end connections of the original test setup was modified to investigate connection detailing for welded overlap core steel encased BRBs. As shown in Figure 2.4, the test setup was modified twice, the first one to accommodate pin ended BRB specimens and the second one for the rigidly connected BRB specimens. The vertical distance between the center of the pin support and the workpoint of the brace to column connection was 2060 mm and resulted in a BRB length of 3639 mm for pin connected BRB specimens and 3730 mm for rigidly connected BRB specimens. This geometry generated brace angles of 34.5 and 36.5 degrees measured from the horizontal for pin connected and rigidly connected BRB specimens respectively.

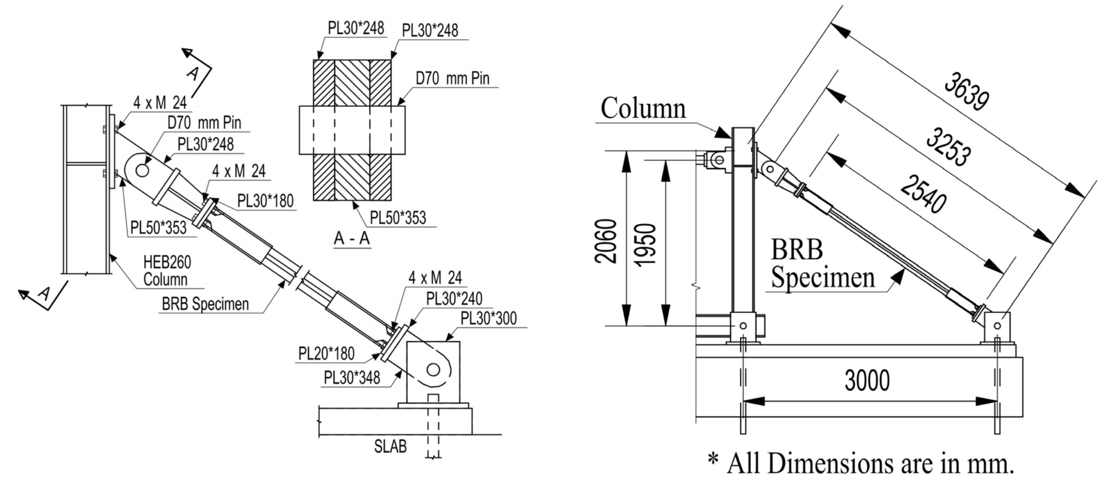


(a) Pin connected BRB

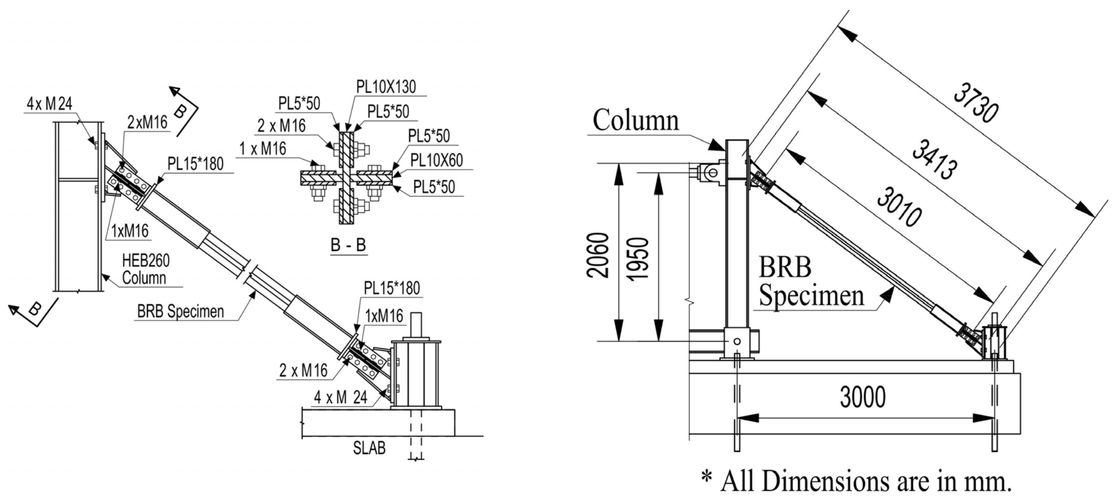


(b) Rigidly connected BRB

Figure 2.4 Connection details and dimensions of the test setup used for the third phase of the research program

The loading protocol recommended by the AISC Seismic Provisions for Structural Steel Buildings (AISC341-10 (2010)) was adopted with minor changes. The AISC protocol requires 2 cycles of loading at the deformation corresponding to $\Delta_{by}$, $0.50\Delta_{bm}$,

$1.00\Delta_{bm}$, $1.50\Delta_{bm}$, and $2.00\Delta_{bm}$ where $\Delta_{by}$ is the value of deformation quantity at first significant yield of test specimen and $\Delta_{bm}$ is value of deformation quantity corresponding to the design story drift. Additional complete cycles of loading corresponding to $1.50\Delta_{bm}$ is required to achieve a cumulative inelastic axial deformation of at least 200 times the yield deformation. This requirement, however, is for an individual buckling restrained braced tested under uniaxial loading and is not required for a subassemblage specimen. The AISC protocol requires predetermining the value of design story drift and the brace deformation which corresponds to the design story drift. A study by Tremblay *et al.* (2006) indicated that the brace deformation that corresponds to design story drift depends on many factors such as the brace angle, ratio of length of the yielding segment to the length of the brace, contribution of other framing members to lateral stiffness and etc. A parametric study conducted by researchers revealed that the strain demand of the yielding segment generally remains within the range 1%-2% unless the brace core is made significantly shorter in which case strain values up to 3%-5% can be expected. In this research the deformation demand that corresponds to the design drift was considered to be equal to 0.01 times the yielding length of the BRB. In other words, the strain demand at the design drift was considered equal to 1%. Accordingly, 2 cycles of deformation corresponding to 1/3 $\Delta_{by}$, 2/3 $\Delta_{by}$, $\Delta_{by}$, $0.50\Delta_{bm}$ (0.5%), $1.00\Delta_{bm}$ (1.0%), $1.50\Delta_{bm}$ (1.5%), $2.00\Delta_{bm}$ (2.0%), $2.50\Delta_{bm}$ (2.5%) were conducted. The difference between the AISC protocol and the applied protocol stems from the early and late cycles. Early cycles at 1/3 $\Delta_{by}$ and 2/3 $\Delta_{by}$ were conducted to observe any manufacturing defects that can cause detrimental effects prior to plastic behavior. The late cycles at 2.5% deformation were conducted to observe the ultimate deformation capacity of BRBs beyond the 2% limit.

### 2.3. Details of Test Specimens

Typical cross sectional details of the specimens are given in Figure 2.5, dimensions and welding details are given in Figures 2.6, 2.7, 2.8, 2.9. In a typical BRB the core plate is sandwiched between built-up steel members which form the buckling restraining mechanism. Two different core plate arrangements were adopted in the experimental program. The specimens used for Phase 1 testing utilized a constant width core plate whereas the specimens used for Phase 2 and Phase 3 testing utilized welded overlap core plates. The specimens used for Phase 1 and Phase 2 testing had a length of 2500 mm whereas the specimens used for Phase 3 testing had a length of 3253 mm and 3010 mm for pin connected and rigidly connected specimens respectively. Cruciform ends were formed by welding 5 mm thick and 25 mm wide plates to both ends of the specimens. The cruciform ends extend for a distance of 200 mm from both ends. Teflon pads having a thickness of 0.5 mm were used between the core plate and the bucking restraining mechanism. These pads were placed on both sides of the core plate. The core segment was tack welded to the buckling restraining mechanism at mid-length to avoid slipping of the encasing (Eryaşar and Topkaya (2010)). Geometrical and material properties of the core plates are given in Table 2.1.

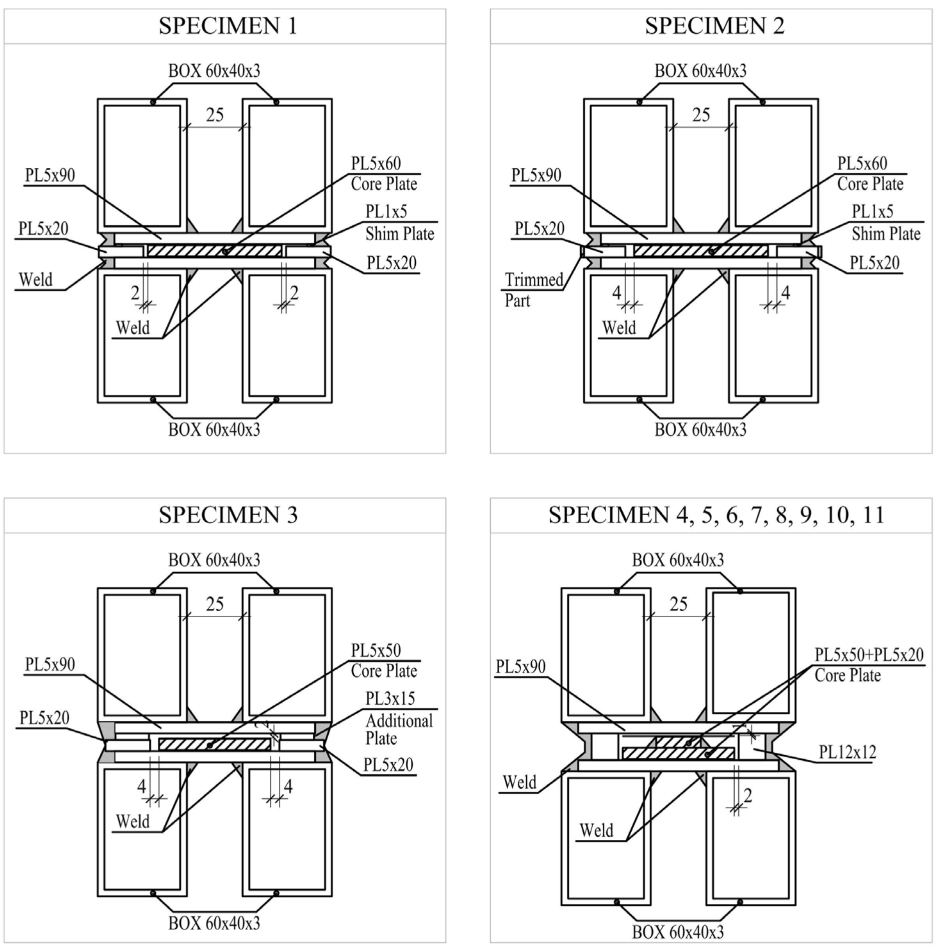


Figure 2.5 Cross-sectional details of BRBs

### 2.3.1. Details of Core Plates – Phase 1 Testing

The core plates of Phase 1 testing were made up of flat bars having a thickness of 5 mm. The width of the core plate was 60 mm for Specimens 1 and 2 and 50 mm for Specimen 3. The total length of the yielding segment was 2100 mm (Figure 2.6 and 2.7). The main difference between the specimens used in Phase 1 testing stems from the differences in gap sizes. When a BRB core is subjected to compressive forces, axial compressive strains produce extensions in two orthogonal directions of the cross section due to the Poisson's effect. In order to allow for this type of a deformation a certain amount of gap has to be provided. The first two specimens adopt a gap detail where a gap is provided through the width of the core plate. As shown in Figure 2.5, the movement of the core plate in through width direction was restrained by making use of filler plates. Gaps of 2 mm were used on both edges for Specimen 1 and the size of the gap is increased to 4 mm for Specimens 2 and 3. For the first two specimens no gap was provided in through thickness direction and the core plate was in direct contact with the teflon pad which was in direct contact with the buckling restraining mechanism. In Specimen 3 a gap size of 2 mm in the through thickness direction was utilized. The aim of providing different gap sizes in these specimens is to study the effect of gap size on the local performance of the core.

### 2.3.2. Details of Core Plates – Phase 2 Testing

The core plates of Phase 2 testing were made from welded overlap flat bars. This detail enables to adjust the lengths of the yielding and nonyielding segments. The weld detailing adopted for these specimens and the cross sectional properties are given in Figure 2.6 and 2.7. The idea behind the development of welded overlap cores is to keep the yielding portion outside the connection area of the BRB. The length of the yielding segment was 1500 mm for all specimens in Phase 2 testing. Overlap core BRB is formed by welding different width flat bars to each other. A base flat bar having a width of 50 mm and a thickness of 5 mm was used for Phase 2 testing.

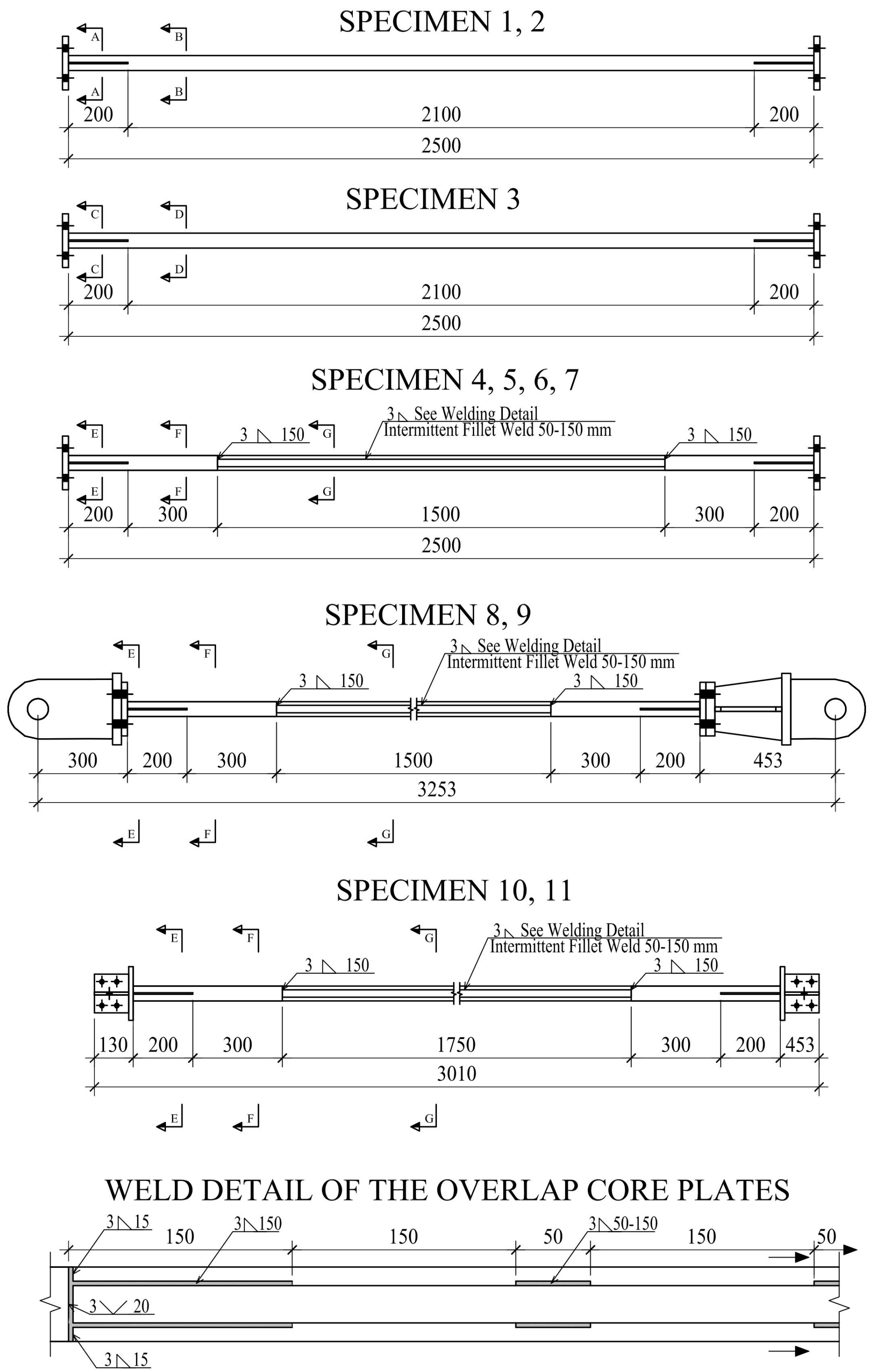


Figure 2.6 Weld detailing of core plates for specimens

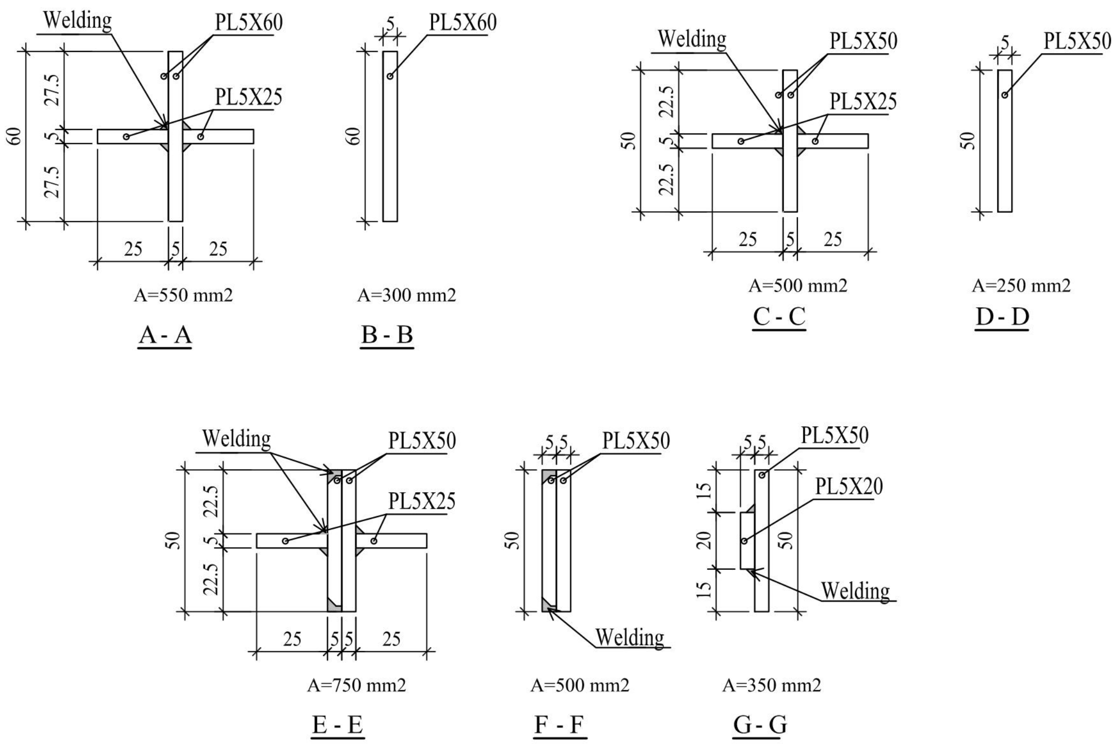


Figure 2.7 Cross-sectional weld detailing for specimens

Overlapping flat bars were fillet welded to the base flat bar. The width of these flat bars was determined to constrain yielding to the center 1500 mm length of BRB. Flat bars having the same width, 5 mm thickness and 500 mm length were welded to the base flat bar from both ends to form non-yielding regions. A flat bar having a width of 20 mm and a thickness of 5 mm was welded to the base flat bar at the center and this formed the yielding segment for each specimen. The width of the flat bar placed at the center was selected to allow for yielding in this segment. It should be noted that after the center portion, which has a reduced cross sectional area, yields the axial resistance of the BRB continues to increase due to strain hardening. The cross sectional area of the nonyielding segment was 1.43 times the cross sectional area of the yielding segment. The reduced width flat bar was welded to the base flat bar using intermittent welding. Fillet welds of 50 mm in length were deposited at 150 mm intervals to connect these two plates together. Electrode welding was adopted due to the welding equipment available in the laboratory. Continuous welding was not utilized because this procedure results in significant distortions of the core segment and can adversely affect the global performance of BRBs. It should be noted that the difference in yield strengths between the connected flat bars is unavoidable unless these are formed by CNC cutting of the same plate. As shown in Figure 2.5 the gap configuration used in Phase 2 testing was the same for all specimens. Essentially a 2 mm gap was provided on both sides in the through width direction. A 1 mm gap was provided in the through thickness direction.

### 2.3.3. Details of Core Plates – Phase 3 Testing

The core plates of Phase 3 testing are identical to those of Phase 2 testing except few changes. The length of the yielding segment was 1500 mm for pin connected specimens and 1750 mm for rigidly connected specimens. Pin connection end details for specimen 8 and 9 were constructed by making use of gusset plates having a thickness of 30 mm and a steel bar having a diameter of 70 mm. The rigid connection details for specimen 10 and 11 were constructed by making use of 8 M16 bolts and gusset plates having a thickness of 5 mm. The idea behind Phase 3 testing is to investigate the need for collar plates of the welded overlap core steel encased BRBs with different connection details.

Table 2.1 Properties of specimens

Properties of specimens

| Spec. no. | Core Plate | | | | | | | Connection | | Encasing | | | | |
|---|---|---|---|---|---|---|---|---|---|---|---|---|---|---|
| | Dim. (mm) | | $F_y$ (MPa) | | $F_u$ (MPa) | | Welded Overlap Core | Type | Collar | Weld Type | Py(kN) | $P_{cr}$(kN) | $\frac{P_{cr}}{P_{ysc}}$ | Cum. Axial Strain |
| | BFB | OFB | BFB | OFB | BFB | OFB | | | | | | | | |
| 1 | 60x5 | - | 272 | - | 383 | - | N | - | Y | INT1 | 81.6 | 670.8 | 8.2 | 159 |
| 2 | 60x5 | - | 272 | - | 383 | - | N | - | Y | INT1 | 81.6 | 670.8 | 8.2 | 408 |
| 3 | 50x5 | - | 334 | - | 412 | - | N | - | Y | INT1 | 83.4 | 670.8 | 8.0 | 210 |
| 4 | 50x5 | 20x5 | 334 | 363 | 412 | 510 | Y | - | Y | INT1 | 119.7 | 670.8 | 5.6 | 301 |
| 5 | 50x5 | 20x5 | 334 | 363 | 412 | 510 | Y | - | Y | INT2 | 119.7 | 670.8 | 5.6 | 195 |
| 6 | 50x5 | 20x5 | 334 | 363 | 412 | 510 | Y | - | Y | CONT | 119.7 | 670.8 | 5.6 | 217 |
| 7 | 50x5 | 20x5 | 310 | 353 | 453 | 451 | Y | - | Y | CONT | 112.8 | 670.8 | 5.9 | 419 |
| 8 | 50x5 | 20x5 | 373 | 373 | 585 | 510 | Y | PIN | Y | CONT | 130.5 | 670.8 | 5.1 | 401 |
| 9 | 50x5 | 20x5 | 373 | 373 | 585 | 510 | Y | PIN | N | CONT | 130.5 | 670.8 | 5.1 | - |
| 10 | 50x5 | 20x5 | 373 | 373 | 585 | 510 | Y | RIGID | Y | CONT | 130.5 | 510.2 | 3.9 | 280 |
| 11 | 50x5 | 20x5 | 373 | 373 | 585 | 510 | Y | RIGID | N | CONT | 130.5 | 510.2 | 3.9 | 280 |

BFB: Base Flat Bar; OFB: Overlapping Flat Bar; $F_y$: Yield Strength; $F_u$: Ultimate Strength; Y:Yes; N:No; CONT: Continuous
INT1: Intermittent (50-150); INT2: Intermittent (100-100); $P_{cr}$:Critical Buckling Load; $P_{ysc}$: Yield Load of Core Braces;
Spec: Specimen; Dim: Dimension; Cum: Cumulative.

### 2.3.4. Buckling Restraining Mechanism

Buckling restraining mechanisms should be designed to avoid global buckling of a BRB. Watanabe et al. (2012) suggested that the steel encasing be designed for sufficient flexural stiffness such that

$$\frac{P_{cr}}{P_{ysc}} \geq 1.5 \tag{2.1}$$

where $P_{cr}$ is the elastic buckling strength of steel encasing and $P_{ysc}$ is the yield strength of the core.

There are also other constrains in the design of buckling restraining mechanism. Large local deformations that form in the BRB core apply significant amount of contact pressures on the buckling restraining mechanism and lead to large deformations in this member. Therefore, local stiffness of the buckling restraining mechanism is also a concern. In addition, large rotational demands are imposed on BRBs when a subassemblage is considered. As will be explained in the following section, a collar system was adopted in the present study to enhance the performance of end details. The buckling restraining mechanisms used in this study are shown in Figure 2.8. In general, two rectangular hollow structural sections with 60 mm height 40 mm width and 3 mm thickness were welded to flat bars having a width of 90 mm and thickness of 5 mm. The selection of these sections was based on market availability. As shown in Figure 2.9, the rectangular hollow sections were connected to the flat bar by making use of intermittent fillet welds with 50 mm length and 150 mm spacing. A gap of 25 mm was retained in between the walls of the rectangular hollow sections. The encasings used on each side of the core segment are similar and the total length of encasing was 2300 mm for specimen 1, 2, 3, 4, 5, 6, 7, 8, 9 and 2550 mm for specimen 10, 11. For all specimens a 150 mm by 15 mm portion at both ends of the encasing members were removed to allow for free shortening and elongation of the core segment. Filler plates with various widths and thicknesses were used depending on the width of the core plate and the gap sizes.

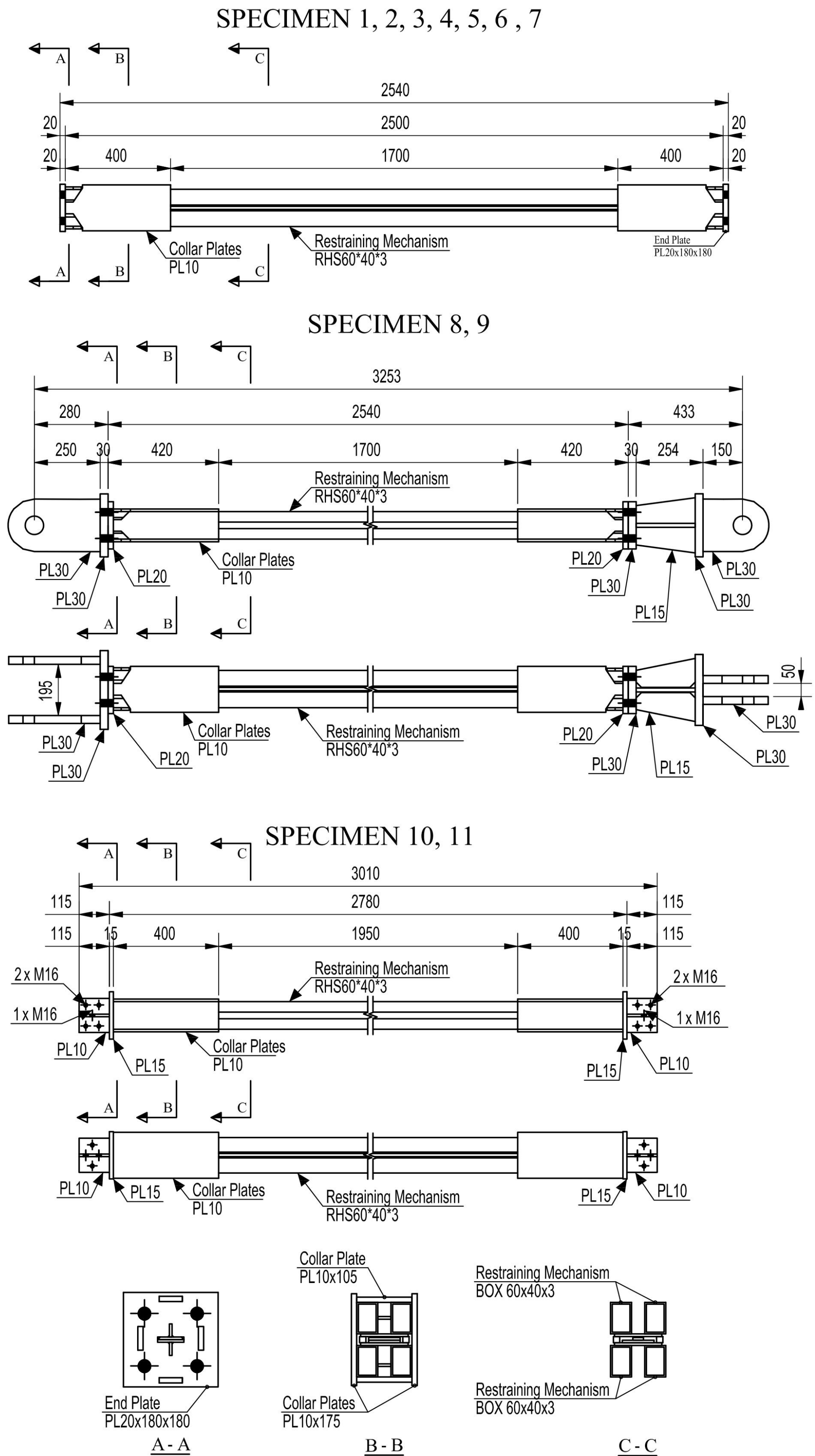


Figure 2.8 Buckling restraining mechanism for specimens

In some cases shim plates were provided to increase the thickness of the filler plates to allow for a specific gap size. The $P_{cr}/P_{ysc}$ ratio of the specimens varied between 3.9 to 8.2 and are reported in Table 1. In calculating these ratios the length between center of pins was used for specimen 1, 2, 3, 4, 5, 6, 7, 8, 9 and the end of the rigid connections was used for specimen 10 and 11.

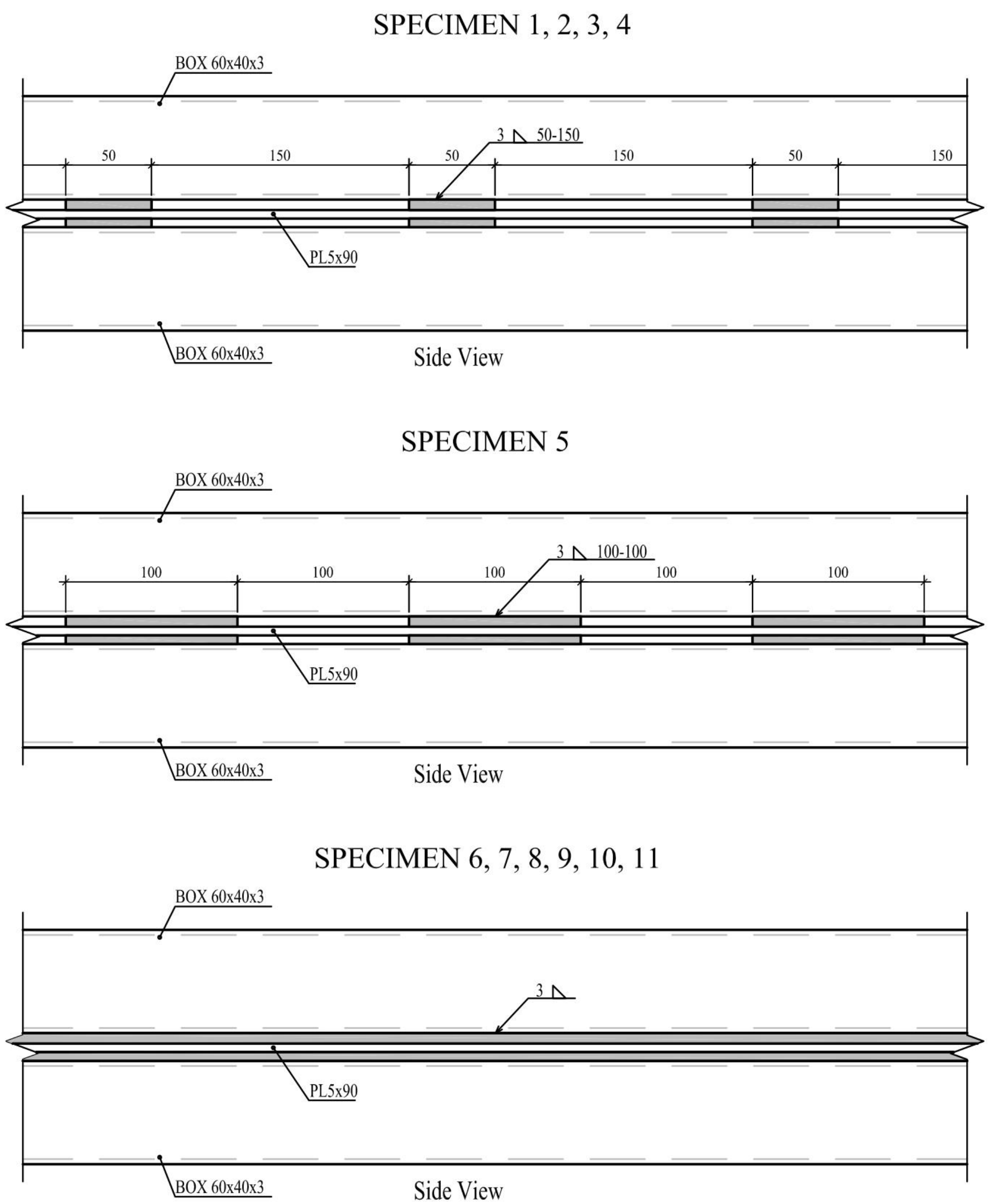


Figure 2.9 Weld detailing for buckling restraining mechanism

The built-up encasings on both sides of the core plate were connected to each other by welding. The weld detailing was considered as a variable in this research program. In Phase 1 testing the encasings were connected by intermittent welding with 50 mm welds spaced at 150 mm intervals as shown in Figure 2.9. Specimen 4 in Phase 2 testing utilized similar weld details. For Specimen 5 the weld length and spacing were modified by depositing 100 mm welds with 100 mm spacing. Specimens 6, 7, 8, 9, 10 and 11 utilized continuous welds to connect the built-up encasings.

### 2.3.5. Collar Detailing

In subassemblage testing large rotational demands are imposed at the BRB ends. These large rotations together with yielding at the BRB ends can result in premature failures. In order to decrease the detrimental effects of end rotations, a collar system was utilized at both ends of the BRBs for all specimens except specimens 9 and 11. The collar system shown in Figure 2.10 consisted of 10 mm thick plates welded to the connection plate used to fasten the specimens to the pinned connections. Teflon pads with 0.5 mm thickness were placed in between the encasing and the collar system in order to minimize frictional forces developing between these members. The collar plates were in direct contact with the teflon pads which were also in direct contact with the encasing.

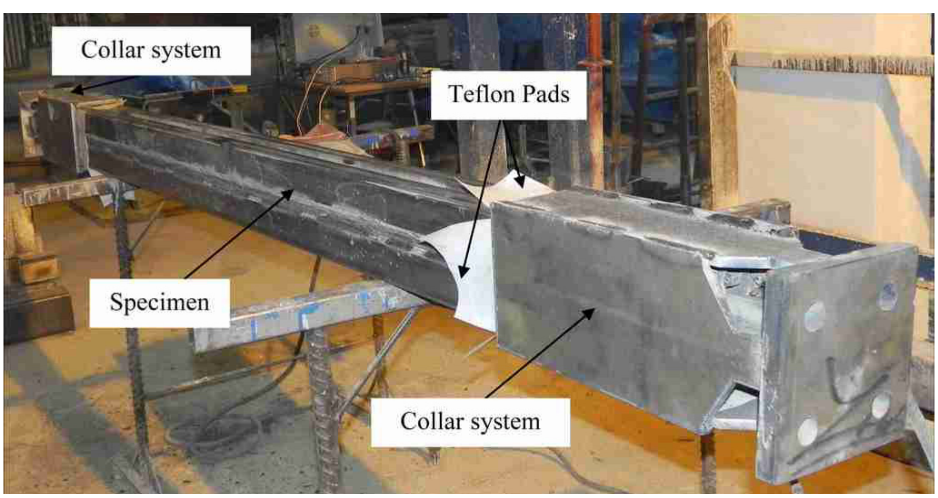


Figure 2.10 Collar system

The collars extended for a length of 400 mm from both ends. The primary function of the collar is to transfer the rotational demands to the encasing as opposed to transferring the demands directly to the core segment. Moreover, in order to further investigate which connection details require collar details, specimen 9 having pin connection and specimen 11 having rigid connection were tested without collar plates.

Table 2.2 Adjustment factors for each cycle

β and ω factors for post yield strain amplitudes

| Specimen no. | 0.50% | | | | 1.00% | | | | 1.50% | | | |
|---|---|---|---|---|---|---|---|---|---|---|---|---|
| | 1st cycle | | 2nd cycle | | 1st cycle | | 2nd cycle | | 1st cycle | | 2nd cycle | |
| | β | ω | β | ω | β | ω | β | ω | β | ω | β | ω |
| 1 | 1.77 | 1.50 | 1.70 | 1.64 | 1.62 | 2.07 | 1.45 | 2.40 | 1.29 | 2.82 | 1.29 | 2.83 |
| 2 | 1.38 | 1.09 | 1.30 | 1.15 | 1.34 | 1.17 | 1.38 | 1.20 | 1.51 | 1.23 | 1.51 | 1.33 |
| 3 | 1.39 | 0.88 | 1.46 | 0.84 | 1.51 | 0.89 | 1.49 | 0.95 | 1.61 | 1.00 | 1.73 | 1.05 |
| 4 | 1.23 | 1.08 | 1.25 | 1.05 | 1.30 | 1.12 | 1.20 | 1.18 | 1.18 | 1.25 | 1.15 | 1.28 |
| 5 | 1.22 | 0.96 | 1.20 | 0.97 | 1.25 | 1.03 | 1.20 | 1.07 | 1.23 | 1.12 | 1.17 | 1.16 |
| 6 | 1.21 | 0.97 | 1.20 | 0.98 | 1.27 | 1.02 | 1.24 | 1.07 | 1.26 | 1.13 | 1.25 | 1.16 |
| 7 | 1.21 | 1.04 | 1.20 | 1.04 | 1.26 | 1.10 | 1.25 | 1.15 | 1.30 | 1.19 | 1.26 | 1.25 |
| 8 | 1.19 | 0.85 | 1.20 | 0.87 | 1.23 | 0.91 | 1.23 | 0.95 | 1.20 | 0.99 | 1.20 | 1.03 |
| 9 | - | - | - | - | - | - | - | - | - | - | - | - |
| 10 | 1.22 | 0.84 | 1.24 | 0.85 | 1.26 | 0.92 | 1.26 | 0.94 | 1.31 | 0.99 | 1.28 | 1.02 |
| 11 | 1.22 | 0.81 | 1.22 | 0.82 | 1.30 | 0.87 | 1.26 | 0.91 | 1.32 | 0.95 | 1.28 | 0.99 |

| Specimen no. | 2.00% | | | | 2.50% | | | | | | 3.00% | | | |
|---|---|---|---|---|---|---|---|---|---|---|---|---|---|---|
| | 1st cycle | | 2nd cycle | | 1st cycle | | 2nd cycle | | 3rd cycle | | 1st cycle | | 2nd cycle | |
| | β | ω | β | ω | β | ω | β | ω | β | ω | β | ω | β | ω |
| 1 | - | - | - | - | - | - | - | - | - | - | - | - | - | - |
| 2 | 1.80 | 1.33 | 1.86 | 1.42 | 2.17 | 1.48 | 2.12 | 1.54 | - | - | - | - | - | - |
| 3 | 1.98 | 1.10 | 2.11 | 1.15 | - | - | - | - | - | - | - | - | - | - |
| 4 | 0.70 | 1.29 | 0.71 | 1.23 | 0.57 | 1.29 | - | - | - | - | - | - | - | - |
| 5 | 1.06 | 1.22 | - | 1.23 | - | - | - | - | - | - | - | - | - | - |
| 6 | 1.30 | 1.20 | 1.30 | 1.23 | - | - | - | - | - | - | - | - | - | - |
| 7 | 1.28 | 1.28 | 1.28 | 1.34 | 1.31 | 1.35 | 1.29 | 1.38 | 1.30 | 1.38 | - | - | - | - |
| 8 | 1.24 | 1.06 | 1.23 | 1.08 | 1.25 | 1.11 | 1.02 | 1.39 | - | - | 1.34 | 1.15 | 1.36 | 1.14 |
| 9 | - | - | - | - | - | - | - | - | - | - | - | - | - | - |
| 10 | 1.31 | 1.06 | 1.27 | 1.09 | 1.16 | 1.11 | 1.17 | 1.30 | - | - | - | - | - | - |
| 11 | 1.31 | 1.04 | 1.28 | 1.05 | 1.13 | 1.07 | 1.05 | 1.21 | - | - | - | - | - | - |

## 2.4.Details of Test Specimens

The AISC Seismic Provisions for Structural Steel Buildings (AISC341-10 (2010)) recommends design of brace connections and adjoining members based on adjusted brace strength. The strength provided by a BRB in compression and tension differs and these resistances are generally obtained from experimental results. The adjusted brace strength ($P_{abs}$) is calculated as follows:

$$P_{abs} = \beta\omega P_{ysc} \quad \text{in compression} \tag{2.2}$$

$$P_{abs} = \omega P_{ysc} \quad \text{in tension} \tag{2.3}$$

where β is the compression strength adjustment factor, ω is the strain hardening adjustment factor.

The compression strength adjustment factor takes into account potential increase in resistance under compression due to Poisson's effect and frictional forces whereas the strain hardening adjustment factor takes into account increase in resistance due to cyclic hardening of the core material. A typical BRB should not only exhibit stable behavior but also provide a reasonable balance between compression and tension resistance. The AISC Specification (AISC341-10 (2010)) mandates that the compression strength adjustment factor be less than 1.3 for acceptable behavior.

Behavior of each specimen is explained in detail in the following sections. The axial strains were calculated using the axial deformations and represent average values along the specimen length. Cumulative axial strains and adjustment factors are reported in Table 2.1 and Table 2.2 respectively. The encasings were removed after testing to observe damage patterns of the core plate. The width of the core plate was measured at 15 locations shown in Figure 2.11 to observe the uniformity of strains in the transverse direction. These changes are reported in Table 2.3. Normalized axial load versus axial strain response obtained for the specimens are given in Figures 2.12 through 2.22.

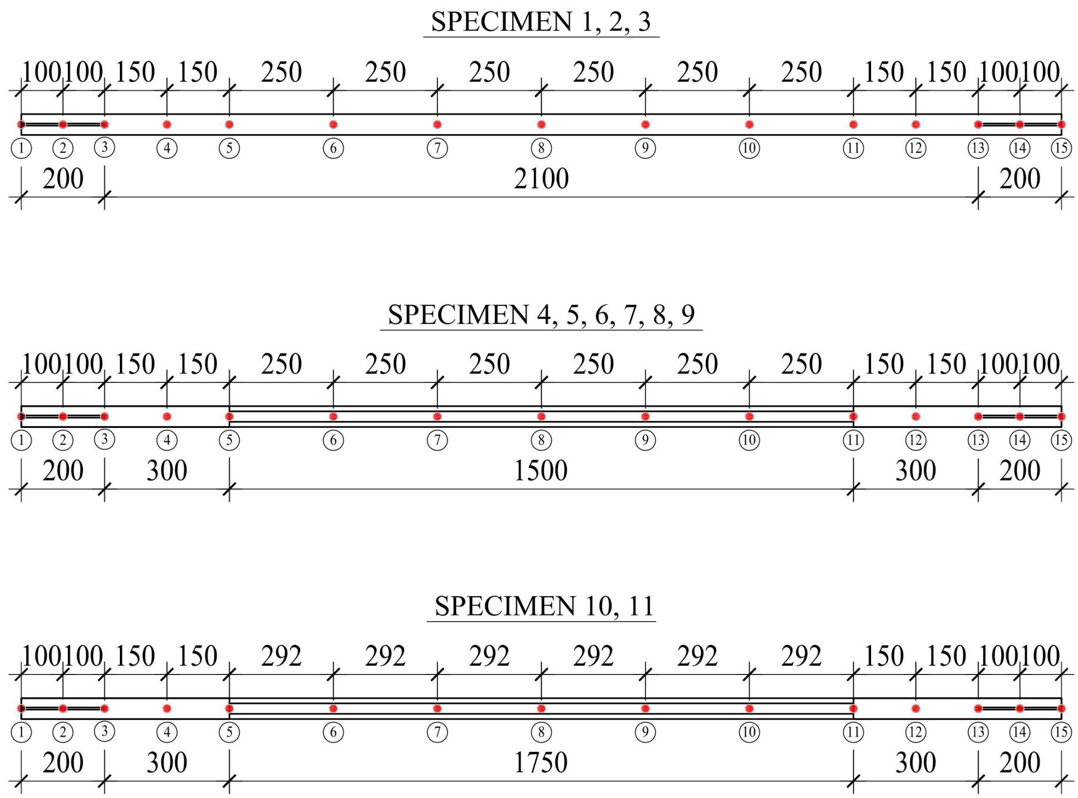


Figure 2.11 Measurement points along the length for change in width of the core segment

Table 2.3 Change in width of the core segment

| | Percentage strain values for width of specimens | | | | | | | | | | |
|---|---|---|---|---|---|---|---|---|---|---|---|
| | Sp.1 | Sp.2 | Sp.3 | Sp.4 | Sp.5 | Sp.6 | Sp.7 | Sp.8 | Sp.9 | Sp.10 | Sp.11 |
| Point number | b(%) | b(%) | b(%) | b(%) | b(%) | b(%) | b(%) | b(%) | b(%) | b(%) | b(%) |
| 1 | -0.67 | -1.50 | 0.60 | 0.00 | 0.20 | 1.60 | 0.20 | 1.00 | -0.16 | 0.40 | -0.84 |
| 2 | -0.67 | -1.83 | -19.80 | 0.00 | 0.00 | 1.40 | 0.40 | 1.10 | 0.00 | 0.66 | 1.02 |
| 3 | -8.83 | -10.50 | -9.60 | 0.00 | 0.00 | 0.40 | 0.20 | 0.60 | -0.10 | 0.06 | 0.68 |
| 4 | 6.17 | -7.17 | -1.60 | 0.00 | -0.40 | 0.80 | 0.00 | -0.36 | -0.72 | 0.06 | 0.74 |
| 5 | 9.83 | -3.17 | 0.00 | 0.00 | 0.40 | 0.40 | 0.20 | -0.06 | -0.12 | 0.94 | 0.90 |
| 6 | 4.00 | 1.50 | 2.20 | 0.80 | 0.80 | 1.40 | 0.20 | 1.80 | -0.36 | 1.88 | 1.18 |
| 7 | 1.50 | 2.17 | 2.20 | 1.40 | 0.60 | 0.40 | 3.00 | 1.74 | 0.36 | 2.62 | 1.72 |
| 8 | -0.67 | 2.50 | 3.00 | 1.40 | 0.60 | 1.20 | 1.20 | 1.74 | -1.06 | 2.90 | 1.60 |
| 9 | -1.67 | 4.17 | 0.60 | 1.00 | 1.40 | 1.40 | 0.00 | 1.66 | 0.46 | 2.60 | 1.64 |
| 10 | -2.00 | 3.83 | -0.60 | 0.60 | 1.20 | 0.20 | -1.20 | 0.90 | -0.12 | 0.68 | 1.06 |
| 11 | -3.50 | -1.00 | -1.20 | 0.00 | 1.00 | 0.40 | 0.20 | 1.04 | 0.56 | 0.38 | 0.80 |
| 12 | -4.00 | -5.50 | -2.00 | 0.00 | -0.80 | 0.80 | -0.40 | 0.06 | -1.44 | 0.22 | 0.60 |
| 13 | -12.33 | -8.83 | -9.60 | 0.00 | -0.40 | 0.60 | -0.20 | 0.60 | -1.24 | 0.66 | 1.60 |
| 14 | -3.17 | 1.33 | 0.20 | 0.00 | 0.00 | 0.40 | 0.00 | 0.26 | 1.10 | 0.74 | 0.42 |
| 15 | -4.00 | 1.00 | -0.20 | -0.20 | 0.20 | 0.80 | 0.00 | 0.88 | -0.60 | 0.70 | 0.44 |

Sp: Specimen; b: Width, "-" means expansion through width direction

### 2.4.1. Behavior of Specimen 1

Specimen 1 developed frictional resistance between the core plate and the encasing in early cycles of loading (Figure 2.12). The difference between the tensile and compressive resistances at 0.5% axial strain was more than 70 percent. The specimen showed stable hysteretic behavior at 1% axial strain. At this strain level the compressive force applied to the subassemblage reached to 250 kN which is equal to the capacity of the hydraulic actuator. After this point the specimen was subjected to tensile axial strain of 1.5% and the compressive strain level was kept at 1% in order not to exceed the capacity of hydraulic actuator. First and second tensile cycles at 1.5% strains were successful, however, the specimen failed in compressive loading which followed the last tensile excursion. The specimen exhibited significantly more tensile resistance when compared with its yield resistance indicating presence of large frictional forces developing.

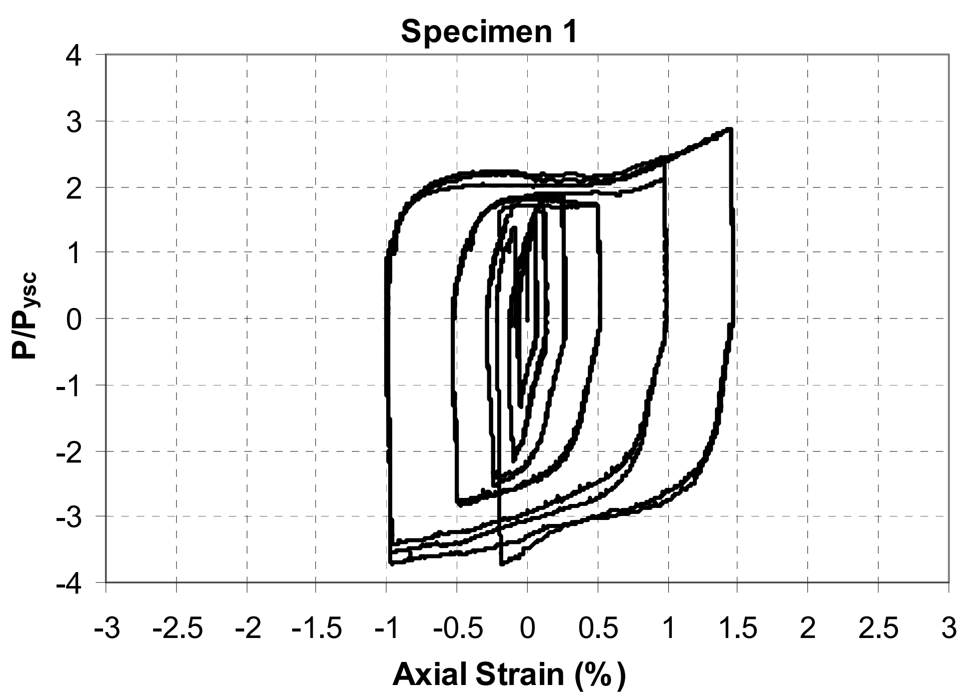


Figure 2.12 Behavior of specimen 1

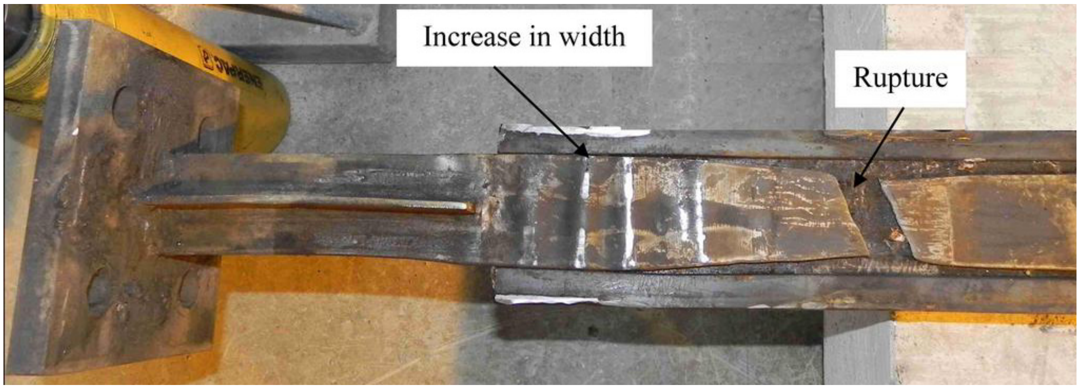


Figure 2.13 Core segment of specimen 1 after testing

Large local deformations and buckles formed at the yielding segment of the core in regions that are close to the cruciform ends as shown in Figure 2.13. These deformations indicate that the axial strains are not uniform along the core segment but concentrate more on the end regions. Deformed pattern of the core segment given in Figure 2.13 indicate that the width of the core segment increased considerably and the core plate came into contact with the filler plates. The contact resulted in force transfer to the encasing member which increased tensile and compressive resistances considerably. The specimen failed through fracture of the core plate at a region close to the ends as shown in Figure 2.13.

### 2.4.2. Behavior of Specimen 2

A larger gap is utilized in Specimen 2 to circumvent the problem associated with Specimen 1. Providing a larger gap in the through width direction resulted in a better performance as shown in Figure 2.14. The friction problem, however, was not completely eliminated. The tensile resistance of the specimen did not increase considerably beyond the yield resistance. The differences between the tensile and compressive resistances were smaller than the differences observed for Specimen 1. Nevertheless, the reported differences are more than 30 percent for the 0.5% axial strain cycle. Transfer of frictional forces between the core and encasing became more pronounced as the axial strains were increased. At the end of the test the reported differences exceeded 100%. The specimen showed stable behavior at 2.5% axial strain.

The final 2.5% compressive cycle was cut short due to increase in applied loading and the specimen was unloaded after 2% axial compressive strain.

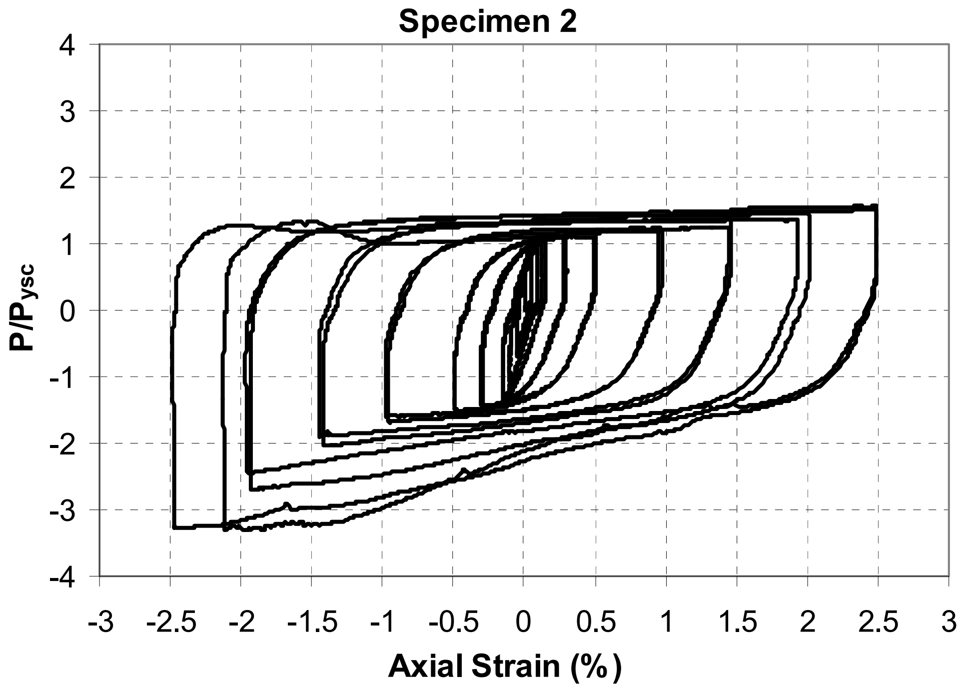


Figure 2.14 Behavior of specimen 2


Figure 2.15 Core segment of specimen 2 after testing

The deformed pattern of the core plate is given in Figure 2.15. This figure suggests that the deformation patterns of Specimen 2 and Specimen 1 are identical. Because of the presence of a larger gap Specimen 2 was more free to expand in the through width direction. This free expansion delayed the force transfer due to contact. As shown in Figure 2.15, the core plate width increased from 60 mm to 66.3 mm and came into contact with the filler plates. Large local deformations and local buckles in Specimen 2 extended for a larger distance when compared with the deformations of Specimen 1.

### 2.4.3. Behavior of Specimen 3

In order to allow for free expansion of the core plate Specimen 3 utilized a 2 mm gap in the through thickness direction in addition to a gap in the through width direction. Specimen 3 showed a poorer behavior when compared with Specimen 2 (Figure 2.16). This specimen showed stable behavior up to 2% axial strain and failed through fracture of the core plate during the tension excursion of 2.5% axial strain.

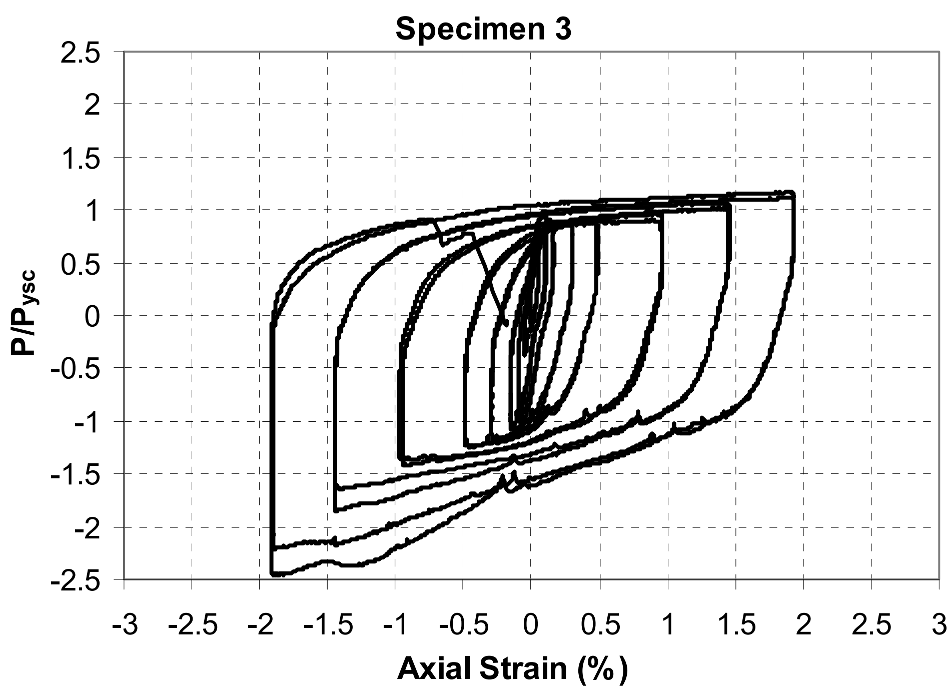


Figure 2.16 Behavior of specimen 3

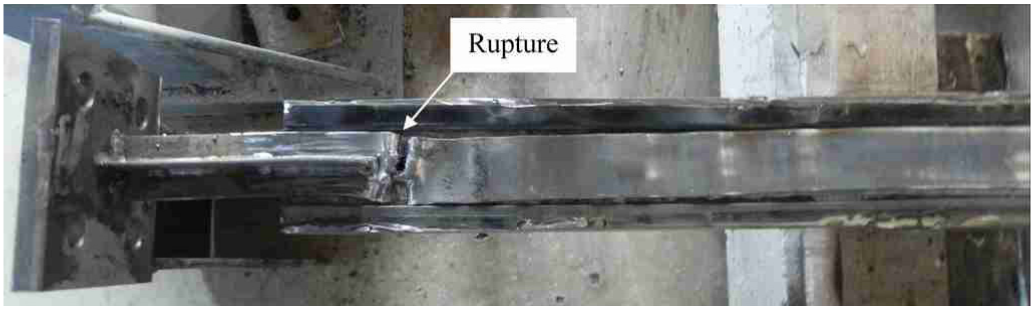


Figure 2.17 Core segment of specimen 3 after testing

Providing a gap in the through thickness direction helped reduce the force transfer between the core plate and the encasing member. The tensile resistance developed by this specimen is lower than the tensile resistance provided by Specimen 2. In any case, the difference between tensile and compressive resistances was more than 30 percent for the early loading cycles and increased to more than 100 percent at the end of the test. As shown in Figure 2.17, fracture of the core plate occurred near the end of the transverse stiffener. Similar to Specimens 1 and 2, large local deformations were observed at the ends of the core plate.

### 2.4.4. Behavior of Specimen 4

Specimen 4 was the first of the overlap core BRBs tested in the experimental program and this specimen showed very stable behavior until the end of the second cycle of 1.5% axial strain (Figure 2.18). The difference between tensile and compressive resistances was kept below 30 percent until the end of cycles at 1.5% axial strain. As shown in Figure 2.19 the encasing deformed excessively during the first cycle at 2% axial strain. This is due to inadequate welding that was deposited to connect the encasings together. Large deformations and buckles formed in the core plate as shown in Figure 2.20 and eventually applied excessive transverse forces to the encasings. These forces resulted in bending of the encasings in the unsupported length between the intermittent welds. Excessive bending resulted in fracture of the welds that connect the encasings.

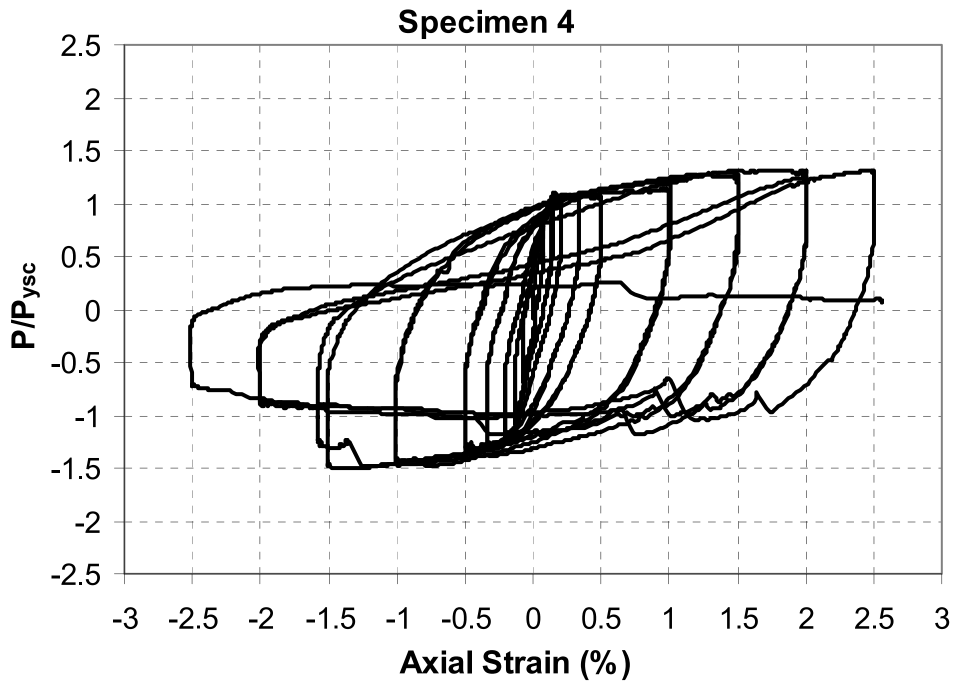


Figure 2.18 Behavior of specimen 4


Figure 2.19 Deformed encasing of specimen 4

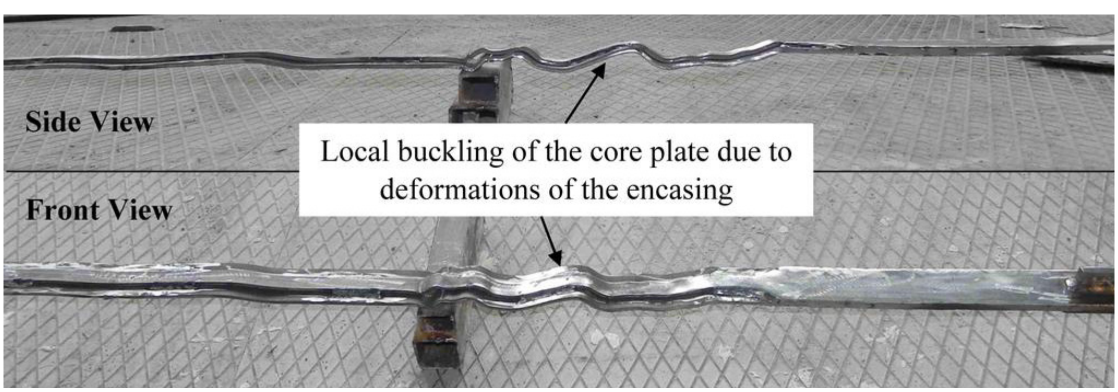


Figure 2.20 core segment of specimen 4 after testing

### 2.4.5. Behavior of Specimen 5

Specimen 5 is identical to Specimen 4 except that longer welds at shorter intervals were used to connect the encasing members. Test results indicated that the behavior of this specimen is very similar to the behavior of Specimen 4 and no significant differences were observed (Figure 2.21). The specimen showed stable behavior during the 1.5% axial strain cycles and excessive bending of the encasings were observed during the 2% axial strain cycles. The differences between tensile and compressive resistances stayed below 30 percent during the loading history. Similar to Specimen 4 large local deformations and buckles formed in the core plates.

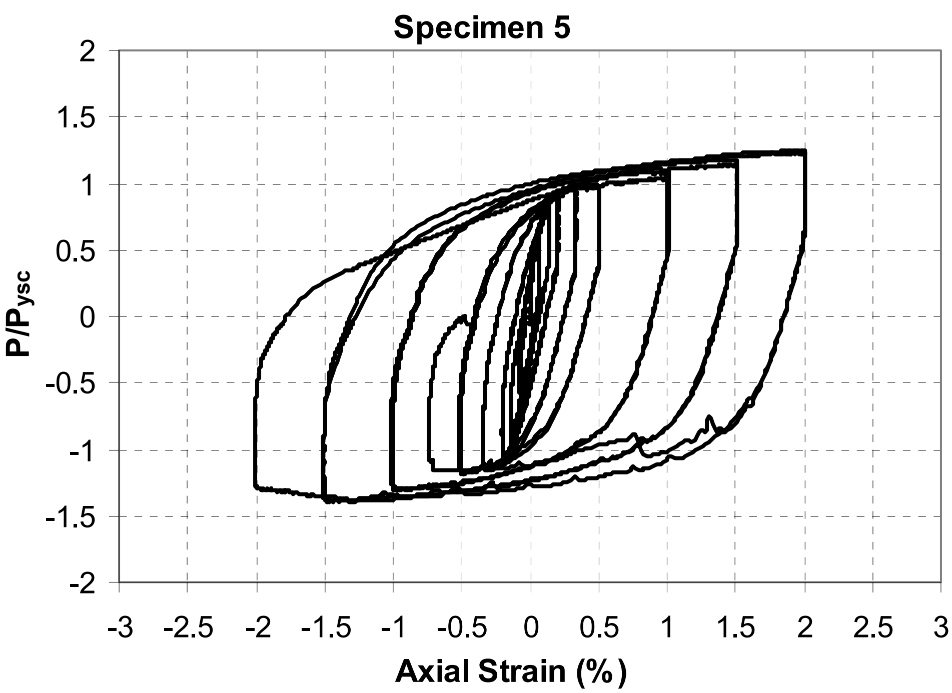


Figure 2.21 Behavior of specimen 5

### 2.4.6. Behavior of Specimen 6

Continuous welds were used to connect the encasing members together in Specimen 6. The specimen showed stable behavior until the end of the second cycle at 2% axial strain (Figure 2.22). Furthermore, the resistances provided in tension and compression did not differ by more than 30 percent throughout the loading history.

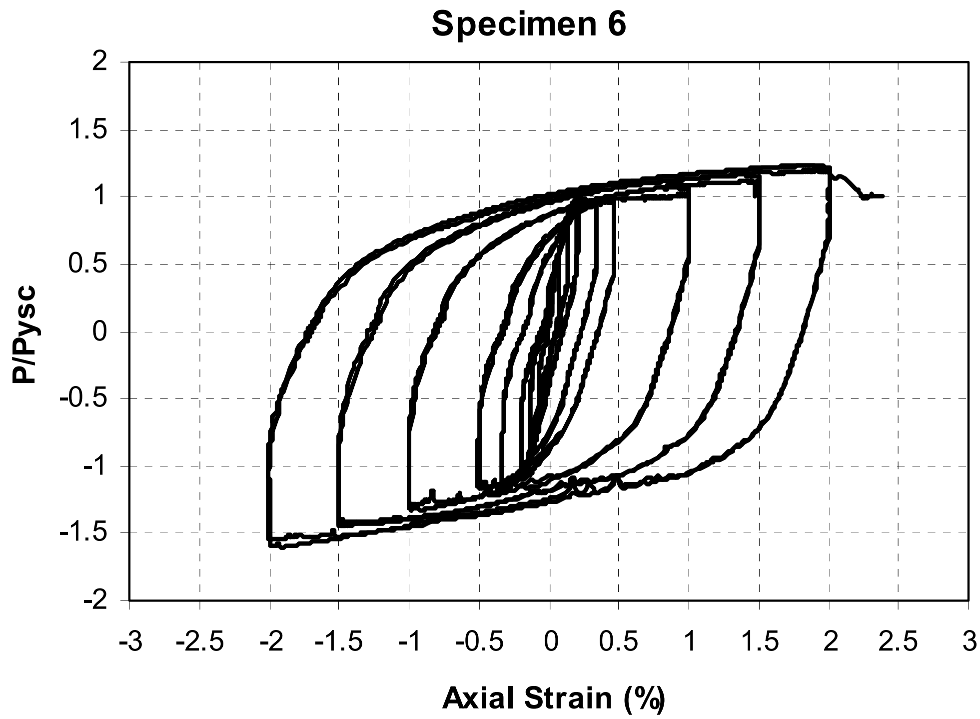


Figure 2.22 Behavior of specimen 6

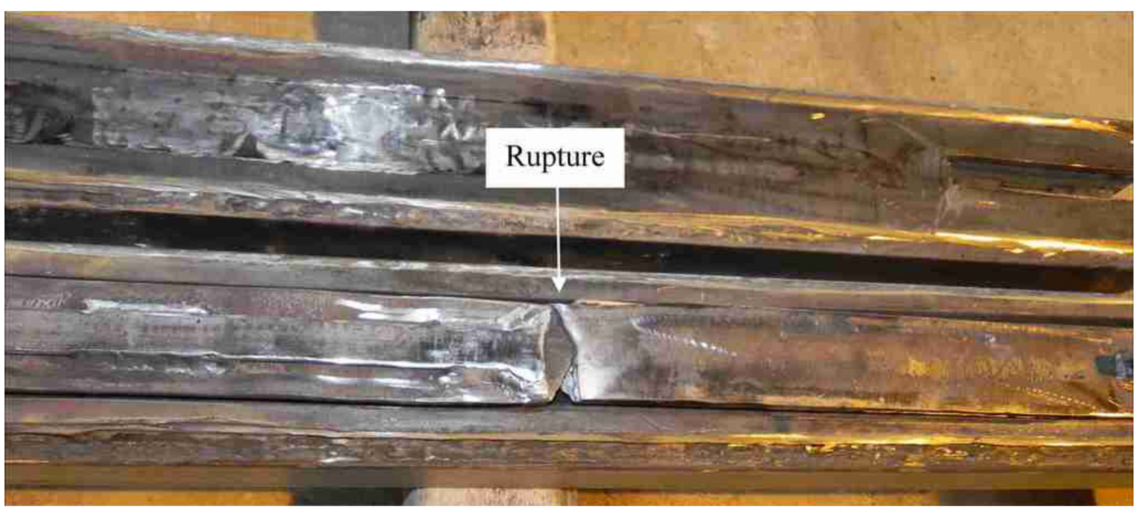


Figure 2.23 Core segment of specimen 6 after testing

The specimen satisfied performance criteria of the AISC Seismic Provisions for Structural Steel Buildings (AISC341-10 (2010)) considering 2% axial strain as the deformation demand corresponding to two times the design story drift. The total plastic deformation was equal to 217 times the yield deformation. The specimen failed during the tensile loading of the first cycle at 2.5% axial strain. The cause of failure was fracture of the welds that connect the overlapped plates at the transition region where a 20 mm wide flat bar is connected to a 50 mm wide flat bar as shown in Figure 2.23. This is the most critical region of the core segment and it is considered that a low quality weld resulted in failure of the specimen at this location.

### 2.4.7. Behavior of Specimen 7

Specimen 7 is similar to Specimen 6 except a few changes. The idea behind testing of this specimen is to improve the weld quality at the region where the width of the overlapping plates change in the core segment. This specimen showed stable behavior at 2.5% axial strain (Figure 2.24). The difference between the resistances in tension and compression stayed mostly below 30 percent except at one cycle where the difference was 31 percent. Additional cycles at 2.5% axial strain were applied after the original loading history was completed. A total of 3 cycles were completed at 2.5% axial strain and the specimen failed in tension during the fourth cycle of loading. The total cumulative plastic deformation was equal to 419 times the yield deformation.

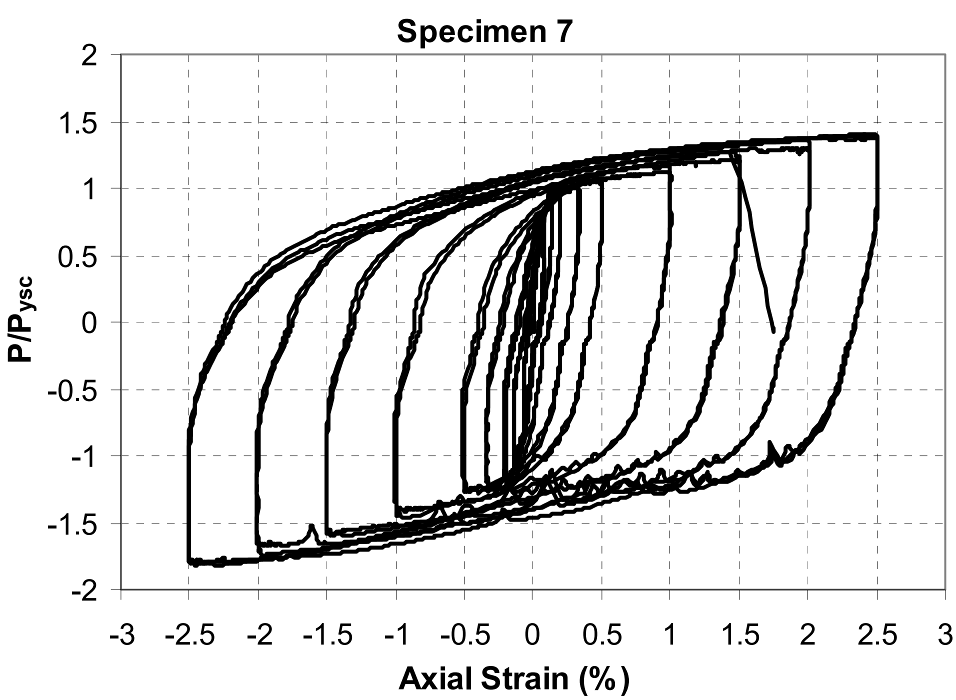


Figure 2.24 Behavior of specimen 7

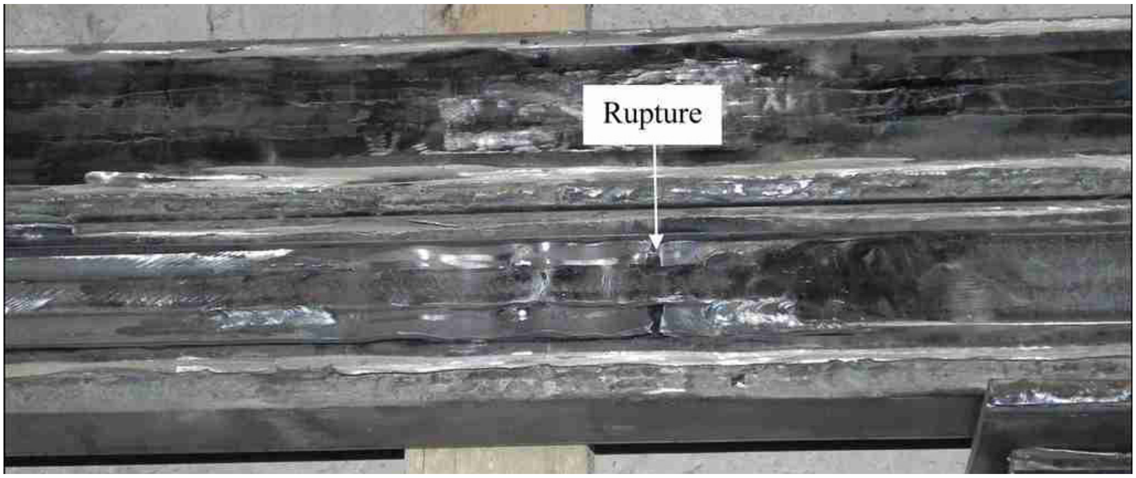


Figure 2.25 Core segment of specimen 7 after testing

The specimen failed through rupture of the core segment away from the welded region. As shown in Figure 2.25, the base flat bar and overlapping flat bar ruptured at different locations due to intermittent welds deposited to connect these bars.

### 2.4.8. Behavior of Specimen 8

Specimen 8 is identical to Specimen 7 except its connection details. This was the first of the pin connected welded overlap core BRB tested in the experimental program. The idea behind testing of specimen 8 through 11 is to investigate the need for collar systems for BRBFs with different end conditions. This specimen showed stable behavior at 3.0% axial strain (Figure 2.26) and satisfied performance criteria of the AISC Seismic Provisions for Structural Steel Buildings (AISC341-10 (2010)) considering 2% axial strain as the deformation demand corresponding to two times the design story drift. The difference between tensile and compressive resistances was kept below 30 percent until the second cycle at 2.5% axial strain. Additional cycles at 2.5% and 3.0% axial strains were applied after the original loading history was completed. A total of 2 cycles were completed at 3.0% axial strain and the specimen failed in tension during the third cycle of loading (Figure 2.27). The total cumulative plastic deformation was equal to 401 times the yield deformation.

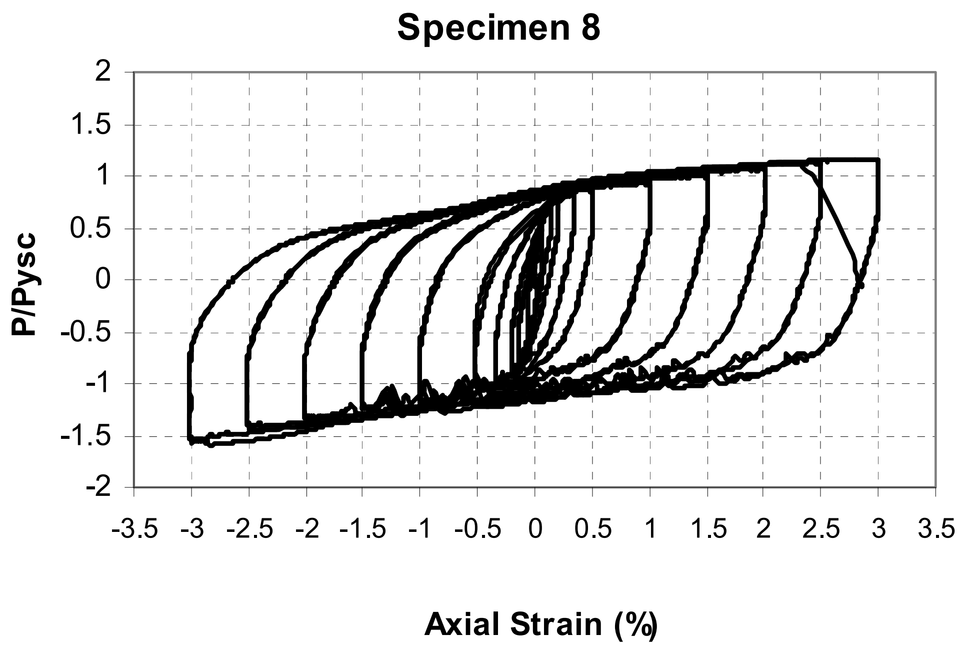


Figure 2.26 Behavior of specimen 8

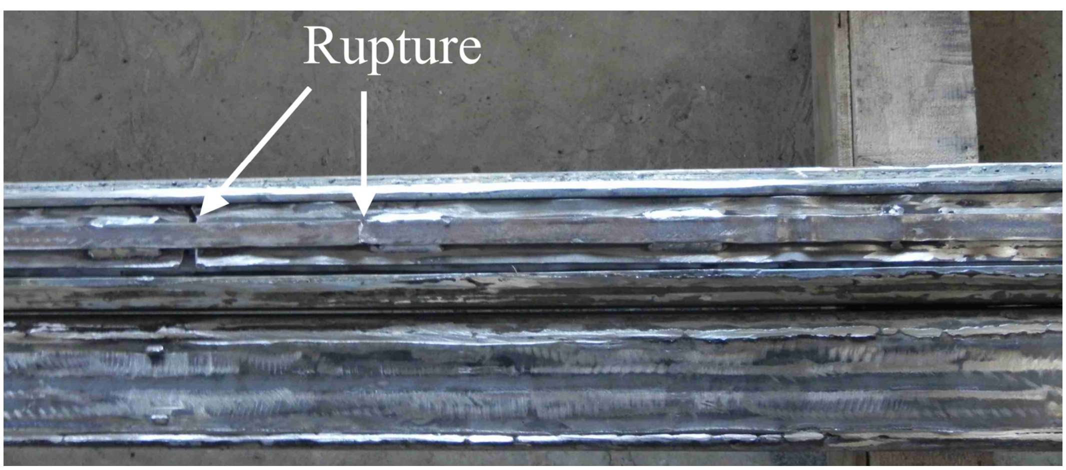


Figure 2.27 Core segment of specimen 8 after testing

### 2.4.9. Behavior of Specimen 9

Specimen 9 is similar to Specimen 8 except that collar plates were not utilized at the end of the specimen to examine response of the pin connected specimen without collar plates under a cycle loading protocol. The specimen showed stable hysteretic behavior until the first yielding initiations on the core plate (Figure 2.28). At this strain level upper end of the specimen experienced flexural bending failure as shown in Figure 2.29 and 2.30. This is attributable to the lack of the collar plates. Significant end rotation of the specimen resulted in a loss of the axial load capacity.

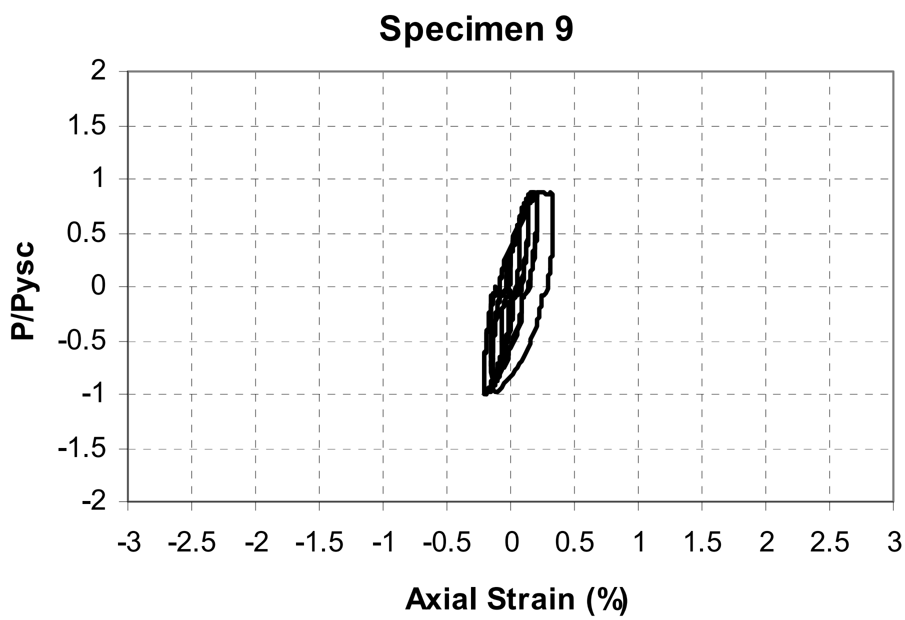


Figure 2.28 Behavior of specimen 9

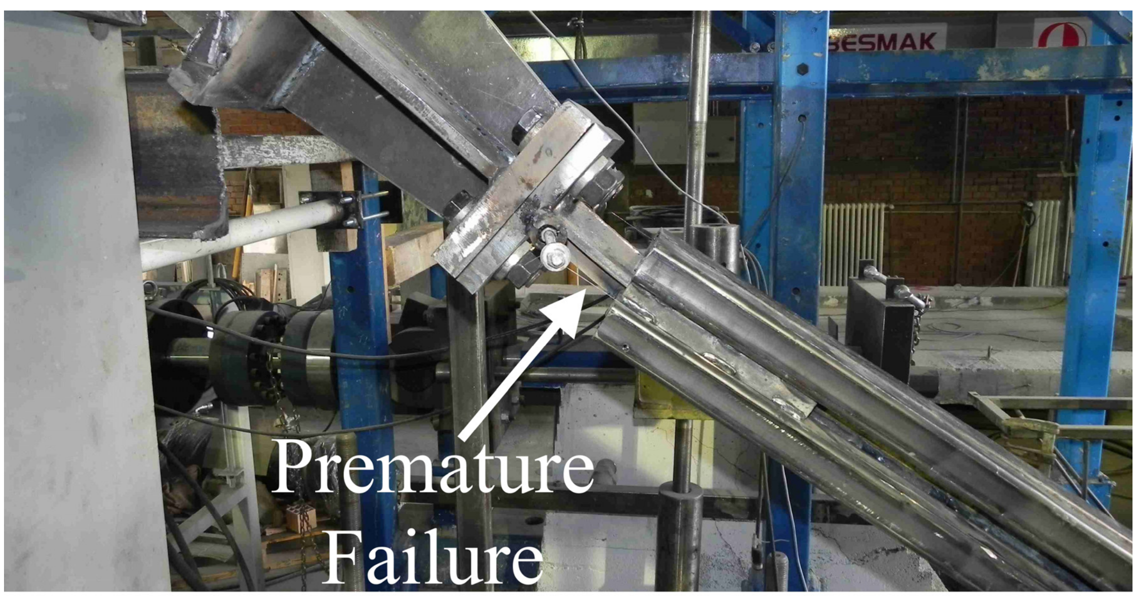


Figure 2.29 Premature failure of specimen 9 after testing

Figure 2.30 Core segment of specimen 9 after testing

### 2.4.10. Behavior of Specimen 10

Specimen 10 was the first of the rigid connected welded overlap core BRBs tested in the experimental program. Yielding length of the core plate increased from 1500 mm to 1750 mm and a collar system was utilized. This specimen showed stable behavior at 2.5% axial strain as shown in Figure 2.31. The difference between the resistances in tension and compression stayed mostly below 30 percent except at two cycles where the difference was 31 percent.

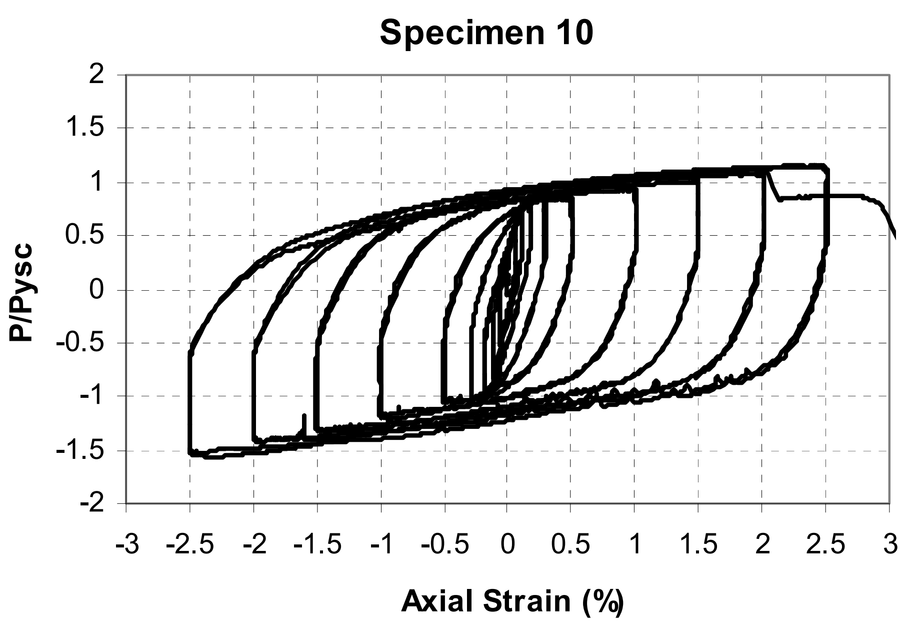

Figure 2.31 Behavior of specimen 10

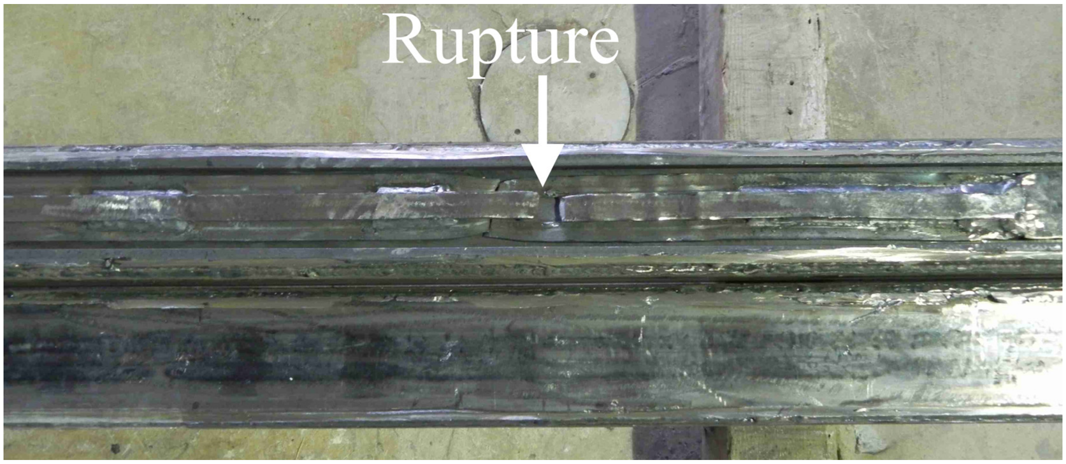

Figure 2.32 Core segment of specimen 10 after testing

Additional cycles at 2.5% axial strain were applied after the original loading history was completed. A total of 2 cycles were completed at 2.5% axial strain and the specimen failed in tension during the third cycle of loading (Figure 2.32). The total cumulative plastic deformation was equal to 280 times the yield deformation.

### 2.4.11. Behavior of Specimen 11

Specimen 11 is identical to Specimen 10 except that collar plates were not used at the end of the specimen to investigate response of the rigidly connected specimen without collar plates. Despite lack of collar plates, the hysteretic behavior of Specimen 11 is similar to Specimen 10 where a collar system was utilized. This specimen showed stable behavior at 2.5% axial strain (Figure 2.33). The difference between the resistances in tension and compression stayed mostly below 30 percent except at two cycles where the difference was 32 percent. Additional cycles at 2.5% axial strain were applied after the original loading history was completed. A total of 2 cycles were completed at 2.5% axial strain and the specimen failed in tension during the third cycle of loading (Figure 2.34). The total cumulative plastic deformation was equal to 280 times the yield deformation. Therefore, the specimen satisfied performance criteria of the AISC Seismic Provisions for Structural Steel Buildings (AISC341-10 (2010)) considering 2% axial strain as the deformation demand corresponding to two times the design story drift. Test result showed that a collar system utilized to decrease the detrimental effects of end rotations is not required for rigidly connected BRBs.

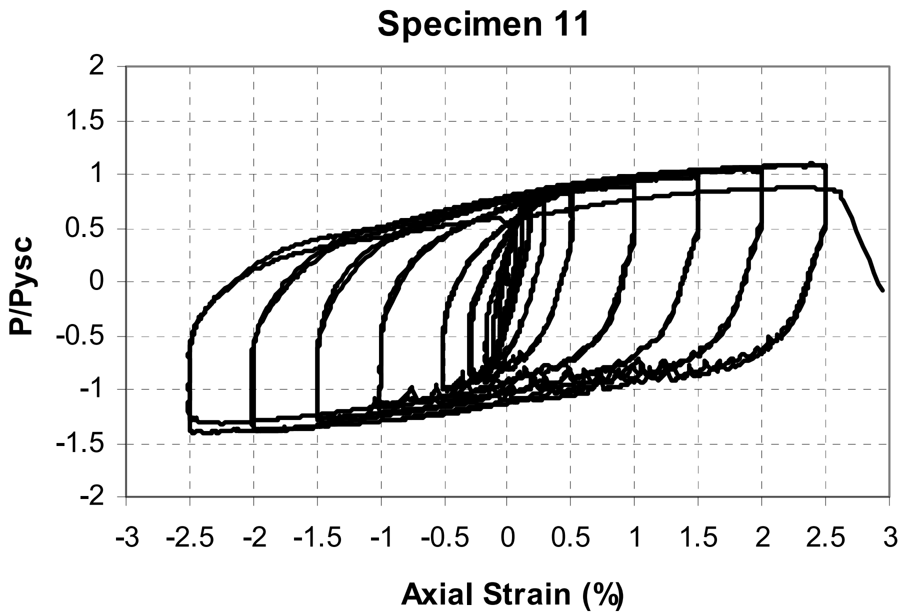


Figure 2.33 Behavior of specimen 11

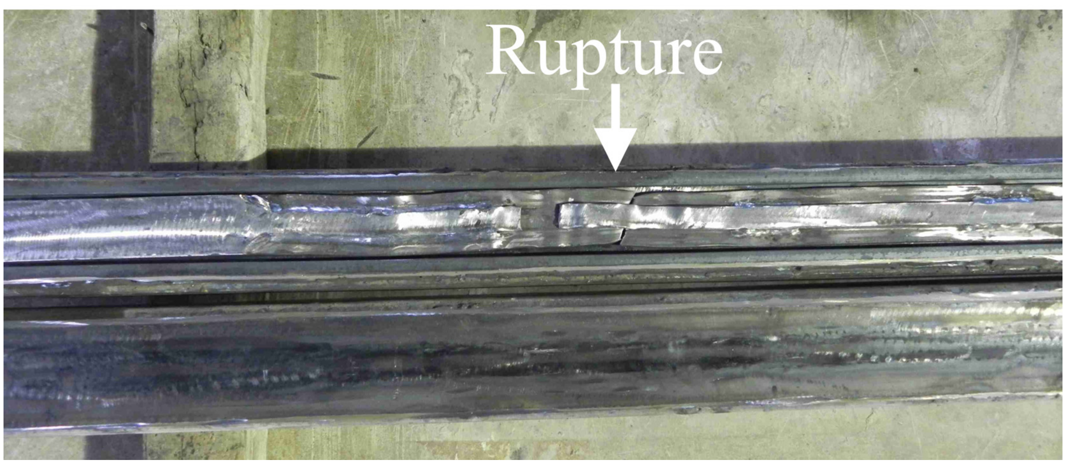


Figure 2.34 Core segment of specimen 11 after testing

## 2.5.Discussion of Results

### 2.5.1. Discussion of Results from Phase 1 Testing

In earlier research works (Eryaşar (2009), Eryaşar and Topkaya (2010)) steel encased BRBs with constant width core plates have shown satisfactory behavior under uniaxial loading of brace-only specimens. A similar type of BRB tested as a part of a subassemblage in this research program has shown poorer behavior when compared with the brace-only specimens. Test results revealed that large local deformations occur at the BRB core plate ends where the deformation demands on the BRB are the highest. Of the three specimens tested in Phase 1 of the research program one specimen was capable of sustaining 2.5% axial strain. All of the specimens, however, developed large differences between tension and compression resistances even at very early stages of loading. The differences between the resistances were generally much larger than the 30 percent limit set forth by the AISC Seismic Provisions for Structural Steel Buildings (AISC341-10 (2010)). It was observed that the core plates deform non-uniformly along the length. The width of the core plates increased excessively and came into contact with the filler plate and resulted in the encasing members to resist axial forces. The maximum change in width within the yielding segment (between points 3 and 13 on Figure 2.8) was 12.33%, 10.50% and 9.60% for Specimens 1, 2 and 3 respectively. The amount of axial strain at points where these maximums were recorded can be found by multiplying the transverse strains with 2.0 by assuming a Poisson's ratio of 0.5 for a yielding material. This conversion suggests that although the overall axial strains are on the order of 2% to 2.5% local strains can vary from 20% to 25%.

Different levels of gap sizes resulted in differences in behavior. In general, increasing the gap size in the through width direction improved the behavior while providing a gap between the encasing and the core in the through thickness direction had a negative impact on the behavior. In an experimental study by Usami *et al.* (2011) researchers examined steel encased BRBs that utilize constant width core plates for the yielding segment with different gaps in the through width direction. Specimens with 2 mm and 6 mm gap showed stable behavior under uniaxial testing and the cumulative inelastic deformations decrease as the gap size is increased from 2 mm to 6 mm. These researchers recommended to keep the gap size between 1 to 2 mm in the through width direction. The results of the present study revealed that increasing the gap size from 2 mm to 4 mm improves the response but the overall performance is still unacceptable. Any recommendations on the gap size should be developed based on subassemblage testing as the results of the uniaxial tests cannot be used directly.

Steel encased BRBs with constant width core plates can be designed to show stable behavior at 2.5% axial strain, however, the differences between tensile and compressive resistances would be at unacceptable levels. In addition, the tensile and compressive resistances differ significantly from the yield resistance due to excessive friction.

### 2.5.2. Discussion of Results from Phase 2 Testing

Welded overlap core BRBs were proposed for the first time in this study and the aim of this type of core is to eliminate the problems associated with constant width core plates. In this system flat bars with different widths are overlapped to create yielding and non-yielding regions in a core segment. Although the welding process is not preferred due to quality concerns, this system eliminates the need for costly CNC cutting of plates to reduce the core segment width.

Four steel encased BRBs with welded overlap cores were tested and the results revealed that properly detailed and manufactured systems can sustain 2.5% axial strain. The differences between tensile and compressive resistances were generally less than the 30 percent limit making these systems acceptable.

Intermittent welding used to connect the encasing members was found to limit the axial strain capacity. The specimens which employed intermittent welds sustained axial strains between 1.5% and 2%. At larger strains bending of the encasings resulted in reduction in load carrying capacity. Continuous welding improved the specimen behavior considerably and resulted in axial strain capacity of 2.5%.

Welding of overlapped flat bars should be exercised with care as low quality of welding may cause premature failure of the core segment. Properly detailed and inspected welded overlap core BRBs can sustain 2.5% axial strain and develop cumulative deformation capacity equal to 419 times the yield deformation.

The axial strains in welded overlap core BRBs were much more uniform along the length when compared with the constant width core BRBs. The gap sizes of 2 mm in the through width direction and 1 mm in the through thickness direction were found to be adequate for acceptable performance.

### 2.5.3. Discussion of Results from Phase 3 Testing

Performance of the welded overlap core BRBs was investigated further by testing four more experiments. Phase 3 testing concentrated on the use of two commonest end details that can be employed in real practice. The need for collars was specifically investigated to understand if these members could be eliminated to come up with systems that are more economical.

Both the pin connected and the rigidly connected specimens showed excellent performance indicating that welded overlap core steel encased BRBs can be designed with both end conditions. The collar system on the other hand is required for pin ended BRBs. One pin ended specimen without collars failed prematurely indicating that pin ended BRBs without collars should not be utilized. For rigidly connected BRBs the systems that utilize collars and the ones without collars provided similar performance.

### 2.5.4. Evaluation of Adjustment Factors

The adjustment factors reported in Table 2.2 were examined in detail and compared with their counterparts obtained using uniaxial testing. The strain hardening adjustment factor, $\omega$, mainly depends on the steel properties and to a certain extent the amount of friction that develops between the core segment and the encasing. The cyclic stress-strain properties of steel differ significantly from the monotonic stress-strain behavior (Cofie and Krawinkler (1985)) because cyclic hardening, cyclic softening, and mean stress relaxation takes place during repeated loading. Cyclic stress-strain curve for a particular steel can be obtained by conducting multi-step tests. In such a test procedure, a steel coupon is cycled at various strain levels beyond the yield strain until a saturation stress is reached. Cofie and Krawinkler (1985) conducted a multi-step test on an A36 specimen and defined the inelastic portion of the cyclic stress-strain curve as follows:

$$\bar{\sigma} = K\left(\bar{\varepsilon}_p\right)^n \tag{2.4}$$

where, $\bar{\sigma}$: normalized stress (note that $\bar{\sigma}$ is equivalent to ω), $\bar{\varepsilon}_p$ : normalized plastic strain, *K*: cyclic stress-strain curve strength coefficient, *n*: cyclic stress strain curve hardening factor.

The *K* and *n* vales obtained from their experiments were 0.9 and 0.19, respectively. A plot of the cyclic stress-strain curve is given in Figure 2.35. The cyclic hardening adjustment factors obtained from the uniaxial testing program of Eryaşar and Topkaya (2010) and the ones from Phase 2 and Phase 3 testing of the current research program are also indicated in the same figure. Data points were grouped according to the yield strength of the core plate. The data points usually fall below the cyclic stress-strain curve reported by Cofie and Krawinkler (1985). This is due to the differences in loading protocols applied to the specimens. These researchers obtained stress-strain curve by conducting multi-step tests where the material is cycled 10 to 20 times at a constant strain amplitude to reach to a saturation stress. In the BRB test programs, only two cycles of loading were applied for each strain amplitude. In fact the strain hardening adjustment factor increases in the second excursion when compared with the first excursion.

In general, the strain hardening adjustment factors obtained from subassemblage testing are greater than the ones obtained from uniaxial testing. These can be attributable to the differences in material properties and to the degree of frictional resistance. The core plate materials used in these test programs are different and the amount of frictional resistance developing in the BRB specimens are likely to be higher in subassemblage testing when compared with uniaxial testing. When the subassemblage tests are considered an enveloping curve depicted by *K*=1 and *n*=0.12 can be used to represent the data.

The compression strength adjustment factors, β, obtained from uniaxial testing and subassemblage testing are compared in Figure 2.36. The β values are mostly influenced by the amount of frictional resistance. Uniaxial testing revealed that attachment details used for encasings have a major influence on this factor. In the uniaxial test program encasings were connected to each other by welding, hand-tight bolting or snug-tight bolting. The β values were the highest for encasings connected by snug-tight bolts and lowest for hand-tight bolts. In order to make a fair comparison the results for welded BRBs are reported in Figure 2.36 for the uniaxial test program. Data shown in Figure 2.36 indicate that compression strength adjustment factors increase as the normalized plastic strain increases in uniaxial testing. For subassemblage testing, however, the reported values are generally higher than the values obtained from uniaxial testing. The β values varied between 1.15 and 1.32 throughout the loading history for all 4 specimens in Phase 2 testing. The results indicate that compression strength adjustment factors obtained from uniaxial testing cannot be directly used to determine the value of this factor for BRBs tested under subassemblage testing.

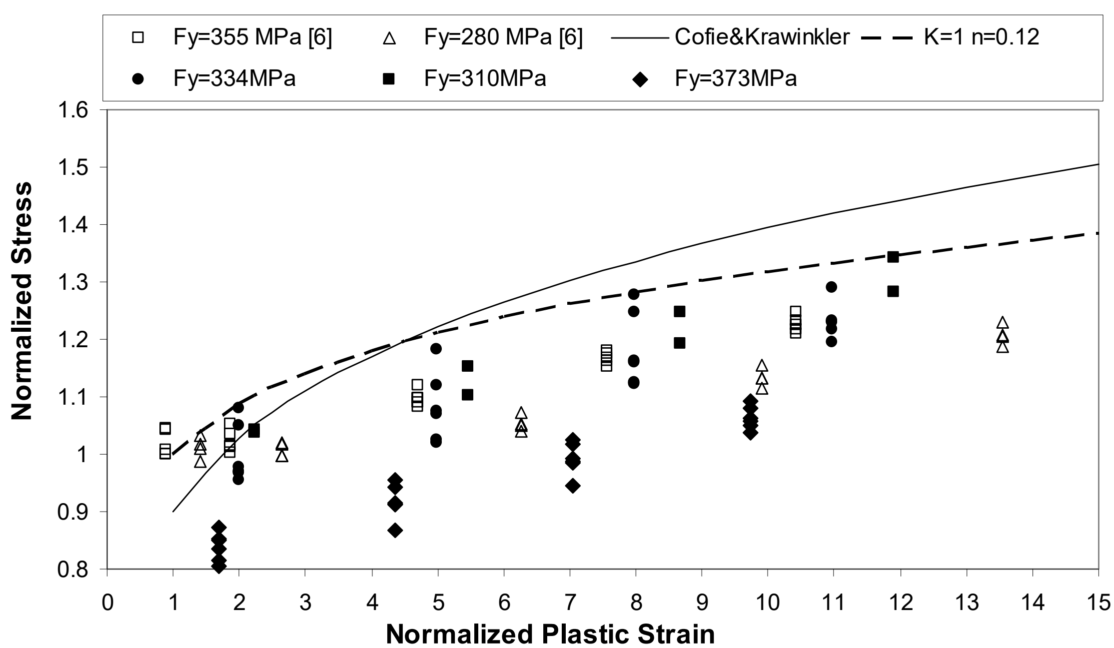

Figure 2.35 Evaluation of strain hardening adjustment factor

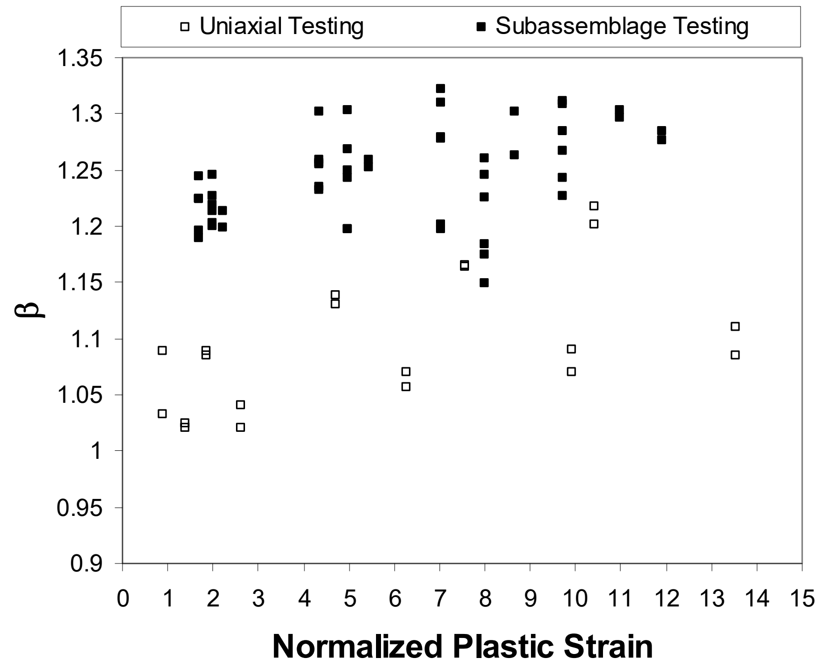


Figure 2.36 Evaluation of compression strength adjustment factor

### 2.6. Design Implications and Future Research Needs

The results of Phase 1 testing revealed that constant width core plates should not be utilized for steel encased BRBs. Although this kind of a core segment produced acceptable results under uniaxial testing, its performance under subassemblage testing prevents its use for practical applications.

Welded overlap core BRBs can be a potential solution for the problems associated with constant width core plates. Yielding of the BRB ends that are subjected to the highest rotational demands should be avoided. The welded overlap core enables to concentrate yielding to the center portion of the core segment thereby allowing the BRB ends to remain essentially elastic. The encasings should be connected by continuous welding to avoid any kind of premature failure. The core plate can be connected to the encasings using tack welding to prevent any kind of slipping of the encasings. In the absence of additional research, the $P_{cr}/P_{ysc}$ ratios should be kept above 3.9 which was the lowest limit experimented as a part of this research program. Care should be exercised in preparing the welded overlap core plates. The region at which two overlapping flat bars with different widths meet is the most critical point of the core segment. The weld deposited to connect these flat bars to the base flat bar should be inspected carefully to avoid any defects. Intermittent welding of the overlapping flat bar to the base flat bar can be used. A gap of 2 mm on both sides on the core plate in through width direction and a gap of 1 mm on one side in the through thickness direction can be employed for acceptable performance.

The test results of Phase 3 testing revealed that collars must be used for welded overlap steel encased BRBs with pin ended connections. On the other hand, rigidly connected BRBs can function properly without the need for collars.

Future research should concentrate on welding details to improve the performance and cost of welded overlap core steel encased BRBs. Continuous welding of the overlapping flat bar should be examined in detail to observe its performance. Similarly intermittent welding of the encasings should be studied by concentrating on weld lengths and spacing that are not investigated in this research program.

The present study is based on a loading protocol recommended by the AISC Seismic Provisions for Structural Steel Buildings (AISC341-10 (2010)). Performance of welded overlap core steel encased BRBs should be studied from a low cycle fatigue point of view. Different loadings that subject the BRB member to constant strains at various amplitudes must be adopted to determine low cycle fatigue life. This will enable direct comparison of these BRBs with their counterparts developed by other researchers (Usami *et al.* (2011)) and identify potential fracture locations.

# CHAPTER 3

# REPLACEABLE LINKS FOR ECCENTRICALLY BRACED FRAMES

## 3.1. Background

In this chapter, the findings of the second experimental research program, which aimed at developing a new replaceable link with direct brace attachments and gusset plated brace attachments, is presented. Pursuant to this goal, an experimental research program has been undertaken at Structural Mechanics Laboratory of Middle East Technical University to develop new replaceable EBF links which can potentially enhance the existing details. The concept of the proposed links is explained first by providing its advantages and potential applications. The experimental program undertaken to study link behavior is explained next. Finally, results of the experiments are given alongside design recommendations.

## 3.2. Proposed Replaceable Link Concept

The proposed replaceable link details require splicing the beams outside the link and the braces as shown in Figure 3.1. Braces can be directly attached to the replaceable link or can be attached by making use of gusset plates. The former detail is studied in the first phase whereas the latter detail is studied in the second phase. The splice connection detail employs standard bolted details where the bolts can be designed as either bearing type or slip-critical type depending on the application. In general, splice plates on both sides are used for the flanges and the web to connect members together. The use of splice plates on both sides helps increase the shear, bearing and frictional resistance of a connection and reduces the connection length. In this proposed replaceable link, the connections are moved away from the link such that the link is not affected by the strength and stiffness of the connections. The link member is continuous in between the spliced ends thereby allowing a similar load deformation behavior to the conventional EBF links. According to widely accepted design specifications, such as the AISC Seismic Provisions for Steel Buildings (AISC341-10 (2010)), lateral bracing should be provided at the link ends. As shown in Figure 3.1, the replaceable link utilizes connection plates that are directly welded to the end stiffeners and bolted to the secondary members that function as lateral braces.

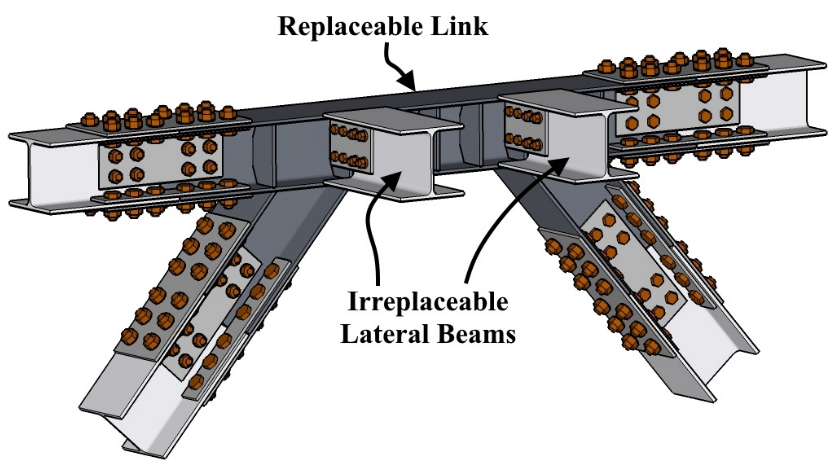


(a) Direct brace attachment

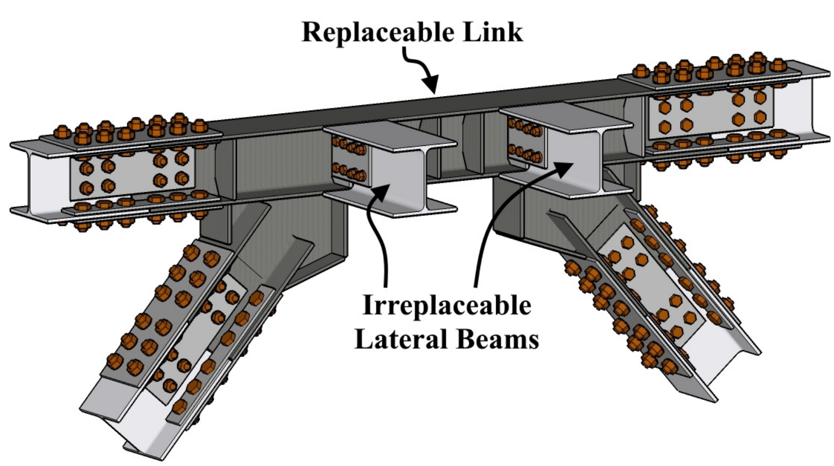


(b) Gusset plate connected brace attachment

Figure 3.1 Proposed replaceable link details

The direct brace attachment detail is similar yet different to a detail applied after the 2010 and 2011 New Zealand earthquakes (Gardiner et al. (2013)) for replacement of active links. Two types of links were utilized for the replacement of active links of a 22 story EBF building (Gardiner et al. (2013)). The first type is similar to the proposed direct brace attachment link except that the connections employed full penetration groove welds. The existing links were removed by cutting out the braces and the beams outside the link and fabricating the new link segment with braces based on a template obtained after removal of the link. The second type of replaceable link applied in the repair process is an extended end-plate replaceable link where the end plates extend beyond the link and the beam outside the link.

The proposed replaceable link concept has several advantages. First of all, the splice details used in this type of a link enable erection tolerance (gap) to be provided at the connections. The gap between the replaceable link and the other members eliminates the need for a manually operated hydraulic jack which can be needed to push the braces or the beams outside the link apart so that the links can be replaced. The use of a bolted detail instead of a welded detail enhances the replaceability of the link member and eliminates the need for flame cutting of links. The proposed replaceable link does not require that the beams outside the link be greater in depth when compared with the depth of the link while allowing to select different I-shapes for these two members.

The proposed replaceable link detail is well suited for both the V and inverted-V brace configurations as shown in Figure 3.2. A concrete deck is not typically utilized for industrial type construction and the proposed link type can be used without any special detailing for deck attachment. Two alternatives given in Figure 3.2 may be adopted for building type structures where a composite deck is present. These two alternatives can be utilized for either the V or inverted-V configurations. In the first alternative the concrete deck acts compositely with the beam outside the link as shown in Figure 3.2a. It is recommended that shear studs be placed in a region bounded by the end of the beam and the end of splice plates. An opening in the concrete deck needs to be provided in the region occupied by the replaceable link to allow easy access to the link.

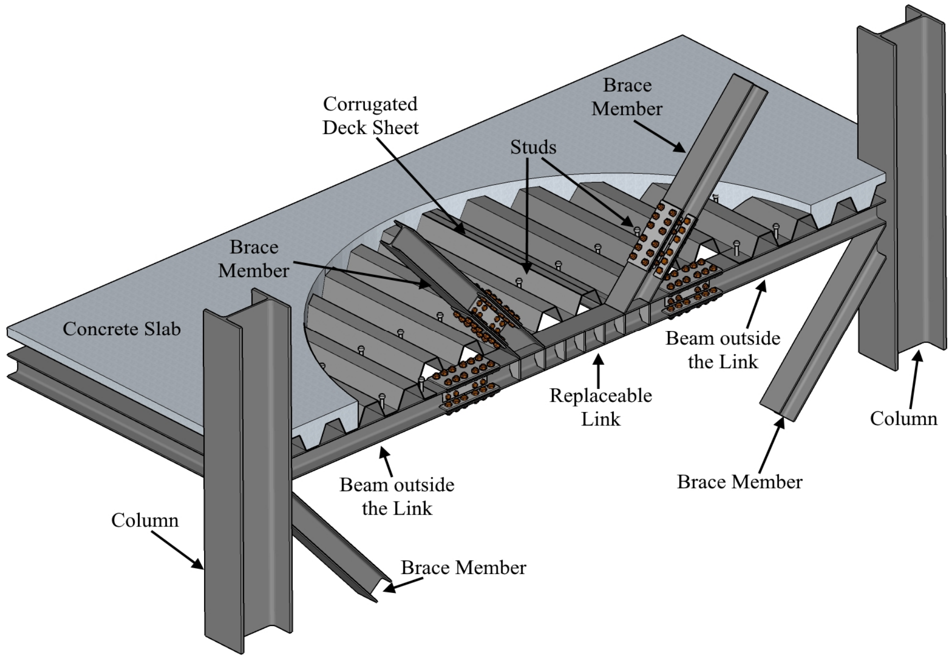


(a) V brace configuration

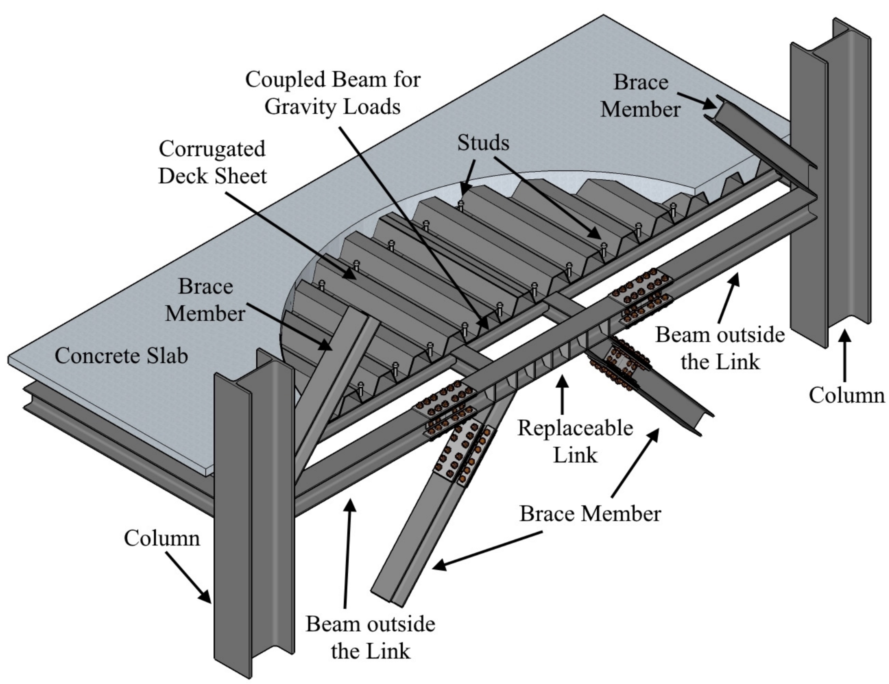


(b) Inverted-V brace configuration

Figure 3.2 Configurations for Proposed Replaceable Link Detail

In customary designs the concrete deck is not connected to the link. The use of welded headed shear studs over the link is not permitted by the AISC Seismic Provisions for Steel Buildings (AISC341-10 (2010)) because the link is considered to be part of the protected zone. In the second alternative the concrete deck is terminated at a distance away from the EBF as shown in Figure 3.2b. Typical to what has been proposed by Perretti (1999) two floor beams are used in each level of the EBFs to avoid interaction between the floor deck and the link. The coupled beam sustains gravity loads while the main beam contains the link and carries the seismic loads. These alternatives were tested as a part of the DUAREM project (Sabau et al. (2014), Ioan et al. (2016)) where the flush end-plate replaceable links were utilized. The specimen had two frames in the loading direction where each one utilized either one of these deck attachment alternatives. The composite deck, however, was continuous over the beam with no attachment to the replaceable link. Experiments revealed that the frame with the second alternative has a better re-centering capability when compared with the first alternative. Furthermore, the non-composite system does not require concrete deck repair which is a major issue that needs to be tackled (Sabau et al. (2014), Ioan et al. (2016), Mansour (2011)). In both alternatives, the opening in the slab can be covered by a combination of cold formed steel sections and plates. It is worth mentioning that the replacement procedure requires temporary shoring of the beams outside the link similar to what was applied after the New Zealand earthquakes for link replacement (Gardiner et al. (2013).

## 3.3.Experimental Program

### 3.3.1. Test Setup and Instrumentation

Typical braced bay widths vary between 6m and 9m and story heights vary between 3.5m and 4.3m for braced frames used in office buildings (Becker and Ishler (1996)). Testing of one-story one-bay EBFs was conducted by making use of a setup indicated in Figures 3.3 and 3.4. The test frame was 5m wide by 3.5m high and represents nearly full scale braced frame dimensions (Figure 3.5). Loading was applied by making use of a 1500kN capacity servo-controlled hydraulic actuator which was attached to a strong wall. EBFs were tested in V configuration which enabled easy replacement without the need for scaffolding to reach to higher levels. In addition, the replaceable link specimen and its connections can be easily monitored due to their proximity to the ground level. Beams and braces were attached to the columns by making use of moment connections. The columns were pin connected to the base beam and the loading beam. The applied load is distributed almost evenly to both columns by making use of the loading beam. The link is subjected to a constant shear force ($V_{link}$) which can be determined from the following expression:

$$V_{link} = F_{actuator} \frac{h}{L} \tag{3.1}$$

where $F_{actuator}$ = the force applied by the actuator, $h$ = the distance between the pin supports at column ends which is equal to 2.7m, $L$ = the frame width measured between the pinned column bases which is equal to 5m.

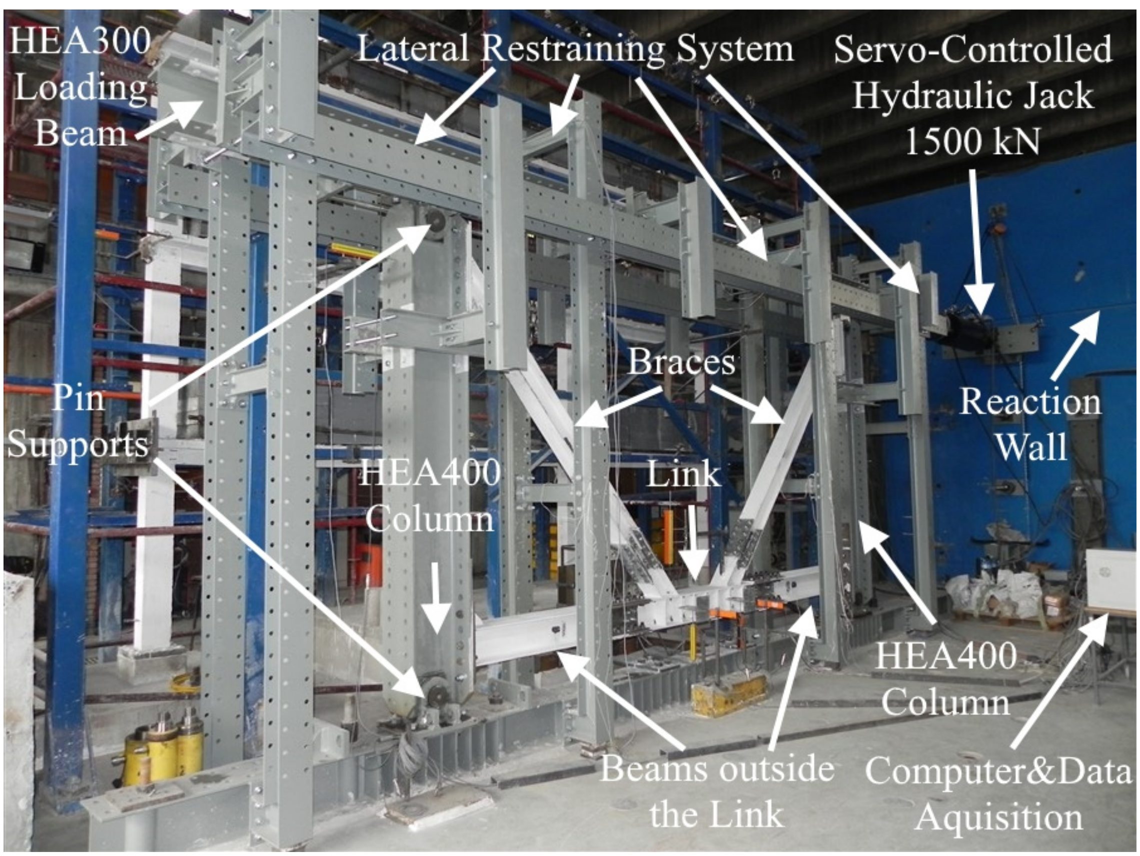


Figure 3.3 Photo of the test setup (general view)

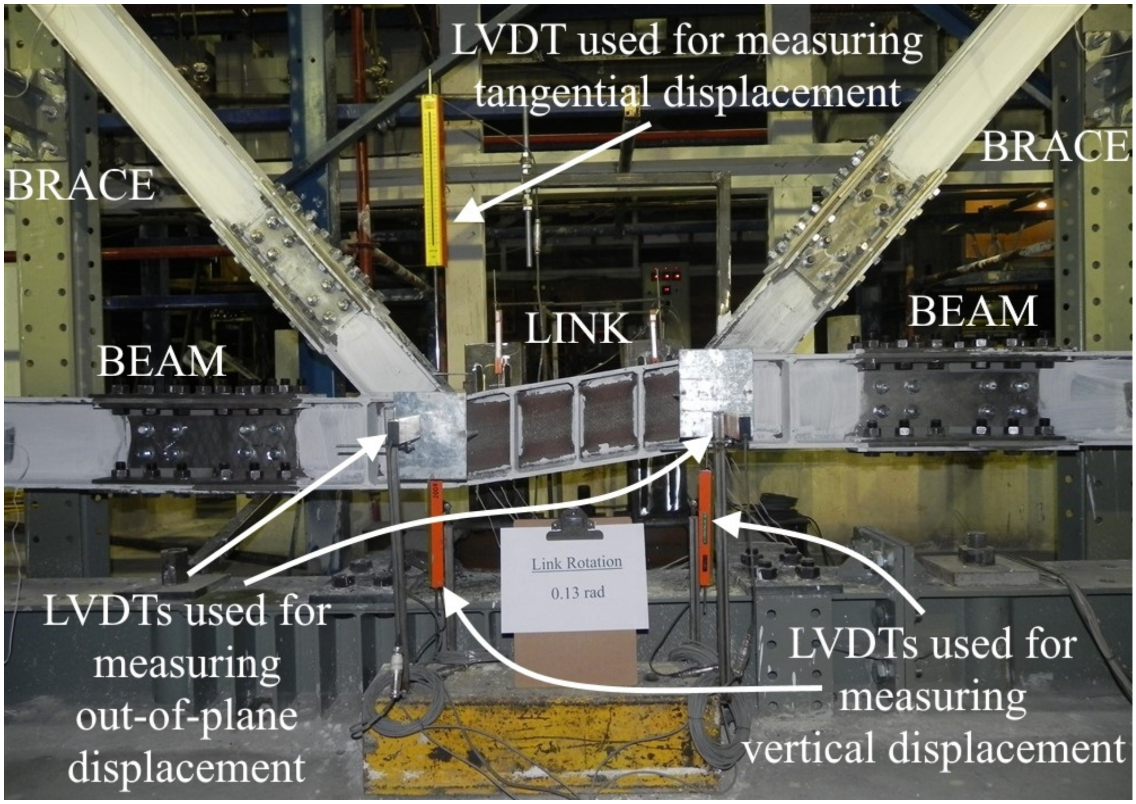


Figure 3.4 Photo of the test setup (close-up view)

The ends of the link were laterally braced by making use of a frame system specially designed to allow for in-plane movements of the link ends and restrain the out-of-plane movement. The entire frame was also supported laterally by restraining the out-of-plane movements of the loading beam and the columns. Horizontal displacement of the frame columns were measured using LVDTs that were placed 2465mm above the bottom pin supports. Strain gages were placed at mid lengths of the beams outside the link and braces on the neutral axis of their cross-section. The strain readings were used to calculate the axial forces in these members. Two different approaches were used to monitor the link rotation angle. The vertical displacement of the link ends were monitored with respect to the stationary strong floor using LVDTs (Figure 3.4). The differences between these individual measurements were used to calculate the link rotation angle. Furthermore, an LVDT was attached to an L-shaped frame (Figure 3.4) which was welded to one of the brace-to-link joints. This LVDT measured the tangential deviation of one of the link ends with respect to the other and provided a control measurement. Both the approaches are affected by the deformations that take place in members outside of the link. The individual link end measurements are influenced by the global rotation of the test frame due to the flexibility at the pins and also by the slip that takes place in splice connections. These influences are eliminated when the tangential displacements are measured. However, the tangential displacement measurements are adversely affected due to the rotation at link ends which in turn creates a rotation of the L-shaped frame.

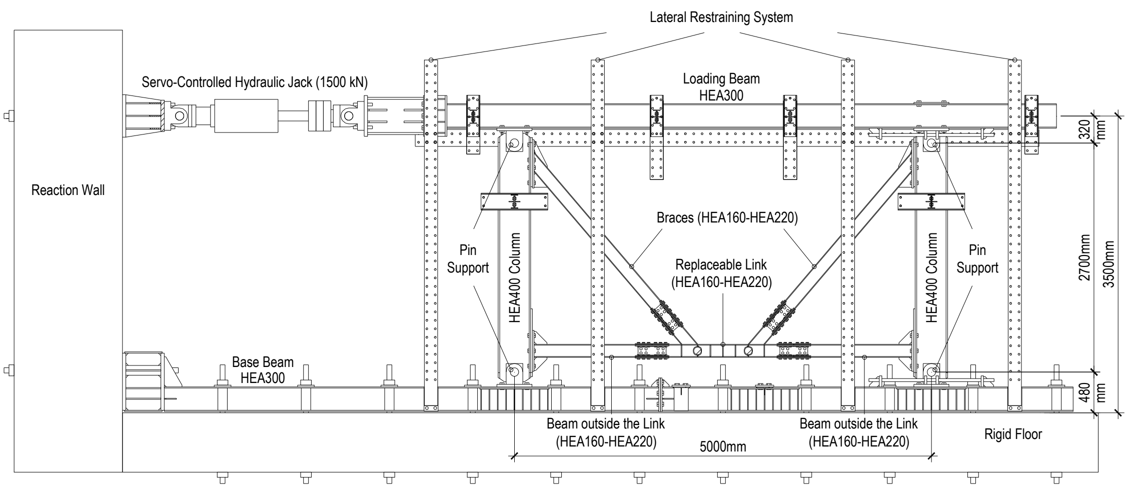


Figure 3.5 Details of the test setup

### 3.3.2. Geometrical and Material Properties of I-Sections

The nominal shear capacity of I-section shear links is calculated as follows according to AISC341-10 (2010):

$$V_n = 0.6F_y\left(d - 2t_f\right)t_w \tag{3.2}$$

where $d$ = depth of the section, $t_f$ = flange thickness, $t_w$ = web thickness, $F_y$ = nominal yield strength.

Archetype designs conducted by various research teams (Mansour (2010), Dubina et al. (2008), Richards and Uang(2006), Özhendekci and Özhendekci (2008), Rossi and Lombardo (2007), Kuşyılmaz and Topkaya(2016)) were considered to identify the range of nominal shear capacity possessed by shear links used in practical applications. A survey consisting of 19 archetypes which have number of stories that range between 3 and 12 revealed that the nominal capacity changes between 90 kN and 1324 kN with an average of 502 kN. The selection of link sections was based on the available equipment capacity. Two different European rolled I-sections, namely HEA160 and HEA220 were used in the experimental program. The commonest European steel grade S275 with a nominal yield strength ($F_y$) of 275 MPa and an ultimate strength ($F_u$) of 430 MPa according to EN 10025 (2004) was selected for both I-sections. Four different heats were obtained for HEA160 whereas only one heat of steel was obtained for HEA140 and HEA220. Tensile tests were conducted on coupons extracted from the I-shapes according to EN 10002 (2001). The measured cross sectional properties and measured material properties of I-sections are given in Tables 3.1 and 3.2 respectively. The width-to-thickness ratios of the web and the flanges of link members satisfy provisions of AISC 341-10 (2010) except for three specimens where intermediate links were employed. The nominal shear capacities provided by HEA160 and HEA220 links with S275 grade steel are 133kN and 217 kN respectively. The HEA 160 link is relatively small in size when compared with typical links used in practice. This link section was selected to study effect of different variables and to provide a proof-of-concept. The HE220 link section is among the sections that can be used in practice for the upper stories. For example upper 2 floors of 4 story and 12 story frames designed by Rossi and Lombardo (2007) employed links with similar capacity.

Table 3.1 Geometrical properties of rolled I-sections

| Type | Section | Heat | Nominal | | | | Measured | | | |
|---|---|---|---|---|---|---|---|---|---|---|
| | | | $d$ (mm) | $b_f$ (mm) | $t_w$ (mm) | $t_f$ (mm) | $d$ (mm) | $b_f$ (mm) | $t_w$ (mm) | $t_f$ (mm) |
| 1 | HEA140 | 1 | 133 | 140 | 5.5 | 8.5 | 132.53 | 140.61 | 5.45 | 8.20 |
| 2 | HEA160 | 1 | 152 | 160 | 6 | 9 | 152.52 | 159.40 | 6.85 | 8.79 |
| 3 | HEA160 | 2 | 152 | 160 | 6 | 9 | 152.53 | 159.67 | 6.70 | 8.88 |
| 4 | HEA160 | 3 | 152 | 160 | 6 | 9 | 152.34 | 159.61 | 6.68 | 8.82 |
| 5 | HEA160 | 4 | 152 | 160 | 6 | 9 | 153.09 | 160.06 | 6.72 | 8.76 |
| 6 | HEA220 | 1 | 210 | 220 | 7 | 11 | 213.72 | 220.97 | 7.81 | 10.67 |

Table 3.2 Material properties of rolled I-sections

| Type | Section | Heat | Web | | | | | Flanges | | | | |
|---|---|---|---|---|---|---|---|---|---|---|---|---|
| | | | $F_{yL}$ (MPa) | $F_{yu}$ (MPa) | $F_{y,0.2}$ (MPa) | $F_u$ (MPa) | *%E* | $F_{yL}$ (MPa) | $F_{yu}$ (MPa) | $F_{y,0.2}$ (MPa) | $F_u$ (MPa) | *%E* |
| 1 | HEA140 | 1 | 367 | 386 | 369 | 500 | 26 | 325 | 338 | 332 | 488 | 30 |
| 2 | HEA160 | 1 | 276 | 301 | 286 | 407 | 25 | 272 | 303 | 286 | 403 | 35 |
| 3 | HEA160 | 2 | 275 | 291 | 278 | 421 | 33 | 281 | 300 | 290 | 426 | 32 |
| 4 | HEA160 | 3 | 278 | 301 | 285 | 417 | 31 | 285 | 305 | 294 | 430 | 32 |
| 5 | HEA160 | 4 | 383 | 402 | 393 | 501 | 29 | 320 | 333 | 324 | 445 | - |
| 6 | HEA220 | 1 | 299 | 318 | 305 | 421 | 32 | 268 | 290 | 278 | 408 | 37 |

$F_{yL}$ = lower yield stress, $F_{yu}$ = upper yield stress, $F_{y,0.2}$ = yield stress at 0.2% permanent elongation, $F_u$ = ultimate strength, *%E* = percent elongation.

### 3.3.3. Test Variables and Test Specimens

Link length ratio (ρ), stiffening of the link, loading protocol, brace to link connection type, location of the brace to link connection, bolt connection type, bolt pretension, spacing between members, demand-to-capacity ratio of braces and the beam outside the link were considered as the prime variables. Using the aforementioned test setup, a total of eight link tests with direct brace attachment and a total of nine link tests with gusset plate connected attachment were conducted in the first and second phases respectively. In the second phase, five specimens with gusset plate connected attachments, three specimens with compact gusset plate connected attachments and one specimen with pin connected attachment were tested. The details of the replaceable links are given in Table 3.3, Figures 3.6, 3.7, 3.8 and 3.9.

For all specimens tested in the first phase the braces were directly attached to the link by making use of Gas Metal Arc Welding (GMAW) whereas for all specimens tested in the second phase the braces were attached to the gusset plates and these gusset plates, in turn, were attached to the link by making use of GMAW. SG2 electrodes similar to ER70S-6 electrodes with a nominal tensile strength of 540 MPa were used. The welding details of the brace-to-beam connection are indicated in Figures 3.6, 3.7, 3.8 and 3.9. In general, full penetration groove welds with reinforcing fillet welds were employed for the flanges and fillet welds were employed for the web of the braces for the specimens where the direct brace attachment was utilized. On the other hand, only fillet welds were employed for the specimens where the gusset plate connected attachment were utilized. In general, after each test the replaceable link portion was removed and the beams and braces outside the replaceable link were reused. The following outlines the details of test variables.

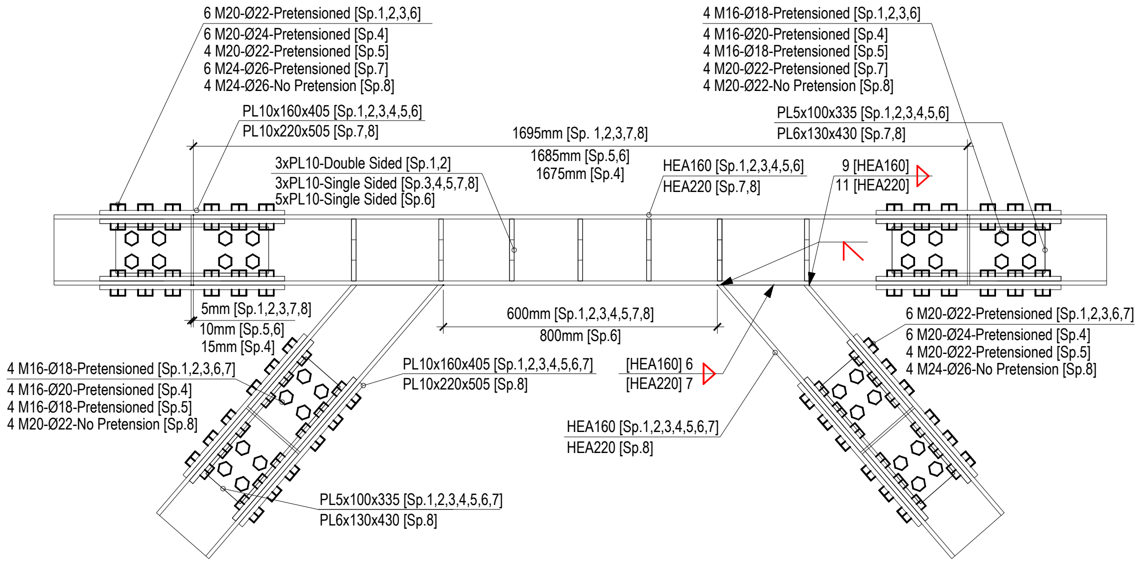


Figure 3.6 Details of direct brace attachment

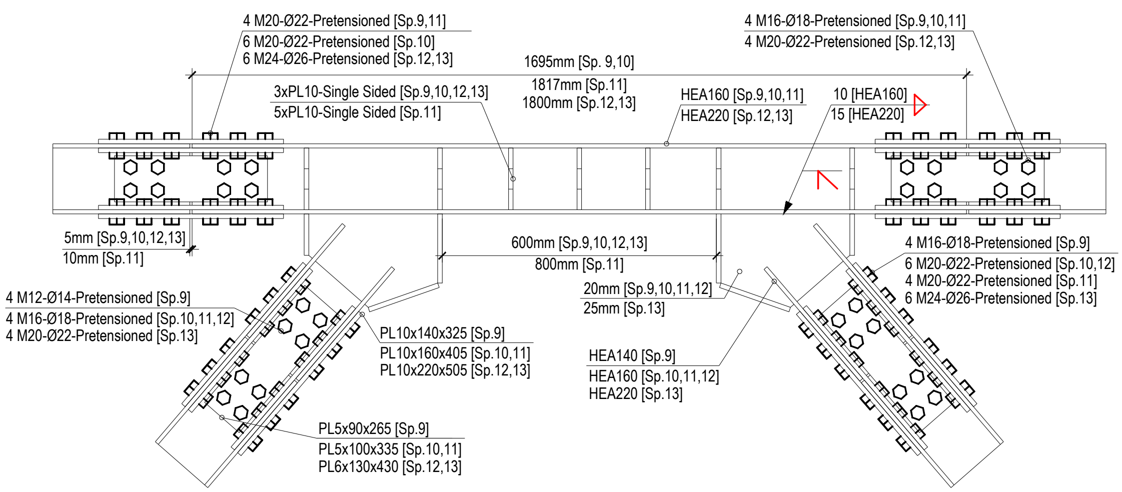


Figure 3.7 Details of gusset plate connected brace attachment

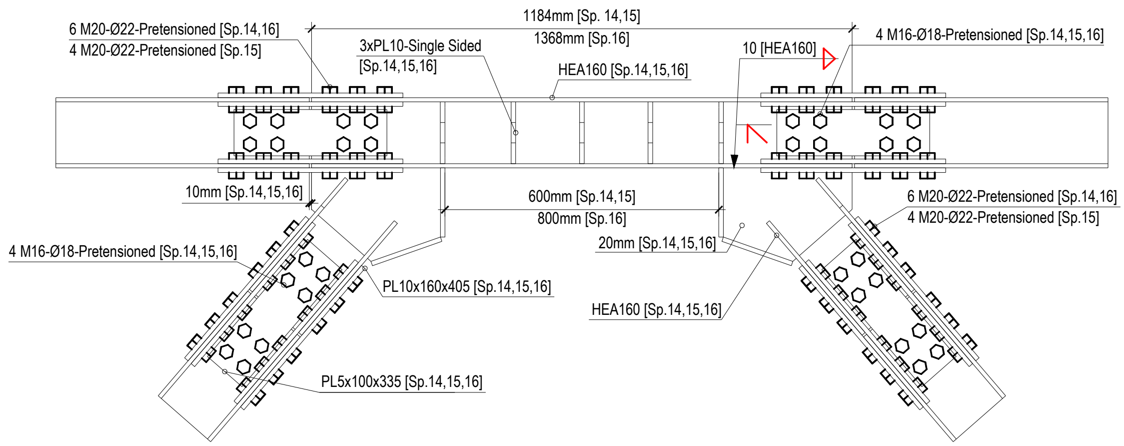


Figure 3.8 Details of compact gusset plate connected brace attachment

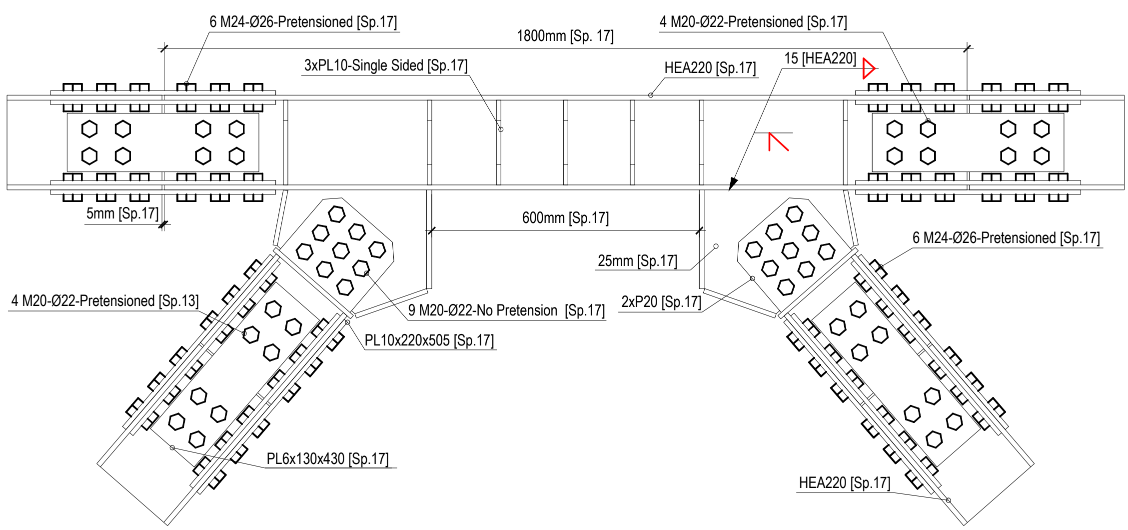


Figure 3.9 Details of pin connected brace attachment

### 3.3.3.1.Link length ratio (ρ)

Link lengths (*e*) of 600 mm and 800 mm were used in the test program. These link lengths correspond to *e*/*L* ratios of 0.12 and 0.16 which cover a practical range of interest. The link length ratios calculated based on both nominal and measured geometrical and material properties are reported in Table 3.3. Link length ratios based on measured properties (ρ) of 1.04, 1.31, 1.32, 1.39, 1.74, and 1.78 were obtained by using combinations of different cross sections and different link lengths. The experimented links were primarily shear yielding links which were expected to exhibit stable energy dissipation. In addition, short links should be selected for easy replacement due to their decreased weight (Ji et al. (2015)). Too short links, however, will impose very high link rotational demands which cannot be tolerated by the link. The 800 mm long links for Specimens 6, 11 and 16 were selected to have a nominal ρ=1.59; however, the measured ρ is equal to 1.74, 1.78 and 1.74 respectively due to the increased web thickness and qualified as an intermediate link.

Table 3.3 Properties of specimens

| Sp. # | Link Section | H. | Brace Section | H. | Link Length (mm) | Brace Con. Type | ρ Nm. | ρ Me. | Load Prot. | Stf. | Bolt Con. Type | Pre. | Gap Size (mm) |
|---|---|---|---|---|---|---|---|---|---|---|---|---|---|
| 1 | HEA160 | 1 | HEA160 | 1 | 600 | DB | 1.19 | 1.39 | LP1 | D | SC | Y | 5 |
| 2 | HEA160 | 1 | HEA160 | 1 | 600 | DB | 1.19 | 1.39 | LP2 | D | SC | Y | 5 |
| 3 | HEA160 | 1 | HEA160 | 1 | 600 | DB | 1.19 | 1.39 | LP1 | S | SC | Y | 5 |
| 4 | HEA160 | 2 | HEA160 | 2 | 600 | DB | 1.19 | 1.31 | LP1 | S | SCO | Y | 15 |
| 5 | HEA160 | 2 | HEA160 | 2 | 600 | DB | 1.19 | 1.31 | LP1 | S | B | Y | 10 |
| 6 | HEA160 | 2 | HEA160 | 2 | 800 | DB | 1.59 | 1.74 | LP1 | S | SC | Y | 10 |
| 7 | HEA220 | 1 | HEA160 | 1 | 600 | DB | 0.84 | 1.04 | LP1 | S | SC | Y | 5 |
| 8 | HEA220 | 1 | HEA220 | 1 | 600 | DB | 0.84 | 1.04 | LP1 | S | B | N | 5 |
| 9 | HEA160 | 3 | HEA140 | 1 | 600 | GB | 1.19 | 1.32 | LP1 | S | B | Y | 5 |
| 10 | HEA160 | 3 | HEA160 | 3 | 600 | GB | 1.19 | 1.32 | LP1 | S | SC | Y | 5 |
| 11 | HEA160 | 4 | HEA160 | 4 | 800 | GB | 1.59 | 1.78 | LP1 | S | B | Y | 10 |
| 12 | HEA220 | 1 | HEA160 | 3 | 600 | GB | 0.84 | 1.04 | LP1 | S | SC | Y | 5 |
| 13 | HEA220 | 1 | HEA220 | 1 | 600 | GB | 0.84 | 1.04 | LP1 | S | SC | Y | 5 |
| 14 | HEA160 | 3 | HEA160 | 3 | 600 | CGB | 1.19 | 1.32 | LP1 | S | SC | Y | 10 |
| 15 | HEA160 | 2 | HEA160 | 2 | 600 | CGB | 1.19 | 1.31 | LP1 | S | B | Y | 10 |
| 16 | HEA160 | 2 | HEA160 | 2 | 800 | CGB | 1.59 | 1.74 | LP1 | S | SC | Y | 10 |
| 17 | HEA220 | 1 | HEA220 | 1 | 600 | PGB | 0.84 | 1.04 | LP1 | S | B | Y | 5 |

LP1: AISC341-10 Loading Protocol, LP2: AISC341-02 Loading Protocol, H: Heat, Y: Yes, N: No, DB: Direct brace attachment, GB: Gusset plate connected brace attachment, CGB: Compact gusset plate connected brace attachment, PGB: Gusset plate pin connected brace attachment, SC: Slip Critical, SCO: Slip Critical Connection with Oversize Holes, B: Bearing Type, D: Double-Sided Stiffeners, S: Single-Sided Stiffeners; Nm.: Nominal, Me.: Measured, Pre: Pretension, Stf: Stiffeners.

#### 3.3.3.2.Stiffening of the link and loading protocol

The stiffener spacing recommended in AISC Seismic Provisions (AISC341-10 (2010)) was used in the program which resulted in three and five intermediate stiffeners for 600mm and 800mm long links respectively. Single-sided stiffeners are allowed by AISC 341-10 (2010) when the depth of the link is less than 635 mm. In the research program single-sided stiffeners were mostly used except two specimens where the stiffeners were double-sided. Based on the recommendation of Okazaki et al. (2005) the stiffener welds were terminated a distance of $5t_w$ from the k-line of the link section. Two different loading protocols were used in the experimental program. In all specimens except one, the loading protocol recommended by the AISC341-10 (2010) was utilized. One of the specimens was subjected to the old AISC protocol which was defined in the 2002 version of AISC Seismic Provisions (AISC341-02 (2002)).

#### 3.3.3.3.Brace to link connection type

Different brace to link connection types utilized in real practice were investigated in this experimental program. Direct brace attachment was employed in the first phase whereas gusset plate connected attachment, compact gusset plate connected attachment and pin connected brace attachment were employed in the second phase.

#### 3.3.3.4.Bolt connection type, bolt pretension, and spacing

The experimental program investigated the use of bearing type and slip-critical type bolted connections for beam and brace splices. According to the AISC341-10 (2010) Specification the bolted connections of the seismic load resisting system can be designed as bearing type and the use of slip-critical connections is not mandated. However, clause D2.2.(4) of AISC 341-10 (2010) recommends that the bolts be fully pre-tensioned and the faying surfaces should have slip coefficients equal to or greater than the coefficient ($\mu$=0.3) given for Class A surfaces in AISC360-10 (2010). The two approaches were studied in order to understand the impact of using bearing type connections on the global frame response. The number of bolts used for the flanges and the web were determined according to capacity design principles. The force corresponding to the fully yielded web or flange plate was considered to determine the required number of bolts for each element. Grade 8.8 high strength bolts, which conform to ISO standard (ISO 898-1 (1999)), were utilized in the connections. All faying surfaces were manually sand blasted to achieve Sa2.5 surface conditions with a reported coefficient of friction between 0.47 and 0.5 (European Commission (2012)). In all specimens except for one the bolts were fully pretensioned by making use of a calibrated torque wrench.  In one of the specimens (Specimen 8), where the connections were designed as bearing type, the bolts were kept snug-tight.  The purpose of having limited pretension was to observe the global frame response under this tightening condition.  Bearing type connections with fully pretensioned bolts were utilized in Specimen 5, 9, 11, 15, and 17 as recommended by the AISC341-10 Specification (2010).

In general, all specimens except one utilized standard holes according to AISC360-10 (2010) as recommended by AISC341-10 (2010).  Oversize holes were used in Specimen 4 where the connections were designed as slip-critical type.  The use of oversize holes is expected to promote easy replacement because of the larger tolerance provided between the bolt and the bolt holes.  In addition, the replacement procedure can be made easier if a gap is provided at the splice connections.  In this research the same level of gap is provided at the beam and brace splices.  Increasing the gap size promotes easy replacement.  On the other hand, using a large gap size increases the connection eccentricity for the web connections and also increases the buckling length of splice plates making them weaker under compressive actions.  For ten specimens, a 5mm gap was provided between the link and the beam outside the link.  Six of the specimens employed a 10mm gap. For the specimen with oversize holes the gap size was increased to 15mm.  The reason for increasing the gap size in this specimen was to study an extreme case where a larger gap is utilized with a larger tolerance provided at the bolt holes.

#### 3.3.3.5.Demand-to-capacity ratio of members

Design of brace members in EBF systems depend on many factors most important being the brace angle. A survey consisting of 19 archetypes (Mansour (2010), Dubina et al. (2008), Richards and Uang(2006), Özhendekci and Özhendekci (2008), Rossi and Lombardo (2007), Kuşyılmaz and Topkaya(2016)) revealed that the ratio of plastic moment capacity of the link to that of the brace varies between 0.49 and 3.98.  In this research, brace sections were determined by considering the forces and bending moments that can be produced by the selected link section. In addition, the ratios of plastic moment capacities were considered to be representative of the practical cases. HEA140 and HEA160 brace sections are employed for HEA160 links whereas HEA160 and HEA220 brace sections are employed HEA220 links. In EBF systems the beams outside the link and the braces are subjected to axial force and bending moment and these elements are designed as beam-columns. By selecting different brace sections for a given beam/link section, the demand-to-capacity ratios of the critical members and connections can be changed. The demand-to-capacity ratio is represented as a *PM* ratio in this research work. The following design expressions given in AISC 360-10 (2010), for uniaxial bending, were used for assessing the *PM* ratio.

$$PM = \frac{P_r}{2P_c} + \frac{M_{rx}}{M_{cx}} \quad \text{for } \frac{P_r}{P_c} \leq 0.2 \tag{3.3}$$

$$PM = \frac{P_r}{P_c} + \frac{8}{9}\frac{M_{rx}}{M_{cx}} \quad \text{for } \frac{P_r}{P_c} > 0.2 \tag{3.4}$$

where $P_r$ and $M_{rx}$ = the axial force and bending moment applied to the member, $P_c$ and $M_{cx}$ = the axial load and bending moment capacity of the member according to AISC360-10 (2010).

Table 3.4 Demand-to-capacity ratios

| Beam Section | Brace Section | Link Length (mm) | Brace Connec. | Beam | | | Brace | | |
|---|---|---|---|---|---|---|---|---|---|
| | | | | $PM_1$ | $PM_2$ | $PM_3$ | $PM_1$ | $PM_2$ | $PM_3$ |
| HEA160 | HEA140 | 600 | Rigid | 0.57 | 0.17 | 0.48 | 0.71 | 0.44 | 0.56 |
| HEA160 | HEA160 | 600 | Rigid | 0.54 | 0.17 | 0.47 | 0.57 | 0.32 | 0.48 |
| HEA160 | HEA160 | 800 | Rigid | 0.63 | 0.17 | 0.55 | 0.65 | 0.32 | 0.55 |
| HEA220 | HEA160 | 600 | Rigid | 0.48 | 0.15 | 0.43 | 0.72 | 0.52 | 0.61 |
| HEA220 | HEA220 | 600 | Rigid | 0.38 | 0.15 | 0.35 | 0.44 | 0.25 | 0.40 |
| HEA220 | HEA220 | 600 | Pin | 0.56 | 0.15 | 0.48 | 0.30 | 0.26 | 0.29 |

Both stability checks and cross-section capacity checks were performed by making use of Equations 3.3 and 3.4 and these are reported as different *PM* values. Here $PM_1$ is used for the global stability of members under compression and bending. In order to provide a measure of the relative importance of compressive axial force to the bending action, a demand-to-capacity ratio ($PM_2$) was calculated for axial force (i.e. $P_r/P_c$) only by neglecting the bending contributions. Due to the presence of holes the most critical cross-section is the one that is closest to the welded joint. Demand-to-capacity of the critical cross-section under tension and bending was represented by $PM_3$ where the $P_c$ and $M_{cx}$ were determined based on the properties of the reduced cross-section. The calculated *PM* ratios for the beam outside the link and braces are reported in Table 3.4.

The demands were calculated based on the nominal shear capacity of the link determined using Equation 3.2. The internal forces in the beam and the brace were determined for the condition where the link nominal shear capacity is reached. It should be mentioned that the values in Table 3.4 do not include amplified forces due to overstrength of the link. In general, AISC341-10 (2010) mandates that the forces be amplified by $1.25R_y$ for the braces, where $R_y$ is the ratio of the expected yield stress to the specified minimum yield stress. The same level of increase is recommended for the beam outside the link when this member does not act compositely with a concrete deck. If the link and the beam are from the same member, then the $R_y$ term can be dropped. It should be noted that the reported average $R_y$ for S275 steels based on the upper yield strength is 1.27 (European Commission (2013)). The specimen fabricator was instructed to find out steels that match closely to their specified strengths. According to Table 3.2 the measured $R_y$ values based on lower yield strength of the web is 1.00, 1.00, 1.01, 1.39 1.09 for HEA160 Heat1, HEA160 Heat2, HEA160 Heat3, HEA160 Heat4 and HEA220 sections respectively. Ideally the $PM_1$ ratio should be kept below 0.8 (1/1.25) to take into account link overstrength. The values given in Table 3.4 suggest that braces are more critical than the beam outside the link for 5 cases where braces are connected to links as rigid. On the other hand, beam outside the link is more critical than the braces for pin connected case. The $PM_1$ ratios are generally below 0.8 indicating that the designs are acceptable according to AISC341-10 (2010) provided that $R_y$ values are close to unity and geometrical properties match with the nominal ones.

## 3.4.Experimental Results

Tests were controlled by the link rotation angle (γ) which was calculated from the vertical displacement measurements of the link ends. The ratio of maximum link rotation angles measured using the two methods (i.e. considering vertical displacement measurements or tangential deviation) had an average of unity. A maximum difference of 13 percent was reported between the two measurement techniques at the level of maximum link rotation. The two methods provided different measurements of the link rotation angle at early stages of loading when the link still exhibited elastic behavior.

Table 3.5 Summary of test results

| Sp. # | $V_{n,N}$ (kN) | $V_{n,M}$ (kN) | $K_{link}$ (kN/rad) | $K_{frame}$ (kN/rad) | $P/P_y$ Tens. | $P/P_y$ Comp. | ($\gamma_p$) (rad) | ($\theta_p$) (rad) | Link OS ($V_{max}/V_{n,M}$) | Failure Mode |
|---|---|---|---|---|---|---|---|---|---|---|
| 1 | 133 | 153 | 20685 | 133968 | 0.25 | 0.19 | 0.135 | 0.018 | 2.18 | A,B |
| 2 | 133 | 153 | 19436 | 135205 | 0.17 | 0.15 | 0.095 | 0.014 | 2.05 | A,B |
| 3 | 133 | 153 | 18341 | 130201 | 0.19 | 0.16 | 0.135 | 0.019 | 2.17 | A,C |
| 4 | 133 | 149 | 17420 | 125074 | 0.15 | 0.13 | 0.135 | 0.018 | 2.16 | A,B |
| 5 | 133 | 149 | 19560 | 124581 | 0.21 | 0.16 | 0.135 | 0.020 | 2.17 | A,B |
| 6 | 133 | 149 | 16098 | 95543 | 0.25 | 0.16 | 0.114 | 0.022 | 1.85 | A,B,D |
| 7 | 217 | 270 | 48245 | 189756 | 0.11 | 0.10 | 0.119 | 0.019 | 2.03 | E,C |
| 8 | 217 | 270 | 52746 | 209870 | 0.19 | 0.18 | 0.141 | 0.027 | 2.19 | C |
| 9 | 133 | 150 | 24562 | 116915 | 0.24 | 0.21 | 0.157 | 0.026 | 2.20 | E,B |
| 10 | 133 | 150 | 20142 | 142172 | 0.20 | 0.25 | 0.133 | 0.021 | 2.22 | A,B |
| 11 | 133 | 209 | 16302 | 107014 | 0.21 | 0.20 | 0.072 | 0.021 | 1.39 | A,B |
| 12 | 217 | 270 | 47609 | 191123 | 0.15 | 0.14 | 0.119 | 0.019 | 2.01 | A,B |
| 13 | 217 | 270 | 62997 | 210428 | 0.17 | 0.20 | 0.141 | 0.020 | 2.13 | C |
| 14 | 133 | 150 | 19104 | 128647 | 0.15 | 0.14 | 0.133 | 0.021 | 2.15 | A,B |
| 15 | 133 | 149 | 19676 | 139700 | 0.20 | 0.19 | 0.134 | 0.020 | 2.15 | A,B |
| 16 | 133 | 149 | 15009 | 102937 | 0.21 | 0.20 | 0.112 | 0.023 | 1.81 | A,B |
| 17 | 217 | 270 | 60492 | 213407 | 0.18 | 0.17 | 0.141 | 0.021 | 2.09 | C |

$V_{n,N}$: Nominal shear strength, $V_{n,M}$: Measured shear strength, OS: Overstrength, $\gamma_p$: Inelastic Rotation Capacity, $\theta_p$ : Inelastic Story Drift Angle, A: Flange buckling, B: Flange fracture, C: Fracture of web at the stiffener weld, D: Flange buckling in brace connection panel, E: Brace buckling.

As mentioned earlier, the initial measurements were influenced by either the setup flexibility or by the rotations that take place at the link ends. The following expressions were used to calculate the inelastic part of link rotation and story drift angle:

$$\gamma_p = \gamma - \frac{V_{link}}{K_{link}} \qquad\qquad \theta_p = \theta - \frac{F_{actuator}}{K_{frame}} \tag{3.5}$$

where $\gamma_p$ = inelastic link rotation, $\theta_p$ = inelastic story drift angle, $\theta$ = total story drift angle, $K_{link}$ = elastic stiffness of the link, $K_{frame}$ = elastic stiffness of the frame.

The results indicate that the loading and unloading stiffnesses differ from each other due to the aforementioned factors that influence the measurements. The initial loading stiffness of the link is on average 23 percent higher than the unloading stiffness when the link rotation is calculated using the vertical measurements of the link ends. On the other hand, the initial loading stiffness of the frame is on average 18 percent lower than the unloading stiffness. The unloading stiffness is influenced less by the factors that affect the measurements and these stiffnesses which are reported in Table 3.5 was used in calculating inelastic angles. The stiffness values reported in Table 3.5 were compared with stiffnesses obtained using elastic 3D finite element analysis employing shell elements. The ratios of the experimental link stiffness to the value from numerical analysis have an average of 1.07, a maximum of 1.16 and a minimum of 0.95. Similarly the ratios for the frame stiffness have an average of 0.92, a maximum of 0.99 and a minimum of 0.77. According to AISC341-10 (2010) the inelastic link rotation capacity ($\gamma_p$) of the links is defined as the maximum level of inelastic rotation sustained for at least one full cycle of loading prior to the link shear strength dropping below the nominal link shear strength ($V_n$). The link shear strength based on nominal ($V_{n,N}$) and measured ($V_{n,M}$) properties are reported in Table 3.5. The measured shear strength ($V_{n,M}$) calculated based on measured section dimensions and measured lower yield strength was considered in defining inelastic link rotation capacity. Hysteretic inelastic link rotation versus link shear response of all specimens is given in Figures 3.10, 3.11, and 3.12. In these figures, the shear strengths based on measured properties are shown with dashed lines.

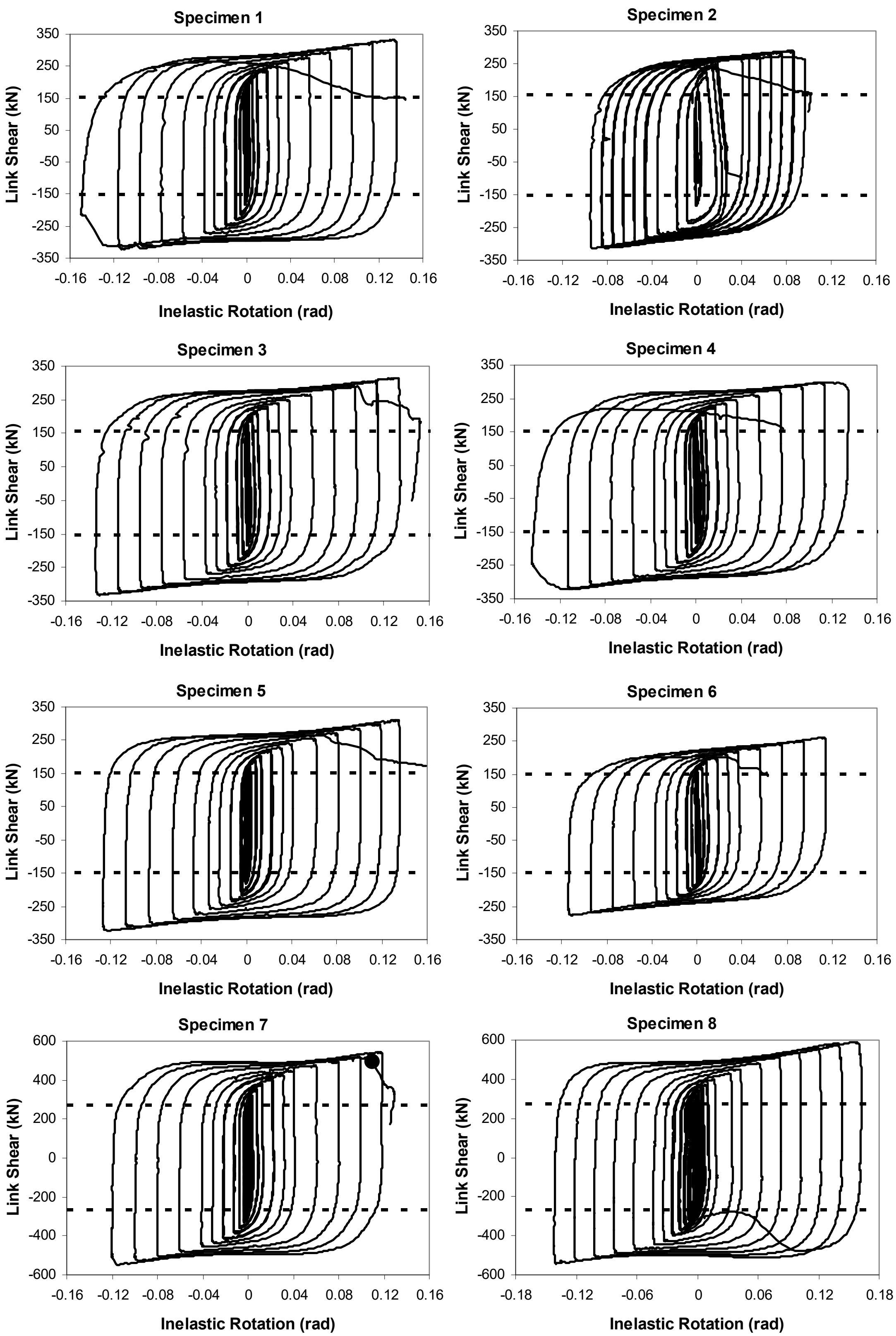


Figure 3.10 Hysteretic response of specimens (Specimens 1 through 8)

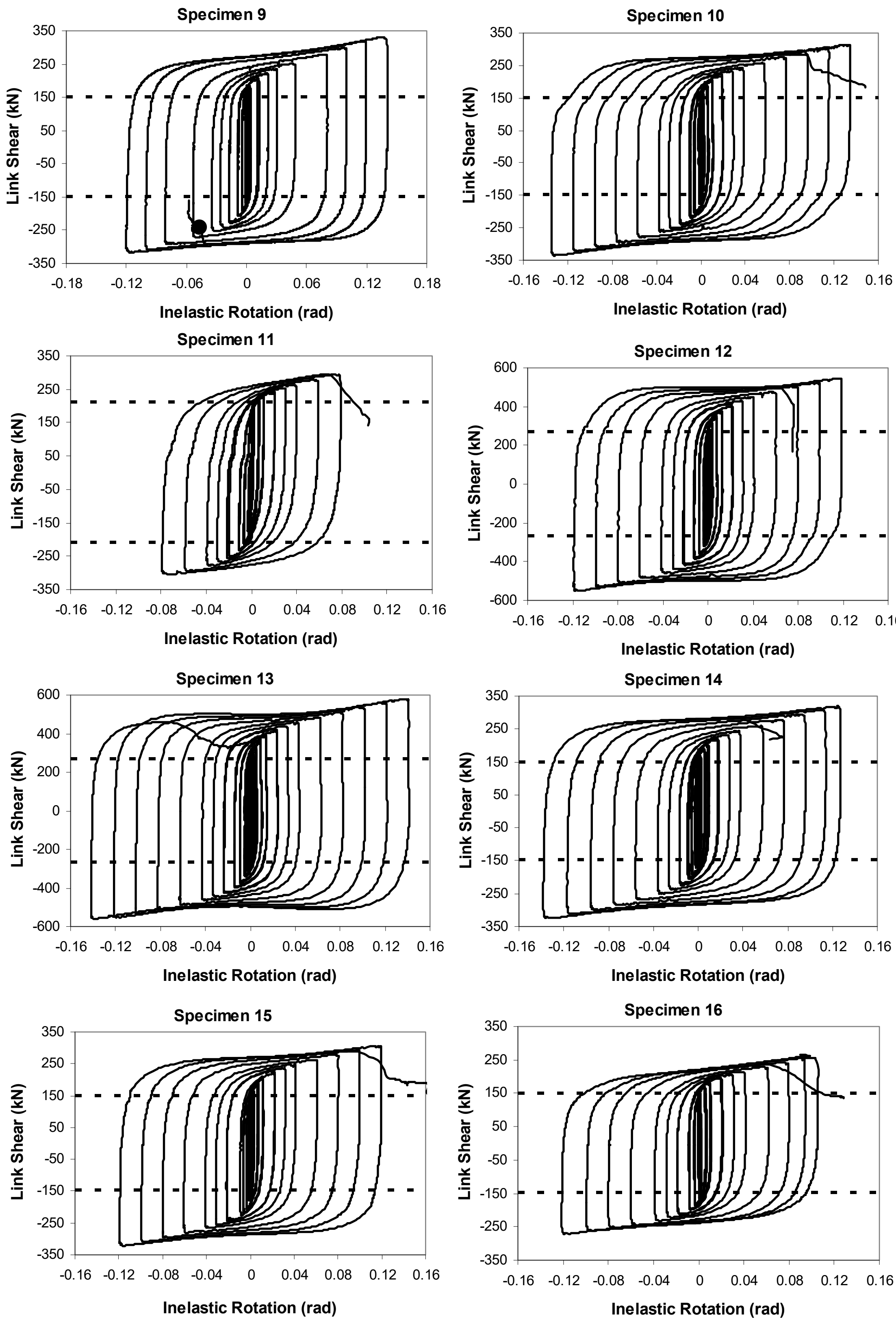


Figure 3.11 Hysteretic response of specimens (Specimens 9 through 16)

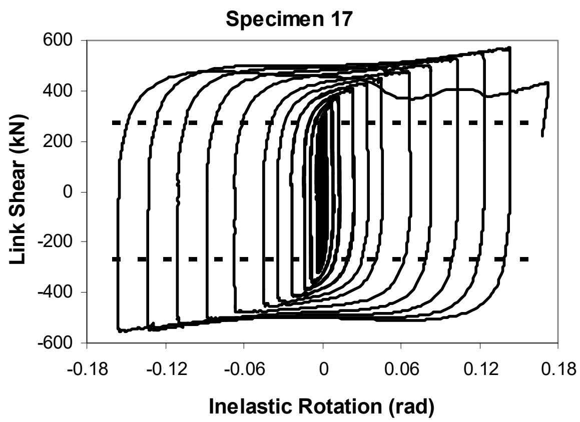


Figure 3.12 Hysteretic response of Specimen 17

For the specimens which employed slip critical connections except Specimen 14 and Specimen 16 which utilized compact gusset plate connection, the link rotation was obtained by making use of displacement readings at link ends. For Specimens 5, 8, 9, 11, 15 and 17 which employed bearing type connections and Specimen 14 and 16 which employed compact gusset plate connection, the tangential deviation measurements were used for link rotation angle. Three distinct failure modes given in Figures 3.13 and 3.14 were observed in the experimental program. For most of the specimens with link length ratios of 1.04, 1.31, 1.32, 1.39, 1.74, and 1.78 flange buckling followed by fracture in the flange at the link-to-brace connection was observed (Figures 3.13a and 3.14a). For specimens with shorter link length ratios (ρ= 1.04) fracture of web at the stiffener weld was responsible for the failure (Figures 3.13b and 3.14b). In two of the experiments (Specimens 7 and 9) the brace under compression buckled at later loading cycles causing the entire system to loose its resistance (Figures 3.13c and 3.14c). The point at which the strength degradation starts due to brace buckling is indicated by a filled marker in Figures 3.10 and 3.11. For the intermediate link specimen (ρ= 1.74) flange buckling at the brace connection panel was also observed (Figure 3.13d). Axial forces in the braces and the beams outside the link were used to calculate the axial force produced in the link. In general, tensile forces develop at large link rotations. Links also experience compressive forces as the loading direction changes. The maximum tensile and compressive axial force produced in the link normalized by the link axial capacity ($P/P_y$), the inelastic rotation capacity ($\gamma_p$), overstrength calculated based on measured properties, inelastic story drift angle ($\theta_p$), and controlling failure mode for each specimen are reported in Table 3.5.

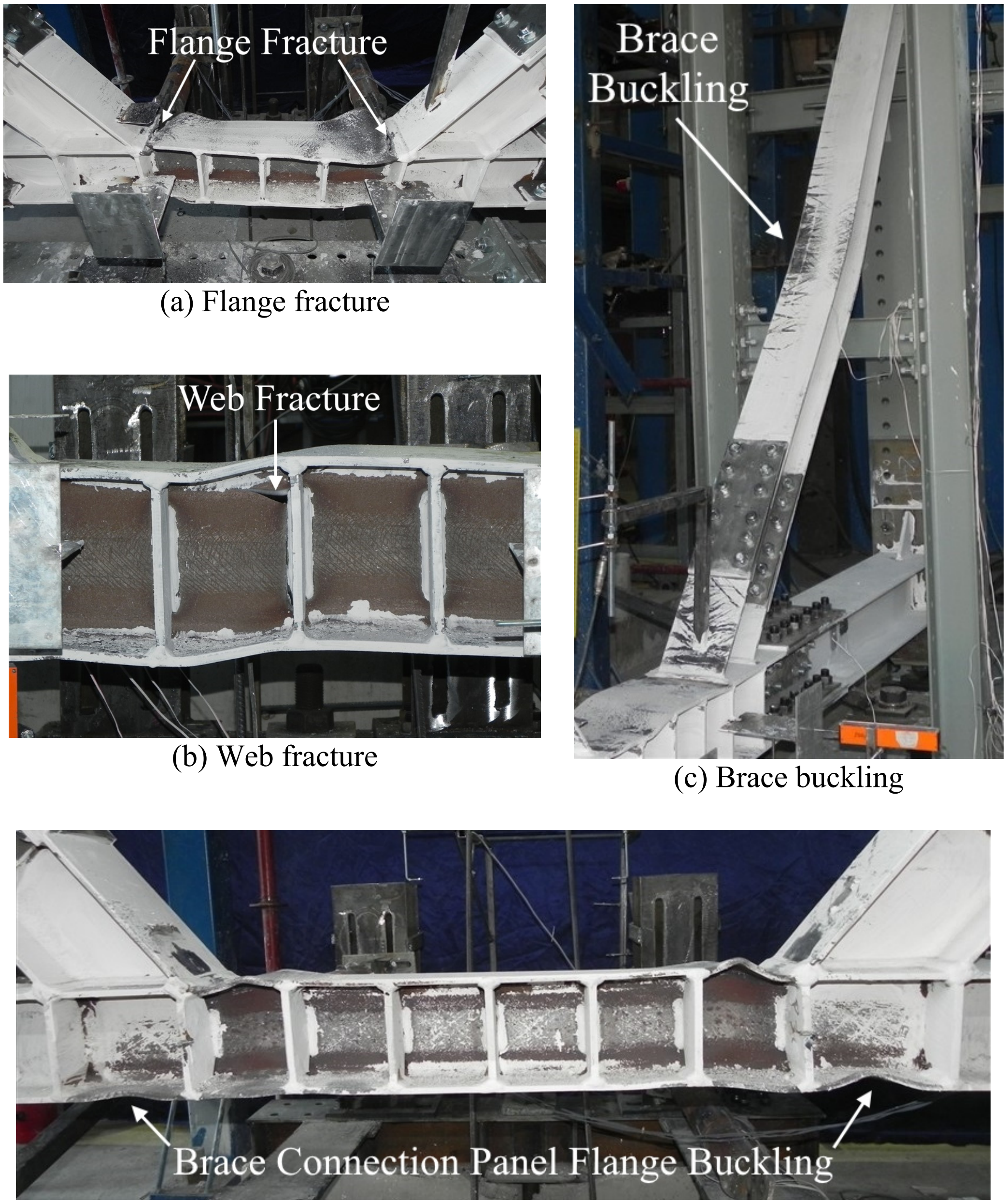


(a) Flange fracture

(b) Web fracture

(c) Brace buckling

(d) Brace connection panel flange buckling

Figure 3.13 Failure modes of specimens tested in Phase 1

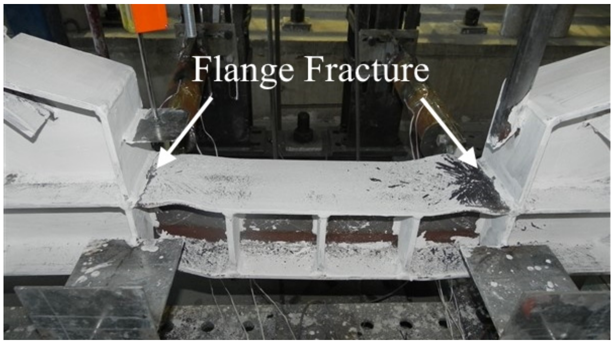


(a) Flange fracture

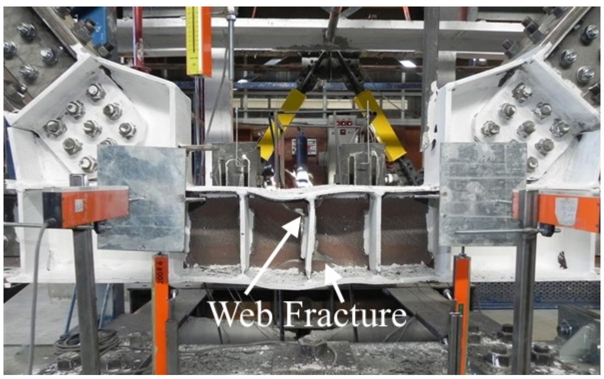


(b) Web fracture


(c) Brace buckling

Figure 3.14 Failure modes of specimens tested in Phase 2

## 3.5.Discussion and Experimental Results

### 3.5.1. Inelastic Rotation Capacity, Loading Protocol, Stiffening of the Link, and Flange Slenderness Ratio

The AISC341-10 Provisions (AISC341-10 (2010)) specify the shear yielding links ($\rho \leq 1.6$) should be capable of developing an inelastic rotation of 0.08 rad, whereas flexural yielding links ($\rho \geq 2.6$) should be capable of developing an inelastic rotation of 0.02 rad. The required inelastic rotation of intermediate links ($1.6 < \rho < 2.6$) is determined by linear interpolation between 0.08 and 0.02 rad. The test results were evaluated by making comparisons with the AISC341-10 (2010) requirements as well as the earlier tests. Data from different research teams (Stratan and Dubina (2004), Mansour et al. (2011), Ji et al. (2015), Okazaki et al. (2005), Hjelmstad and Popov (1983), Malley and Popov (1983), Kasai and Popov (1986), Ricles and Popov (1987), Engelhardt and

Popov(1989), Itani (1997), Chi and Uang (2000), McDaniel et al. (2003), Okazaki et al. (2009), Dusicka et al. (2010), Ciutina et al. (2013)) were collected and combined with the data produced as a part of this study. Test data from earlier studies that belong to premature failures were excluded from the data set. Figure 3.15 plots the inelastic rotation capacity versus the link length ratio. The inelastic rotation capacity of the replaceable shear links exceeded the required rotation levels stipulated by AISC341-10 (2010). The replaceable links behaved similar to conventional links without significant pinching. The links were able to develop required inelastic rotation capacity in the presence of axial load levels reported in Table 3.5.

The effect of loading protocol has a pronounced effect on the inelastic rotation capacity as observed by Okazaki et al. (2005). Specimens 1, 3, 4, 5, 9, 10, 14, and 15 tested under the AISC341-10 (2010) loading protocol exceeded 0.130 rad of inelastic rotation while a similar specimen (Specimen 2) tested under AISC341-02 (2002) loading protocol sustained an inelastic rotation of 0.095 rad. Nevertheless, the rotation capacity of Specimen 2 exceeded the limit of 0.08 rad. When the behavior of Specimens 1 and 3 are compared it can be concluded that no discernable differences exist between using single-sided or double-sided stiffeners for these shallow link sections.

The findings of this study can be used to re-evaluate the flange slenderness ratio for links. Based on the work of Okazaki et al. (2005), the flange slenderness limit in the AISC Seismic Provisions (AISC341-10 (2010)) were modified to $0.38(E/F_y)^{1/2}$ from $0.30(E/F_y)^{1/2}$, where $E$ is the elastic modulus of structural steel. This modification is only applied to shear yielding links ($\rho \leq 1.6$). A number of long link specimens tested by Okazaki et al. (2005) with flange slenderness at the limit of $0.38(E/F_y)^{1/2}$ experienced local flange buckling but achieved inelastic rotations well beyond the required levels. However, a single specimen failed to achieve the required inelastic rotation due to local buckling. For S275 steel, the flange slenderness limit of $0.38(E/F_y)^{1/2}$ corresponds to 10.2. The flange slenderness ratios of the HEA160 and HEA220 links were 9.07 and 10.4, respectively. The HEA220 links with $\rho$=1.04 did not experience local buckling and failed through either brace buckling, fracture of the web or fracture of the flange.

Local bending of the flange at 0.07 rad followed by local flange buckling at rotations that vary between 0.11 rad and 0.13 rad were observed for the HEA160 links (Specimens 1 through 5, Specimen 9, 10, 14 and 15) which had rather longer normalized link lengths when compared with HEA220 links. Although these specimens experienced local buckling the post buckling response was relatively stable and local buckling did not result in a loss of shear load carrying capacity. These specimens eventually failed through fracture of the flange. It is considered that large local strains that develop at the brace-to-link connection were responsible for this failure mode. Earlier tests (Okazaki et al. (2005)) were conducted on isolated link specimens where the links were attached to end plates. In the present study the forces were transferred to the links through the braces and this causes a much more different loading condition. Both link sections showed excellent behavior for the short link specimens ($\rho \leq 1.6$) providing an independent verification of the findings of Okazaki et al. (2005). The intermediate link specimens (Specimens 6, 11 and 16) violated the limit of $0.30(E/F_y)^{1/2}$ which corresponds to 8.09 for S275 steel. Although the flange slenderness ratio of these intermediate links exceeded the AISC341-10 (2010) requirement, the specimens provided excellent behavior. The cyclic response obtained from these specimens is an addition to the data set of longer link specimens with higher flange slenderness ratios that showed acceptable performance.

### 3.5.2. Link Overstrength

The link overstrength factor has a paramount importance in EBF design. The braces and the beam outside the link are proportioned based on capacity design principles where the forces acting on these members are directly related to the link overstrength. Popov and Engelhardt (1988) recommended an overstrength factor of 1.5 to account for expected link strength and its strain hardening. The current AISC341-10 (2010) provisions address the overstrength using three different factors. The forces are amplified by $1.25R_y$ where the 1.25 factor takes into account the strain hardening effect and $R_y$ takes into account the differences between actual and nominal material properties. The commentary to AISC341-10 (2010) indicates that the use of resistance factors or safety factors also contribute to the level of assumed overstrength. Considering resistance factors to safeguard against larger overstrength is open judgment as these factors are used for the uncertainties in the resistance side rather than the loading side.

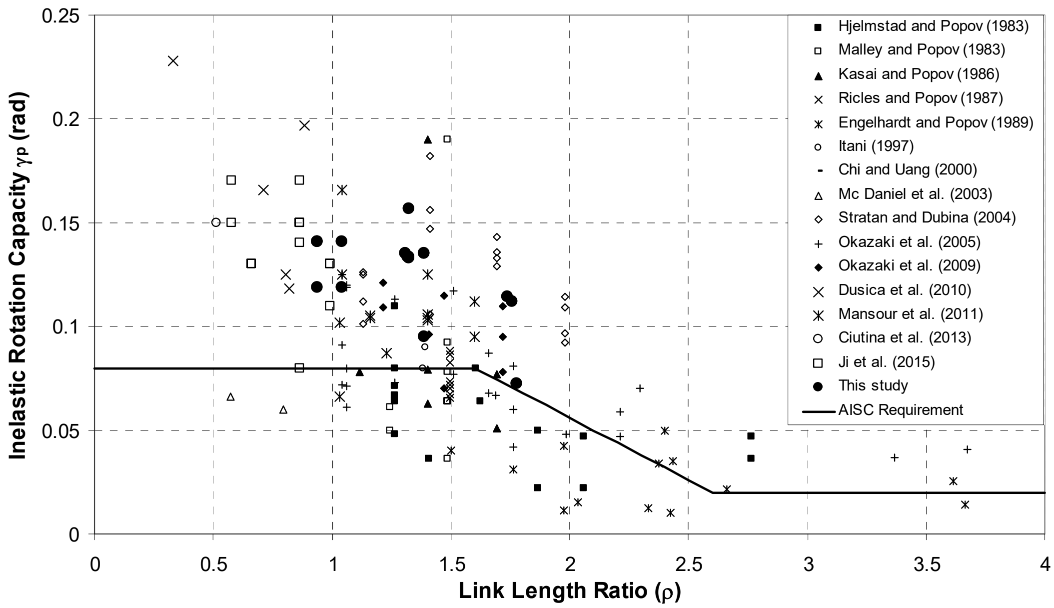


Figure 3.15 Comparison of Inelastic Rotation Capacity of Links with Past Tests

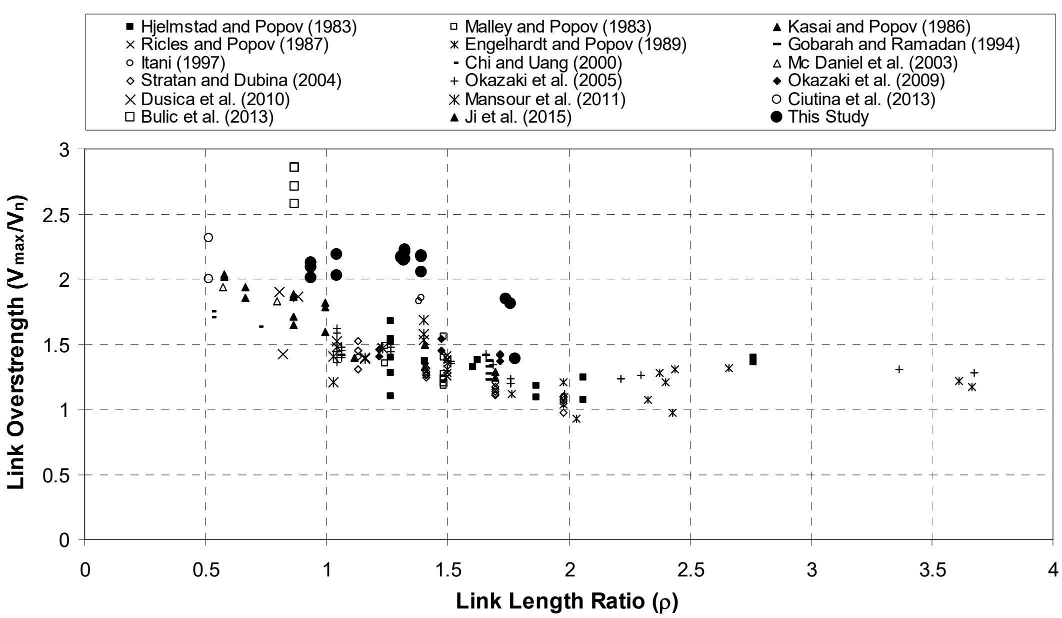


Figure 3.16 Comparison of Link Overstrength with Past Tests

The replaceable links tested as a part of this research program provided very large overstrengths that reached to a maximum of 2.22 for Specimen 10. The data from this research was compared with data from various research teams (Stratan and Dubina (2004), Mansour et al. (2011), Ji et al. (2015), Okazaki et al. (2005), Hjelmstad and Popov (1983), Malley and Popov (1983), Kasai and Popov (1986), Ricles and Popov (1987), Engelhardt and Popov(1989), Itani (1997), Chi and Uang (2000), McDaniel et al. (2003), Okazaki et al. (2009), Dusicka et al. (2010), Ciutina et al. (2013), Ghobarah and Ramadan et al. (1994), Bulic et al. (2013)) in Figure 3.16. In this figure the $V_{max}/V_n$ ratio is plotted against the link length ratio, where $V_{max}$ is the reported maximum shear strength of a link. The capacity of the link ($V_n$) is calculated as the smaller of $V_p$ or $2M_p/e$, where $V_p$ and $M_p$ were computed using the measured dimensions and measured material properties. Because the measured properties are used, the differences between the nominal and actual properties are already taken into account and the overstrengths presented in Figure 3.16 are representative of the overstrengths that arise due to strain hardening and other possible factors.

The reasons for having higher overstrengths were studied in the past. Based on the work of Richards (2004), the commentary to AISC 341-10 (2010) recommends considering the possibility of strain hardening factors in excess of 1.25 for built-up sections with very thick flanges and very short lengths ($\rho \leq 1.0$). Large overstrength values for very short links were reported after recent experimental studies. Ji et al. (2015) investigated built-up links having length ratios ranging between 0.58 and 0.97 and reported a maximum link overstrength of 2.04. Ciutina et al. (2013) tested EBFs with short links ($\rho$=0.5) comprised of HEA200 sections where overstrength values of 2.0 and 2.3 were reported for monotonically and cyclically loaded specimens respectively. Bulic et al. (2013) tested HEA100 section shear links ($\rho$=0.9) under monotonic loading where the links were subjected to an inelastic rotation of 0.2 rad. The overstrength values ranged between 2.56 and 2.84. The overstrengths provided by the links tested in this research program are significantly higher than the overstrengths provided by the links in the same category ($1.0<\rho<1.75$). This is the first study to report such high overstrengths for links that qualify as short or intermediate links. Della Corte et al.

(2013) studied overstrength of links through finite element analysis and proposed an equation to predict the level of overstrength at an inelastic link rotation of 0.08 rad. The ratio of the area of flange to shear area, cross section depth, link length, strain hardening and axial restraint were found as the prime variables that influence overstrength. The overstrengths calculated based on the proposed formula were compared with the experimental overstrengths at 0.08 rad of inelastic link rotation. The differences between the experimental and calculated overstrengths are on average 15 percent and 22 percent for cases with and without axial restraint respectively. The average of the ratios of calculated overstrength without axial restraint and with axial restraint is 0.92 indicating that axial restraint is not the major source of overstrength. This assertion can be substantiated by calculating the additional shear resistance provided by the effect of axial force. The maximum levels of tensile axial forces reported in Table 3.5 were used to calculate the additional shear resistance due to axial restraint. When all specimens are considered the averages of the contributions of this additional shear to the total shear resistance and nominal shear resistance are 9 percent and 19 percent respectively.

### 3.5.3. Brace Buckling

Most of the experimental EBF studies concentrate on the behavior of isolated link specimens. In these tests it is not possible to observe the behavior of braces and the beam outside the link. The present study is one of the few studies that demonstrated brace buckling in an EBF system. Specimen 7 which employed an HEA220 link and HEA160 brace and Specimen 9 which employed an HEA160 link and HEA140 brace experienced brace buckling due to the large overstrength possessed by the link. Brace buckling should definitely be averted in EBF systems as buckling of any one of the braces trigger a soft story mechanism. As evidenced in Specimen 7 and 9, the load carrying capacity of the system reduced significantly after the initiation of brace buckling.

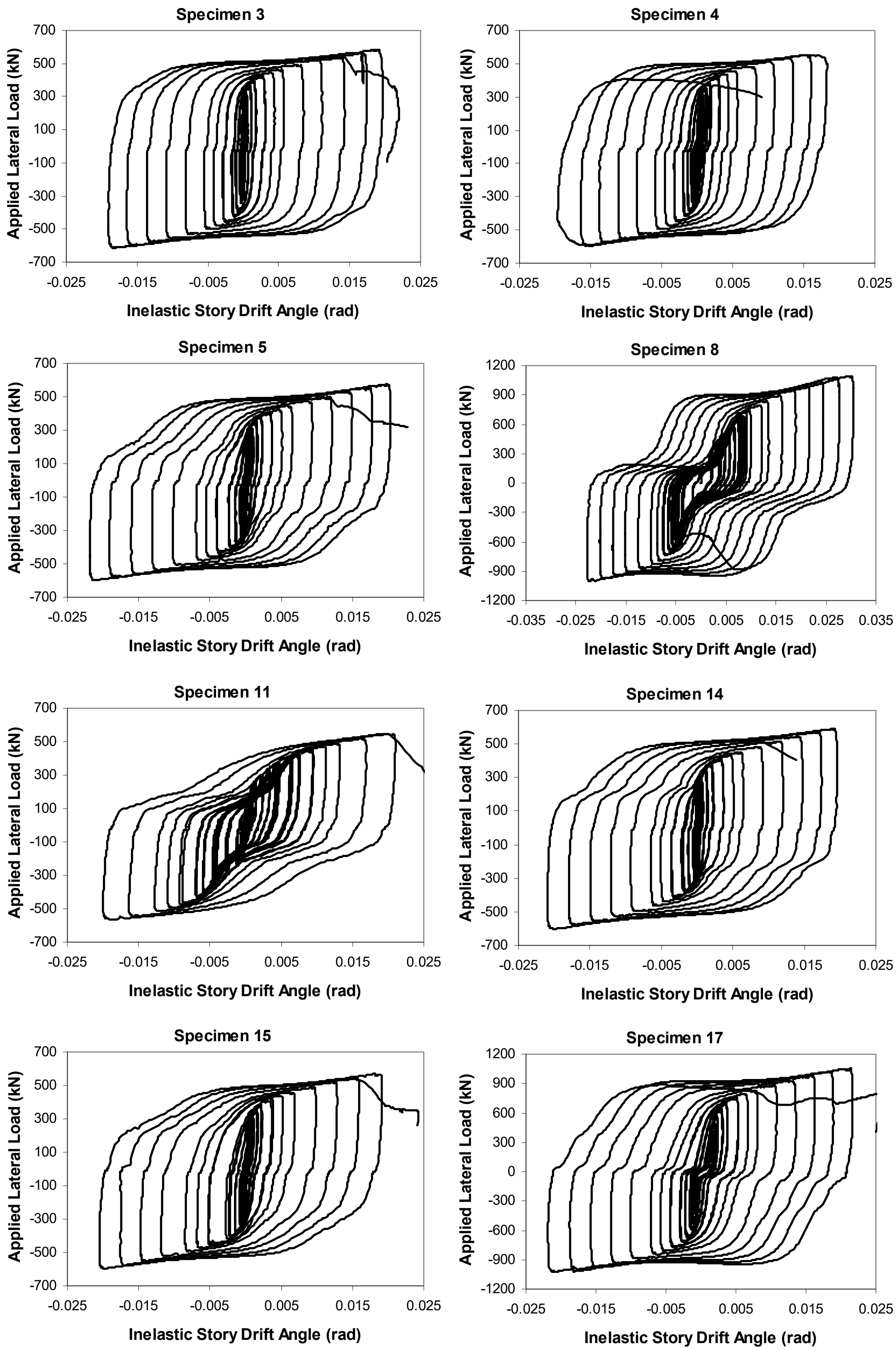


Figure 3.17 Hysteretic Response of EBFs

The $PM_1$ ratios reported in Table 3.4 vary between 0.30 and 0.72 while the $PM_2$ ratios vary between 0.25 and 0.52 for the braces. It is worthwhile to reiterate that the *PM* values reported in Table 3.4 do not contain the overstrength of the link. When the reported *PM* values are multiplied by the overstrength value observed in the tests, the resulting *PM* values exceed unity indicating initiation of yielding and potential of buckling in braces. Specimens 5 and 6 were instrumented with strain gages to observe yielding in the braces. The gages were placed at the flanges of braces close to a location where the brace flange is welded to the replaceable link. Test results revealed that the strains reach to 5500με indicating yielding in these members.

Local yielding in braces does not create significant structural problems as buckling does. Specimen 7 was special in the sense that the $PM_2$ ratio of this specimen ($PM_2$=0.52) was much higher when compared with its counterparts. The $PM_2$ ratio multiplied by the overstrength of the link (Ω=2.03) result in an overall $PM_2$ ratio over unity. This observation suggests that stability of the braces must be ensured by checking the compression resistance of the brace with a higher overstrength factor. A similar design philosophy was experimented in the past by Engelhardt and Popov (1989). In the design of one of the EBF subassemblages, the brace section was sized only for the ultimate axial force generated in the brace, assuming the brace connection behaves as a pin and transfers no moment to the brace. The brace section was therefore chosen to provide high axial compressive strength with no concern for available flexural strength. The specimen showed stable brace behavior with significant amount of bending deformations of the brace.

### 3.5.4. Replaceability of Links, Connection Detailing and Global Frame Response

The links were easily replaced after each test and the members outside the links were reused. The proposed detail did not require flame cutting of the link or the use of hydraulic jacks to remove and replace the link. The gap provided at the splice connections promotes easy replacement. No discernable differences were observed for specimens with different gap sizes (5, 10, 15 mm). A gap size of 10mm should be sufficient for practical applications. The demands on the splice plates and the bolts must be determined by considering the increased splice plate length and web connection eccentricity due to the presence of a gap.

The force transfer mechanism has a strong influence on the EBF system. As mentioned before AISC341-10 (2010) does not mandate slip critical connections; however, frictional resistance at faying surfaces and full bolt pretension are recommended. Slip was not directly measured in the research program. The main aim was to observe the effects of different connection types on the global response measures. Effect of using different splice connections on the global frame response is indicated in Figure 3.17. In this figure behaviors of Specimens 3, 4, 5, 8, 11, 14, 15, and 17 are compared. Specimen 3 and 4 employed slip critical connections where standard holes were utilized in Specimen 3 and oversize holes were used in Specimen 4. No significant loss of stiffness was observed in these tests. The results show that both frames exhibit similar response indicating that oversize holes can be utilized if the connections are designed as slip-critical. It is worthwhile to mention that the replacement procedure for Specimen 4 was much easier compared with the replacement of other specimens.

The recommendations of AISC341-10 (2010) were followed in Specimen 5, 11 and 15 where the faying surfaces were sand blasted and the bolts were fully pre-tensioned. The required number of bolts; however, was determined based on shear strength of the bolts and bearing strength at bolt holes. This specimen showed a pinched global frame behavior when compared with the behavior of Specimen 3 which employed slip-critical connections. At higher load levels there was a loss of stiffness observed together with loud bangs from the setup. It was considered that these indicators were a result of slip in the splice connections. The pinching does not have a detrimental effect on the behavior. Therefore, the use of bearing type connections together with the recommendations of AISC341-10 (2010) for surface preparation and bolt pretension are recommended herein. Specimen 8 did not conform to the AISC341-10 (2010) requirements as the bolts were only snug-tight as opposed to being fully pre-tensioned. The global response of this specimen exhibits significant amount of pinching. There was a significant loss of stiffness at early stages of loading even before the link starts to yield. It is considered that slip was responsible for loss of stiffness at service load levels which is inadmissible. Therefore, it is recommended to reduce the amount of slip at the splice connections by employing the recommendations of AISC341-10 (2010).

In the Specimen 14 where compact gusset plate connected attachments was employed, since the link to beam outside the link connection is within the panel zone, bolts were subjected the significant amount of shear force when compared to the specimens with direct brace attachment or the specimens with gusset plate connected attachment. Therefore, Specimen 14 indicated a pinched global frame behavior when compared with the behavior of Specimen 3 which employed direct brace attachment and slip-critical connections. Pin connected brace attachment utilized for Specimen 17 is one of the most preferred connection type in real practice for brace members. Global frame behavior of this specimen is similar to the specimens where bearing type connection was employed. Test results revealed that pin connected brace attachments may be an alternative for EBFs where rigid brace attachment is used.

The rigid plastic mechanism is generally used to find out inelastic link rotations at the design stage. The method provides relationships between the inelastic story drift angle and the inelastic link rotation. According to commentary to AISC341-10 (2010) the following relationship holds for the type of EBF geometry tested in this research program.

$$\theta_p = \gamma_p \frac{e}{L} \tag{3.6}$$

The inelastic story drift angle was calculated using Equation 3.6 and the inelastic link rotations reported in Table 3.5. The calculated values are compared with the measured inelastic story drift angles reported in Table 3.5. The measured inelastic story drift angles are on average 25 percent larger than the calculated ones. The difference between the measured and calculated values increases as the amount of slip in connections increases. For Specimen 8 where the bolts were not pre-tensioned the difference reaches to 60 percent.

# CHAPTER 4

# SUMMARY AND CONCLUSIONS

## 4.1. Summary

This thesis reports findings of a three-phase experimental research program on steel encased buckling-restrained braces (BRBs) and a two-phase experimental research program on eccentrically braced frames with replaceable links.

The first experimental research program composed of three phases examined potential use of steel encased BRBs which utilize constant width core plates and welded overlap core plates under subassemblage testing. Furthermore, connection details with particular emphasis on the use of collar plates were studied for the welded overlap core BRBs.

The second experimental research program composed of two phases reports findings of an experimental study conducted on replaceable links for steel eccentrically braced frames. While the replaceable links with direct brace attachments were investigated in the first phase of this experimental program, replaceable links with gusset plated brace attachments were examined in the second phase. The aim of this research program was to come up with new replaceable links providing many advantages in terms of replaceability compared with the other replaceable links investigated to date for eccentrically braced frames.

## 4.2. Conclusions

### 4.2.1. Conclusions about Steel Encased Buckling Restrained Braces

The results of the first phase indicated that behaviors of steel encased BRBs with constant width core plates under uniaxial testing and subassemblage testing are markedly different. Subassemblage test results revealed that the core plate is subjected to non-uniform strains along the length and the end regions which are subjected large rotational demands develop very large local strains. The width of the core plate increases excessively due to large strain demands. The core plate comes into contact with the encasings and results in axial resistances reaching to unacceptable levels.

Welded overlap core steel encased BRBs were developed and tested for the first time in this research program. This kind of a core enables to tailor the yielding portion of the core segment and eliminates any disadvantages of CNC cutting procedure. Test results showed that properly detailed and inspected welded overlap core BRBs can provide acceptable performance by sustaining cumulative strains in excess of 400 times the yield strain.

The present study also investigated behavior of the welded overlap core steel encased BRBs with pin ended connections and rigid connections in light of the presence and absence of collars. Test results revealed that a collar system should be used for pin connected BRBs whereas it is not required to be used for rigidly connected BRBs. Both the end connection types can be utilized for welded overlap core steel encased BRBs.

#### 4.2.2. Conclusions about Replaceable Links for Eccentrically Braced Frames

A total of seventeen quasi-static cyclic loading tests were conducted on a nearly full scale framing to validate a proposed replaceable link concept. The link length ratio (ρ), stiffening of the link, loading protocol, brace to link connection type, location of the brace to link connection, bolt connection type, bolt pretension, spacing between members, demand-to-capacity ratio of braces and the beam outside the link were considered as the prime variables. Fourteen of the replaceable links qualified as shear links and three of the links qualified as an intermediate link. Major findings from the study are summarized as follows:

The short links achieved large inelastic rotation capacities that vary between 0.095 and 0.157 rad depending on the applied loading protocol. Specimen 2 tested using the severe loading protocol given in AISC341-02 (2002) had a much lower rotation capacity when compared with its counterparts. Three intermediate link specimen (Specimens 6, Specimen 11, and Specimen 16) achieved an inelastic rotation capacities of 0.114 rad., 0.072 rad, and 0.112 rad. All replaceable links satisfied the rotation limits given in AISC 341-10 (2010).

The use of single-sided or double-sided stiffeners for the shallow link section used in this study did not result in discernable differences.

The overstrength factors of the replaceable links reached 2.22. Data from past experiments suggest even higher overstrength factors for shorter links ($\rho<1.0$). Overstrength factors in excess of 2.0 are the first to be reported in literature for the link categories tested in this research program ($1.0<\rho<1.75$). Finite element studies conducted by Della Corte et al. (2013) also substantiate the level of overstrength observed in the experiments.

The high level of link overstrength caused brace buckling in two of the experiments proving the importance of correctly quantifying this factor at the design level.

The use of slip-critical connections with oversize or standard holes were found to result in adequate response. Bearing type connections with frictional faying surfaces and fully pre-tensioned bolts were also found to provide adequate response. EBFs with this type of connection detail were found to show a pinched response when compared with EBFs having slip-critical connections. Test results revealed that EBFs with bearing type connections having snug-tight bolts result in severely pinched global frame response.

The study included replaceable links where the brace member is connected to the link by making use of a gusset plate. According to test results, inelastic rotation capacity of the specimens where gusset plate connected attachment was used is generally similar to the specimens where direct brace attachment was used. However, since the bolts were subjected to significant amount of shear force for the specimens where compact gusset plate connected attachment was employed, pinched global frame behavior was obtained. Global frame behavior of the specimen where pin connected brace attachment was employed is similar to the specimens where bearing type connection was employed. Test results revealed that pin connected brace attachments may be an alternative for EBFs with rigid brace attachments.

In conclusion, the study demonstrated the potential of using the proposed replaceable link details where standard splice connections are employed for the braces and the beams outside the link. Slip-critical connections with standard or oversize holes are recommended to be used in cases where the required number of bolts is rather low and the connection length is rather short. For sizeable replaceable links bearing type connections are recommended where the surface preparation and bolt pretension recommendations of AISC341-10 (2010) are followed. The required number of bolts should be determined based on capacity design principles. Regardless of the type of the link, the braces of the EBF system should be designed to show stable behavior. For short ($1.0 \leq \rho \leq 1.6$) and very short links ($\rho < 1.0$) it is recommended that the stability of the brace be ensured by considering the axial resistance only without bending effects and using an overstrength factor of at least $2.0R_y$ (i.e. $PM_2 < 1.0$ calculated based on $\Omega = 2.0R_y$). A gap size of 10 mm was found to be sufficient for replacement purposes. The splice connection strength must be verified for a given gap size.

The success of the replacement procedure depends heavily on the amount of residual frame drifts. Full scale laboratory tests indicated that the residual drifts are significantly recovered after the removal of the link. In case where the residual drifts are higher, the replacement method that was implemented after New Zealand earthquakes (Gardiner et al. (2013)) is recommended herein. This method requires post-replacement site measures of the frame geometry to develop a template and fabrication of new replaceable links based on this template. There is currently a need to develop connection details for easy replacement under large residual drifts. Future research should concentrate on testing and validation of such details.

# REFERENCES


American Institute of Steel Construction (AISC), Seismic provisions for structural steel buildings, AISC 341-02, Chicago, 2002.

American Institute of Steel Construction (AISC), Seismic provisions for structural steel buidings, AISC 341-10, Chicago, 2010

American Institute of Steel Construction (AISC), Specification for structural steel buildings, AISC 360-10, Chicago, 2010.

Balut N. and Gioncu V., "Suggestion for an improved 'dog-bone' solution," Proceedings of the 4th International Conference on Behaviour of Steel Structures in Seismic Areas (STESSA 2003), Naples, Italy, 2003.

Becker R. and Ishler M., "Seismic design practice for eccentrically braced frames based on the 1994 UBC", Steel Tips. Structural Steel Education Council, Berkeley, CA, 1996.

Bruneau M., Uang C. M., Sabelli R., "Ductile Design of Steel Structures", Second Edition, McGraw-Hill Companied, 2011.

Bulic M., Causevic M., and Androic B., "Reliability of short seismic links in shear," B. Earthq. Eng., Vol. 11,No. 4, PP. 1083-1098, 2013.

Chi B. and Uang C. M., "Cyclic testing of steel shear links for the San Francisco Moscone Convention Center expansion project," Department of Structural Engineering, University of California, San Diego, La Jolla, CA, Report No. TR-99/06, 2000.

Chuang MC, Tsai KC, Lin PC and Wu AC. Critical limit states in seismic buckling-restrained brace and connection designs. Earthquake Engineering and Structural Dynamics, 2015; 44: 1559-1579.

Ciutina A., Dubina D., and Danku G., "Influence of steel-concrete interaction in dissipative zones of frames: I-Experimental study," Steel Compos. Struct., Vol. 15,No. 3, PP. 299-322, 2013.

Clifton, C., Bruneau, M., MacRae, G., Leon, R., Fussell, A. 2011. "Steel Structures Damage from the Christchurch Earthquake Series of 2010 and 2011", Bulletin of The New Zealand Society for Earthquake Engineering, 44(4), 297-318.

Cofie, NG, Krawinkler, H, Uniaxial cyclic stress-strain behavior of structural steel, Journal of Engineering Mechanics, 1985; 111: 1105-1120.

CSA, Design of Steel Structures, CAN/CSA S16-14. Canadian Standards Association, Mississauga, ON, 2014.

Dubina D., Stratan A., and Dinu F., "Dual high-strength steel eccentrically braced frames with removable links," Earthq. Eng. Struct. D., Vol. 37,No. 15, PP. 1703-1720, 2008.

Dubina D., Stratan A., and Dinu F., "Re-centring capacity of dual-steel frames," Steel Constr., Vol. 4,No. 2, PP. 73-84, 2011.

Dusicka P., Itani A. M., and Buckle I. G., "Cyclic Behavior of Shear Links of Various Grades of Plate Steel," J. Struct. Eng. ASCE, Vol. 136,No. 4, PP. 370-378, 2010.

Dusicka P, Tinker J. Global restraint in ultra-lightweight buckling-restrained braces. Journal of Composites for Construction, 2013; 17: 139-150.

EN 10025-2, Hot rolled products of structural steels. - Part 2: General technical delivery conditions for non-alloy structural steels. European Committee for Standardization, Brussels, 2004.

EN 10002-1, Metallic materials – Tensile testing – Part 1: Method of test at ambient temperature. European Committee for Standardization, Brussels, 2001.

Engelhardt M. D. and Popov E. P., "Behavior of long links in eccentrically braced frames," Earthquake Engineering Research Center, University of California, Berkeley, CA, Report No. UCB/EERC-89/01, 1989.

Engelhardt M. D. and Popov E. P., "On Design of Eccentrically Braced Frames," Earthquake Spectra, EERI, Vol. 5, No. 3, PP. 495-511, 1989.

Eryaşar E, Experimental and numerical investigation of buckling restrained braces, Thesis, Middle East Technical University, Ankara, Turkey, 2009.

Eryaşar E, Topkaya C. An experimental study on steel-encased buckling-restrained brace hysteretic dampers. Earthquake Engineering and Structural Dynamics, 2010; 39: 561-581.

Eurocode 8 (2004), Design of structures for earthquake resistance. – Part 1: General rules, seismic actions and rules for buildings. European Committee for Standardization, Brussels.

European Commission, High-strength tower in steel for wind turbines (Histwin), Directorate-General for Research and Innovation, Contract No RFSR-CT-2006-00031, 2012.

European Commission, Optimising the seismic performance of steel and steel-concrete structures by standardising material quality control (OPUS), Directorate-General for Research and Innovation, Contract No RFSR-CT-2007-00039, 2013.

Fahnestock L, Ricles JM, and Sause R. Experimental evaluation of a large-scale buckling-restrained braced frame. Journal of Structural Engineering, 2007; 133: 1205-1214.

Fujimoto M., Aoyagi T., Ukai K., Wada A., and Saito K., "Structural Characteristics of Eccentric K-Braced Frames," Trans. Architectural Institute of Japan, Vol. 195, PP. 39-49, 1972.

Gardiner G., Clifton C., and MacRae G. A., "Performance, damage assessment and repair of a multistorey eccentrically braced frame building following the Christchurch earthquake series, steel innovations conference 2013," Proceedings of the Steel Innovations Conference 2013, Christchurch, New Zealand, 2013.

Ghobarah A. and Ramadan T., "Bolted link-column joints in eccentrically braced frames," Eng. Struct., Vol. 16,No. 1, PP. 33-41, 1994.

Hjelmstad K. D. and Popov E. P., "Characteristics of Eccentrically Braced Frames," Journal of Structural Engineering, ASCE, Vol. 110, No. 2, PP. 340-353, 1984.

Hjelmstad K. D. and Popov E. P., "Cyclic Behavior and Design of Link Beams," Journal of Structural Engineering, ASCE, Vol. 109, No. 10, PP. 2387-2403, 1983.

Hjelmstad K. D. and Popov E. P., "Seismic behavior of active beam link in eccentrically braced frames," Earthquake Engineering Research Center, University of California, Berkeley, CA, Report No. UCB/EERC-83/15, 1983.

ISO 898-1, Mechanical properties of fasteners made of carbon steel and alloy steel -- Part 1: Bolts, screws and studs, 1999.

Ioan A., Stratan A., Dubina D., Poljansek M., Molina F. J., Taucer F., Pegon P., and Sabau G., "Experimental validation of re-centring capability of eccentrically braced frames with removable links," Eng. Struct., Vol. 113,PP. 335-346, 2016.

Itani A. M., "Cyclic behavior of Richmond-San Rafael tower links," Center for Civil Engineering Earthquake Research, University of Nevada, Reno, NV, Report No. CEER 97-4, 1997.

Ji X., Wang Y., Ma Q., and Okazaki T., "Cyclic behavior of very short steel shear links," J. Struct. Eng. ASCE, 2015. (doi:10.1061/(ASCE)ST.1943-541X.0001375)

Kasai K. and Popov E. P., "A study of seismically resistant eccentrically braced frames," Earthquake Engineering Research Center, University of California, Berkeley, CA, Report No. UCB/EERC-86/01, 1986.

Kasai K. and Popov E. P., "Cyclic Web Buckling Control for Shear Link Beams," Journal of Structural Engineering, ASCE, Vol. 112, No. 3, PP. 505-523, 1986.

Kasai K. and Popov E. P., "General Behavior of WF Steel Shear Link Beams," Journal of Structural Engineering, ASCE, Vol. 112, No. 2, PP. 362-382, 1986.

Kasai K. and Popov E. P., "On Seismic Design of Eccentrically Braced Frames," Presented at the 8th World Conference on Earthquake Engineering, IAEE. San Francisco, 1985.

Kazemzadeh Azad S. and Topkaya C., “A Review of Research on Steel Eccentrically Braced Frames,” Journal of Constructional Steel Research, Vol. 128, Pages: 53-73, 2017

Kim DH, Lee CH, Ju YK and Kim SD. Subassemblage test of buckling-restrained braces with H-shaped steel core. The Structural Design of Tall and Special Buildings, 2015; 24: 243-256.

Lin PC, Tsai KC, Wu AC and Chuang MC. Seismic design and test of gusset connections for buckling-restrained braced frames. Earthquake Engineering and Structural Dynamics, 2014; 43: 565-587.

Lin PC, Tsai KC, Wang KJ, Yu YJ, Wei CY, Wu AC, Tsai CY, Lin CH, Chen JC, Schellenberg AH, Mahin, SA and Roeder CW. Seismic design and hybrid tests of a full-scale three-story buckling-restrained braced frame using welded end connections and thin profile. Earthquake Engineering and Structural Dynamics, 2012; 41: 1001-1020.

Manheim D. N. and Popov E. P., "Plastic Shear Hinges in Steel Frames," Journal of Structural Engineering, ASCE, Vol. 109, No. 10, PP. 2404-2419, 1983.

Malley J. O. and Popov E. P., "Design Considerations for Shear Links in Eccentrically Braced Frames," University of California, Berkeley, Report No. UCB/EERC-83/24, 1983.

Malley J. O. and Popov E. P., "Shear Links in Eccentrically Braced Frames," Journal of Structural Engineering, ASCE, Vol. 110, No. 9, PP. 2275-2295, 1984.

Mansour N., "Eccentrically Braced Frames with Replaceable Shear Links," Ph.D. Thesis, Department of Civil Engineering, University of Toronto, Toronto, Ontario, Canada, 2010.

Mansour N., Christopoulos C., and Tremblay R., "Experimental validation of replaceable shear links for eccentrically braced steel frames," J. Struct. Eng. ASCE, Vol. 137,No. 10, PP. 1141-1152, 2011.

McDaniel C. C., Uang C. M., and Seible F., "Cyclic testing of built-up steel shear links for the new bay bridge," J. Struct. Eng. ASCE, Vol. 129,No. 6, PP. 801-809, 2003.

Okazaki T., Arce G., Ryu H. C., and Engelhardt M. D., "Experimental study of local buckling, overstrength, and fracture of links in eccentrically braced frames," J. Struct. Eng. ASCE, Vol. 131,No. 10, PP. 1526-1535, 2005.

Okazaki T., Engelhardt M. D., Drolias A., Schell E., Hong J. K., and Uang C. M., "Experimental investigation of link-to-column connections in eccentrically braced frames," J. Constr. Steel Res., Vol. 65,No. 7, PP. 1401-1412, 2009.

Park J, Lee J and Kim J. Cyclic test of buckling restrained braces composed of square steel rods and steel tube. Steel and Composite Structures, 2012; 5: 423-436.

Perretti A., "Comportamento sismico di telai in acciaio con controventi eccentrici," Ph.D. Thesis, Department of Civil, Building and Environmental Engineering, University of Naples, Naples, Italy, 1999. (in Italian)

Piedrafita D, Cahis X, Simon E, Comas J. A new modular buckling restrained brace for seismic resistant buildings. Engineering Structures, 2013; 56: 1967-1975.

Piedrafita D, Cahis X, Simon E, Comas J. A new perforated core buckling restrained brace. Engineering Structures, 2015; 85: 118-126.

Popov E. P. and Engelhardt M. D., "Seismic eccentrically braced frames," J. Constr. Steel Res., Vol. 10, PP. 321-354, 1988.

Ramsay J. J., Fussell A., and Wilkinson R. G., "Design of Replaceable-Link Eccentric Braced Frames in Post-Earthquake Christchurch," Proceedings of the Steel Innovations Conference 2013, Christchurch, New Zealand, 2013.

Ricles J. M. and Popov E. P., "Composite Action in Eccentrically Braced Frames," Journal of Structural Engineering, ASCE, Vol. 115, No. 8, PP. 2046-2065, 1989.

Ricles J. M. and Popov E. P., "Experiments on eccentrically braced frames with composite floors," Earthquake Engineering Research Center, University of California, Berkeley, CA, Report No. UCB/EERC-87/06, 1987.

Richards P. W., "Cyclic Stability and Capacity Design of Steel Eccentrically Braced Frames," Ph.D. Thesis, Department of Structural Engineering, University Of California, San Diego, San Diego, CA, 2004.

Roeder C. W. and Popov E. P., "Eccentrically Braced Steel Frames for Earthquakes," Journal of the Structural Division, ASCE, Vol. 104, No. ST3, PP. 391-411, 1978.

Sabau G. A., Poljansek M., Taucer F., Pegon P., Molina F. J., Tirelli D., Viaccoz B., Stratan A., Ioan Chesoan A., and Dubina D., "Seismic Engineering Research Infrastructures For European Synergies: Full-Scale Experimental Validation of a Dual Eccentrically Braced Frame with Removable Links (DUAREM)," Institute for the Protection and Security of the Citizen, Publications Office of the European Union, Luxembourg, Report EUR 27030, 2014.

Stratan A., Dubina D., and Dinu F., "Control of global performance of seismic resistant EBF with removable link," Proceedings of the 4th International Conference on Behaviour of Steel Structures in Seismic Areas (STESSA 2003), Naples, Italy, 2003, PP. 175-180.

Stratan A. and Dubina D., "Bolted links for eccentrically braced steel frames," Proceedings of the 5th AISC/ECCS International Workshop: Connections in Steel Structures V. Behaviour, Strength and Design, Delft, The Netherlands, 2004, PP. 223-332.

Tanabashi R., Naneta K., and Ishida T., "On the Rigidity and Ductility of Steel Bracing Assemblage," Presented at the 5th World Conference on Earthquake Engineering, IAEE, Rome, 1974.

Tremblay R, Bolduc P, Neville R, and Devall R. Seismic testing and performance of buckling-restrained bracing systems. Canadian Journal of Civil Engineering, 2006; 33: 183-198.

Turkish Seismic Code 2007, Specification for structures to be built in disaster areas.

Uang C, and Nakashima M. Steel buckling-restrained braced frames. In Earthquake Engineering from Engineering Seismology to Performance Based Engineering, CRC Press, 2004.

Usami T, Wang CL, Funayama J. Developing high-performance aluminum alloy buckling- restrained braces based on series of low- cycle fatigue tests. Earthquake Engineering and Structural Dynamics, 2012; 41: 643-661.

Usami T, Wang C, Funayama J. Low-cycle fatigue tests of a type of buckling restrained braces. Procedia Engineering, 2011; 14: 956-964.

Wang CL, Usami T, Funayama J. Improving low-cycle fatigue performance of high-performance buckling-restrained braces by toe-finished method. Journal of Earthquake Engineering, 2012; 16: 1248-1268.

Wang CL, Usami T, Funayama J, Imase F. Low-cycle fatigue testing of extruded aluminium alloy buckling-restrained braces. Engineering Structures, 2013; 46: 294-301.

Watanabe A, Hitomi Y, Saeki E, Wada A, and Fujimoto,M. Properties of brace encased in buckling-restraining concrete and steel tube. Proceedings, 9th World Conference on Earthquake Engineering, vol. IV., 1988.

Wu AC, Lin PC and Tsai KC. High-mode buckling responses of buckling-restrained brace core plates. Earthquake Engineering and Structural Dynamics, 2014; 43: 375-393.

Xie Q. State of the art of buckling-restrained braces in Asia. Journal of Constructional Steel Research, 2005; 61: 727-748.

Zhao J, Wu B and Ou J. A novel type of angle steel buckling-restrained brace: Cyclic behavior and failure mechanism. Earthquake Engineering and Structural Dynamics, 2010; 40: 1083-1102.

Zhao J, Wu B, and Ou J. Flexural demand on pin-connected buckling-restrained braces and design recommendations. Journal of Structural Engineering, 2012; 138: 1398-1415.

# CURRICULUM VITAE

## PERSONAL INFORMATION


| | |
|---|---|
| Surname, Name: | Bozkurt, Mehmet Bakır |
| Nationality: | Turkish (TC) |
| Date and Place of Birth: | 1 January 1982, Bismil |
| Marital Status: | Married |
| Phone: | +90 533 518 17 57 |
| email: | mehbakboz@gmail.com |


## EDUCATION

| Degree | Institution | Year of Graduation |
|---|---|---|
| MS | ITU Civil Engineering | 2009 |
| BS | ESOGU Civil Engineering | 2004 |
| BS | ESOGU Mechanical Engineering | 2004 |

## WORK EXPERIENCE

| Year | Place | Enrollment |
|---|---|---|
| 2012-2016 | Middle East Technical University | Research Assistant |
| 2011-2012 | Promer Engineering | Structural Designer |
| 2010-2011 | Prota Engineering | Structural Designer |
| 2008-2010 | Nurol Machinery and Industry | Structural Designer |
| 2005-2008 | Famer Engineering | Structural Designer |

## FOREIGN LANGUAGES

Advanced English (IELTS 6.5 (2012))

## JOURNAL PUBLICATIONS


1. Bozkurt, M.B., Topkaya, C. (2017) “Replaceable Links with Direct Brace Attachments for Eccentrically Braced Frames” Earthquake Engineering & Structural Dynamics, DOI: 10.1002/eqe.2896.

2. Bozkurt, M.B., Topkaya, C. (2016) “Development of Welded Overlap Core Steel Encased Buckling-Restrained Braces” Journal of Constructional Steel Research, Vol. 127, Pages 151-164.

## REFEREED CONFERENCE PROCEEDINGS

1. Bozkurt, M.B., Özkılıç., Y.O., Topkaya, C. (2016) “Evaluation of Displacement Amplification Factors for Steel Buckling Restrained Brace Frames" The 8th International Conference on Steel and Aluminium Structures, Hong Kong, China

2. Bozkurt, M.B., Özkılıç., Y.O., Topkaya, C. (2016) “Response of Buckling Restrained Braced Frames with Different Yield Strength and Yielding Length” Proceedings of the 12th International Congress on Advances in Civil Engineering, Istanbul, Turkey.

3. Bozkurt, M.B., Topkaya, C. (2016) “Evaluation of Seismic Response Factors for BRBFs using FEMA P695 Methodology” The International Colloquium on Stability and Ductility of Steel Structures, Timisoara, Romania

4. Bozkurt, M.B. (2015) “Burkulması Önlenmiş Çelik Çaprazlı Sistemler ile Süneklik Düzeyi Yüksek Merkezi Çelik Çaprazlı Sistemlerin Yapısal Maliyet Analizi Karşılaştırması" 6. Ulusal Çelik Yapılar Sempozyumu, Eskişehir, Türkiye.

5. Bozkurt, M.B., Topkaya, C. (2014) “Steel Buckling-Restrained Braces with Cold-Formed Encasings” Proceedings of the 11th International Congress on Advances in Civil Engineering, Istanbul, Turkey.

## RESEARCH PROJECTS

1. Development of Replaceable Links for Steel Eccentrically Braced Frames, Funded by Scientific and Technological Research Council of Turkey Project Number: 114M251, Researcher, 2014-2017, Project Budget: 300860TL.

2. Experimental Investigation on Replaceable Links for Steel Eccentrically Braced Frames, Funded by Middle East Technical University, Project Number: BAP-2016-03-03-03, Researcher, 2014-2015, Project Budget: 14500TL.

3. Experimental Investigation of Large Scale Buckling Restrained Braces, Funded by Middle East Technical University, Project Number: BAP-2014-03-03-02, Researcher, 2014-2015, Project Budget: 20663TL.